RCD-21-181-0

Activity Thresholds, Patient-Specific Modifying Factors, Breastfeeding Interruption Times, and Other Supporting Data

Research Information Letter Report for

Phase 2 Revisions to Regulatory Guide 8.39: Release of Patients Administered Radioactive Material

R.R. Benke, D.M. Hamby, D.L. Boozer,
C.T. Rose, C.D. Mangini, R.P. Harvey and K.M. Tack

submitted by:

RCD RADIATION PROTECTION ASSOCIATES

a subsidiary of:

Renaissance Code Development, LLC
310 NW 5th St., Suite 107
P.O. Box 1778
Corvallis, Oregon 97339
(541) 286-4428 (office/fax)
http://www.rcdsoftware.com

June 30, 2021

David M. Hamby, PhD
Managing Partner
david.hamby@rcdsoftware.com
NRC Contract No. 31310019C0036

Table of Contents

Table of Tables

Table of Figures

1. EXECUTIVE SUMMARY

The U.S. Nuclear Regulatory Commission (NRC) regulation at 10 CFR 35.75 provides requirements for evaluating and releasing patients who have been administered radioactive material. The revision to Regulatory Guide 8.39 (NRC 2020) presents acceptable approaches to demonstrate compliance. This document describes concepts developed for Revision 2 to NRC Regulatory Guide 8.39 and specifically addresses:

- basic thresholds for external radiation dose (Chapter 2)
- internal dose potential for a relatively new radiopharmaceutical (Chapter 3)
- incorporating additional realism with patient-specific modifying factors (Chapter 4)
- thresholds and interruption times for patients who are breastfeeding (Chapter 5)
- emerging technologies and radiopharmaceuticals (Chapter 6)
- unexpected patient death shortly after release from the medical facility (Chapter 7)
- harmonization with international guidance (Chapter 8)

Nothing herein supersedes the requirements stated in 10 CFR Part 35 or guidance published in NRC Regulatory Guide 8.39, Revision 2. Throughout this document, dose equivalents and dose equivalent rates are simply referred to as doses and dose rates, respectively.

2. BASIC THRESHOLDS

Basic thresholds provide a rapid means of assessing potential external doses to individual bystanders exposed to the patient. Theory and parameterization for developing dose-rate kernels specific to patient release, Δ_{pr}, basic activity thresholds, Q_{rel} and Q_{ins}, and basic measurement thresholds, M_{rel} and M_{ins}, for releasing the patient and issuing instructions to the patient are presented below.

Photon Dose-Rate Kernel Specific to Patient Release

Dosimetric calculations implement a point-kernel concept and feature a *total dose-rate constant*, Δ_{pr}, for patient release. The kernel has units of dose rate per unit activity at a specified distance and includes contributions from primary photons (gamma rays, X rays and positron annihilation photons) and secondary photons from bremsstrahlung production arising from electron (beta, internal conversion, and Auger emission) interactions in the patient's body. The point-kernel formulation assumes isotropic emission from a point source within the patient and dose delivery to a point in tissue of a bystander at a distance of 1 m. The source is assumed to be embedded in an infinitely small sphere of tissue so that bremsstrahlung can be generated. Attenuation and buildup in material between the patient and the bystander is not considered in the calculation of Δ_{pr} (i.e., the source and receptor are modeled as separated points of tissue in a vacuum). Analytical calculations were performed and compared with Monte Carlo simulation results.

The dose-rate constant for patient release is the sum of kernels for: (1) primary photon emissions, Δ_{pr}^{γ}; (2) bremsstrahlung photons due to electron emissions from internal conversion and Auger processes, Δ_{pr}^{e}; and (3) bremsstrahlung photons due to positron and negatron decay emissions, Δ_{pr}^{β}. Thus,

$$\Delta_{pr} = \Delta_{pr}^{\gamma} + \Delta_{pr}^{e} + \Delta_{pr}^{\beta}. \qquad \text{Equation [2-1]}$$

Compared to primary photon emissions, bremsstrahlung contributions tend to be insignificant unless the radionuclide is a pure beta emitter (e.g., ^{32}P, ^{90}Y) or when gamma-ray and X-ray emissions are very weak (e.g., ^{89}Sr). Although bremsstrahlung emissions are governed by a small conversion fraction of primary energy, the relatively high activities administered in medical procedures coupled with substantial self-absorption of charged particles by the patient's body results in appreciable bremsstrahlung contributions to bystander dose for certain radionuclides.

For encapsulated sources (as a plaque or implant), bremsstrahlung production increases considerably due to more rapid radiative energy losses in higher atomic number (Z) materials compared to tissue and can also become an important factor for radiation protection. For implants, a spherical 0.05 mm radius titanium encapsulation is assumed. Bremsstrahlung generation is modeled in the titanium along with attenuation and buildup. Because self-attenuation by the radioactive source material is not included in the external dose calculations for bystander exposure and protection, a single geometric model (i.e., single source encapsulation) provides a reasonable representation for numerous encapsulated sources. Although higher energy electrons can penetrate the titanium encapsulation and lose some energy in tissue, bremsstrahlung for implants is assumed to be generated solely in the titanium encapsulation. Overall, implemented modeling assumptions provide additional fidelity for patient release compared to available generic information.

Primary Photon Dose-Rate Kernel

The dose-rate kernel in tissue for primary photon emissions resembles the traditional gamma-ray exposure constant in air and is defined for a given radionuclide as

$$\Delta_{pr}^{\gamma}\left[\frac{mSv\ m^2}{GBq\ h}\right] = k\sum_i\left(E_i \cdot Y_i \cdot \frac{\mu_{\mathrm{en}_i}}{\rho}\right), \qquad \text{Equation [2-2]}$$

where k is a unit conversion constant (including the point-kernel 4π geometry factor)

$$k = \frac{10^9\left[\frac{\mathrm{nt}}{\mathrm{s\ GBq}}\right]\cdot 3{,}600\left[\frac{\mathrm{s}}{\mathrm{h}}\right]\cdot 1.602\times 10^{-10}\left[\frac{\mathrm{mSv\ kg}}{\mathrm{MeV}}\right]}{4\pi} = 45.9\left[\frac{\mathrm{mSv\ kg\ nt}}{\mathrm{GBq\ MeV\ h}}\right]$$

and

E_i energy of photon *i* $\left[\frac{MeV}{\gamma}\right]$;

Y_i emission yield of photon *i* in units of photons per nuclear transition (nt) $\left[\frac{\gamma}{nt}\right]$; and

$\frac{\mu_{\mathrm{en}_i}}{\rho}$ mass energy absorption coefficient in tissue for photon *i* $\left[\frac{m^2}{kg}\right]$.

Calculations used nuclear decay data from the International Commission on Radiological Protection (ICRP) in Publication 38 (ICRP 1983) and Publication 107 (ICRP 2008). However, only results using the data from the ICRP-107 database appear in Revision 2 of Regulatory Guide 8.39 (NRC 2020). For external dose delivered to the bystander, radiation must escape the tissues of the patient, propagate through air and any intervening materials, and partially penetrate and deposit energy in the tissue of the bystander. To avoid non-physical overestimations of dose (e.g., without explicit modeling of self-shielding by patient tissues and air attenuation), dose-rate kernels for patient release are developed by applying a low-energy cutoff at 10 keV. This approach prevents unrealistically large contributions from very low-energy photons in the dose estimation for bystanders.

Mass energy absorption and attenuation coefficients for tissue and other materials are available from the National Institute of Standards and Technology (https://www.nist.gov/pml/x-ray-mass-attenuation-coefficients). In this work, those data have been transformed into various functional fits to simplify calculations. The functional form is generally a ratio of polynomials,

$$\frac{\mu(E)}{\rho} = \frac{\sum_{i=0}^{9}\alpha_i \ln(E)^i}{1+\sum_{i=1}^{8}\beta_j \ln(E)^j}, \qquad \text{Equation [2-3]}$$

where E is photon energy in units of MeV and $\frac{\mu}{\rho}$ is the photon mass attenuation coefficient in units of cm^2/g. Coefficients are specific to the absorbing or attenuating material, in this case, tissue and titanium (refer to **Table *2-1***).

Table 2-1 Coefficients for Equation [2-3] to determine mass energy absorption and mass attenuation for ICRU (1980) 4-component tissue (ρ = 1 g/cm^3) and titanium (ρ = 4.51 g/cm^3)

	Tissue		Titanium
Parameter	$\left(\frac{\mu}{\rho}\right)$	$\left(\frac{\mu_{en}}{\rho}\right)$	$\left(\frac{\mu}{\rho}\right)$
a_0	6.997×10^{-2}	3.067×10^{-2}	5.878×10^{-2}
a_1	-4.154×10^{-3}	1.285×10^{-2}	1.534×10^{-2}
a_2	-6.919×10^{-3}	-2.061×10^{-3}	-5.249×10^{-3}
a_3	1.211×10^{-3}	-1.057×10^{-3}	8.086×10^{-5}
a_4	5.208×10^{-4}	3.150×10^{-4}	1.380×10^{-3}
a_5	-5.960×10^{-5}	1.143×10^{-4}	5.270×10^{-5}
a_6	-2.192×10^{-5}	-1.011×10^{-5}	-7.361×10^{-5}
a_7	7.728×10^{-7}	-5.314×10^{-6}	-8.595×10^{-6}
a_8	7.706×10^{-7}		2.708×10^{-6}
a_9	-2.494×10^{-8}		5.278×10^{-7}
b_1	4.296×10^{-1}	5.972×10^{-1}	7.553×10^{-1}
b_2	3.627×10^{-2}	1.361×10^{-1}	1.739×10^{-1}
b_3	-5.849×10^{-3}	1.239×10^{-2}	-2.154×10^{-3}
b_4	-6.259×10^{-6}	-6.503×10^{-4}	-4.526×10^{-3}
b_5	3.312×10^{-4}	-3.667×10^{-4}	5.503×10^{-4}
b_6	4.527×10^{-5}	-5.769×10^{-5}	3.587×10^{-4}
b_7	1.844×10^{-6}	4.669×10^{-6}	4.769×10^{-5}
b_8		-1.555×10^{-7}	2.124×10^{-6}

Buildup factors, B, are based on a geometric progression approximation from work originally by Harima (1986) and Harima et al. (1986, 1991), and subsequently confirmed by others, most recently by Olarinoye et al. (2019). Buildup is a function of photon energy and the number of mean free paths in the attenuating medium (μx) according to the relationship,

$$B(E_0, \mu x) \approx \begin{cases} 1 + \dfrac{(b-1)(K^{\mu x}-1)}{(K-1)}, & K \neq 1 \\ 1 + (b-1)\mu x, & K = 1 \end{cases}$$

Equation [2-4]

where

$$K(\mu x) = c(\mu x)^a + d\frac{\tanh\left(\frac{\mu x}{\xi} - 2\right) - \tanh(-2)}{1 - \tanh(-2)}.$$

The parameter values of a, b, c, d, and ξ are provided in **Table *2-2*** for ICRU (1980) 4-component soft tissue and in iron (Z=26), for the simulation of titanium (Z=22). Encapsulations in stainless steel or iron would not result in a significant difference in bremsstrahlung or buildup from that of titanium. To demonstrate the importance of photon buildup at low energy, a plot of buildup factors for a nominal 20 mm of attenuating tissue is provided in **Figure *2-1*** as a function of incident photon energy. At photon energies less than about 200 keV, buildup effects are quite important to the estimation of photon flux emanating from the patient as an offsetting effect to calculated absorption within the 20-mm thickness of tissue. At energies greater than about 500 keV, buildup increases flux consistently by approximately 10-20% compared to formulations without buildup.

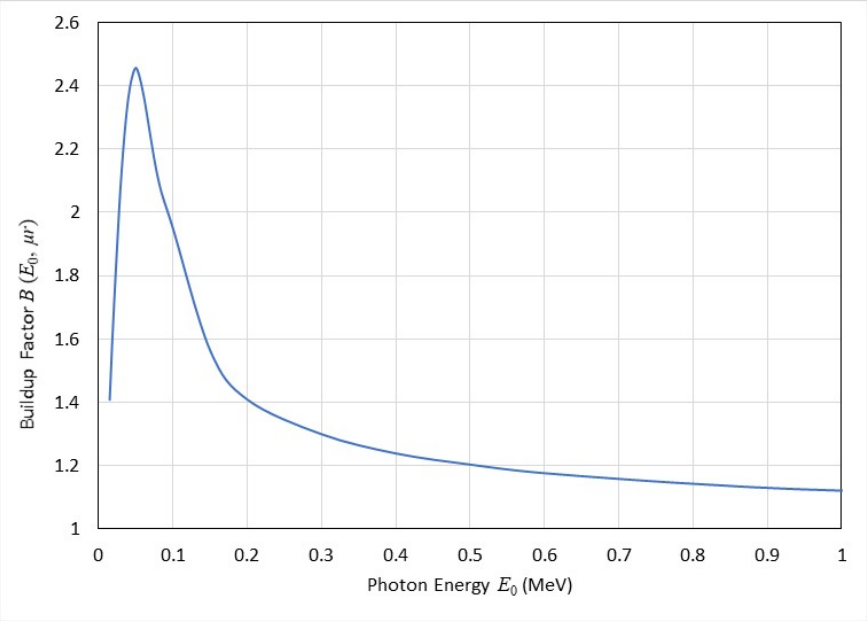

Figure 2-1 Absorption photon buildup factor in 20 mm of ICRU (1980) four-component tissue as a function of photon energy

Bremsstrahlung Dose-Rate Kernel

Bremsstrahlung photons are created as a result of the acceleration of electrically charged particles. These photons populate a continuous spectrum of energies between zero and the maximum kinetic energy of the slowing particles. Generally, bremsstrahlung production in radiation protection addresses the acceleration of light particles (electrons and positrons) in high-Z material because these particles more commonly approach relativistic speeds at comparatively low kinetic energies, which increasing the probability of bremsstrahlung production. A few radionuclides used in medical administrations have very low or no emission yield for photons and emit electrons substantial enough in energy to create bremsstrahlung photons that could result in appreciable contributions to bystander dose.

Many methods for estimating bremsstrahlung generation assume a bulk kinetic energy conversion to photons (Krane 1996; Zanzonico et al. 1999; NCRP 2006; Manjunatha and Rudraswamy 2009). Zanzonico et al. (1999), whose results have been propagated through the years by other researchers (Gulec and Siegel 2007; Manjunatha

and Rudraswamy 2009; Kim et al. 2010), approximated bremsstrahlung production using methods described in Sorenson and Phelps (1987) to generate a specific bremsstrahlung constant, Γ_{br}, analogous to the common gamma-ray exposure constant, Γ_g, and to the dose-rate kernel calculated in this work.

Table 2-2 Coefficients for the geometric progression approximation form of the photon buildup factor

Photon Energy (MeV)	Tissue[a]					Iron[b]				
	a	b	c	d	ξ	a	b	c	d	ξ
0.015	0.176	1.213	0.464	-0.0885	14.33	-0.554	1.004	1.561	0.3524	5.60
0.02	0.139	1.493	0.564	-0.0683	14.91	0.620	1.012	0.13	-0.6162	11.39
0.03	0.062	2.474	0.810	-0.0413	15.88	0.190	1.028	0.374	-0.3170	29.34
0.04	-0.038	3.752	1.210	0.0114	13.55	0.248	1.058	0.336	-0.1188	11.65
0.05	-0.101	4.831	1.568	0.0424	13.78	0.232	1.099	0.366	-0.1354	14.01
0.06	-0.144	5.335	1.864	0.0655	13.69	0.208	1.148	0.405	-0.1142	14.17
0.08	-0.186	5.322	2.216	0.0850	13.37	0.180	1.267	0.47	-0.0974	14.48
0.1	-0.187	5.104	2.272	0.0809	14.31	0.144	1.389	0.557	-0.0791	14.11
0.15	-0.206	3.963	2.425	0.0920	14.14	0.079	1.660	0.743	-0.0476	14.12
0.2	-0.210	3.423	2.431	0.0904	13.46	0.034	1.839	0.911	-0.0334	13.23
0.3	-0.179	2.958	2.134	0.0748	14.07	-0.009	1.973	1.095	-0.0183	11.86
0.4	-0.166	2.714	1.998	0.0701	13.99	-0.027	1.992	1.187	-0.0140	10.72
0.5	-0.142	2.525	1.812	0.0587	14.14	-0.046	1.957	1.261	0.0084	24.77
0.6	-0.132	2.401	1.725	0.0556	14.14	-0.049	1.932	1.274	0.0097	22.82
0.8	-0.111	2.233	1.573	0.0476	14.06	-0.050	1.884	1.27	0.0120	20.30
1	-0.094	2.118	1.464	0.0409	14.04	-0.048	1.841	1.25	0.0140	19.49
1.5	-0.062	1.985	1.286	0.0280	14.37	-0.040	1.750	1.197	0.0110	15.90
2	-0.042	1.876	1.183	0.0189	13.97	-0.028	1.703	1.143	0.0070	20.42
3	-0.014	1.734	1.060	0.0053	13.00	-0.005	1.627	1.059	-0.0132	11.99
4	0.004	1.642	0.987	-0.0062	20.78	0.005	1.553	1.026	-0.0191	12.93
5	0.017	1.569	0.939	-0.0118	14.05	0.012	1.483	1.009	-0.0258	13.12
6	0.028	1.521	0.905	-0.0167	13.44	0.023	1.442	0.98	-0.0355	13.37
8	0.036	1.432	0.877	-0.0257	14.43	0.029	1.354	0.974	-0.0424	13.65
10	0.040	1.367	0.864	-0.0214	13.27	0.042	1.297	0.949	-0.0561	13.97
15	0.047	1.274	0.841	-0.0317	15.16	0.049	1.199	0.957	-0.0594	14.37

[a] coefficients for absorption in ICRU four-component tissue (ICRU 1980; ANSI/ANS-6.4.3 1991)

[b] coefficients for air kerma and an iron medium (ANSI/ANS-6.4.3 1991)

As Zanzonico et al. (1999) explain, their bremsstrahlung constant is approximated from the probability of radiative energy loss $\left(P_{br}^{\beta}\right)_i$ and the mean energy of the resulting bremsstrahlung spectrum $\left(\bar{E}_{br}^{\beta}\right)_i$ generated by emissions of an energy distribution of electrons from decay of the *i*th beta-transition, where

$$\left(P_{br}^{\beta}\right)_i = \frac{Z_{eff}\left(E_{max}^{\beta}\right)_i}{3000} = 3.33x10^{-4}\, Z_{eff}\, \left(E_{max}^{\beta}\right)_i \quad \text{Equation [2-5]}$$

and

$$\left(\bar{E}_{br}^{\beta}\right)_i = 0.11\left(E_{max}^{\beta}\right)_i. \quad \text{Equation [2-6]}$$

Zanzonico et al. (1999) prepared a bremsstrahlung exposure constant as

$$\Gamma_{br} = \sum_{i=1}^{n}\left(f_{\beta}\right)_i \cdot \left(P_{br}^{\beta}\right)_i \cdot \Gamma_{br}\left(\bar{E}_{br}^{\beta}\right)_i, \quad \text{Equation [2-7]}$$

where $\left(f_{\beta}\right)_i$ is the emission frequency (# per transition) of beta-transition *i* and $\Gamma_{br}\left(\bar{E}_{br}^{\beta}\right)_i$ is the *i*th transition bremsstrahlung constant yielding bremsstrahlung photons of mean energy $\left(\bar{E}_{br}^{\beta}\right)_i$.

The *continuous slowing down approximation* (CSDA) is a more precise and calculationally-intensive approach that considers radiative stopping power and underlying energy transformation in a stepwise fashion as charged particles lose energy. CSDA provides a fundamental method of estimating charged particle energy loss (electrons in this case) as the particle travels through a given target material. As a single electron slows, it creates its own bremsstrahlung distribution. Therefore, electrons of various energies released from a singular source, all slowing at the same time and in the same general location, create a complex bremsstrahlung spectrum with photons emanating in all directions. In their fundamental description, Bethe and Heitler (1934) provide an expression for the number of emitted bremsstrahlung photons, $n(E_e, E_p)$, in a given energy interval from E_p to $E_p + dE_p$, when a monoenergetic electron of energy E_e is completely absorbed in a material of atomic density N (units of atoms per unit volume)

$$n(E_e, E_p) = N \cdot dE_p \int_{E_p}^{E_e} \frac{\sigma(E, E_p)}{(-dE/dx)} dE, \quad \text{Equation [2-8]}$$

where

E electron energy corresponding to bremsstrahlung energy E_p

$\sigma(E, E_p)$ bremsstrahlung production cross section, with units of area per unit energy, over all directions for photon energies between E_p and $E_p + dE_p$

$-dE/dx$ electron energy loss per unit path length (or stopping power) in the target (Shivaramu 1990).

For beta emitters, the probability distribution of emitted electron energies, $P_{\beta}(E)$, is continuous, and the bremsstrahlung photon spectrum, $S(E_p)$, provides the number of photons of energy E_p per unit energy interval per beta transition as

$$S(E_p) = \int_{E_p}^{E_{max}} P_\beta(E)\, n(E_e, E_p)\, dE. \qquad \text{Equation [2-9]}$$

For monoenergetic electrons of energy E_e normally incident on a thick target, Wyard (1952) showed that the number of bremsstrahlung photons of energy, E_p, per unit energy and per unit incident electron can be approximated by

$$N_{br}(E_e, E_p) = \frac{16 \cdot Y(E_e)}{5E_e}\left[\left(\frac{E_e}{E_p} - 1\right) - \frac{3}{4}\ln\left(\frac{E_e}{E_p}\right)\right], \qquad \text{Equation [2-10]}$$

where $Y(E_e)$ is the fraction of the incident electron kinetic energy, E_e, subsequently emitted as bremsstrahlung as shown in **Figure *2-2***.

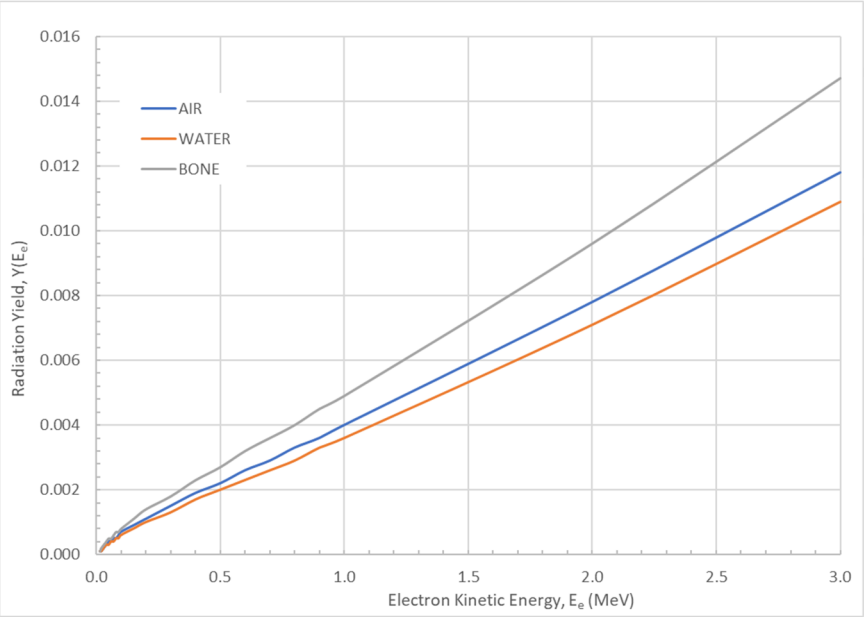

Figure 2-2 Bremsstrahlung yield as a function of electron kinetic energy in air, water, and bone (Johns & Cunningham, 1983)

The Wyard formulation is selected for development of the dose-rate constant for patient release with collective bremsstrahlung generation in tissue represented by isotropic emission from a single generation point. The differential photon fluence $\frac{d\psi}{dE_p}$ at a distance r from this emission point is

$$\frac{d\psi}{dE_p} = N_{br}(E_e, E_p)\frac{B(E_p, \mu x)\, e^{-\mu(E_p)x}}{4\pi r^2}, \qquad \text{Equation [2-11]}$$

where B represents photon buildup and x is the thickness of attenuating material. Buildup is handled in the same manner as detailed above for primary photons. For an electron-emitting radionuclide (i.e., conversion or Auger electrons) the total source strength over all monoenergetic electrons is

$$S_e = A \sum_i f_i,$$ Equation [2-12]

where A is the nuclide activity and f_i is the electron yield, number of electrons emitted per nuclear transition for the i^{th} transition. The photon dose rate at distance r therefore can be calculated (Attix 1986) as

$$\dot{D}(r) = \frac{A\,k}{r^2} \sum_i f_i \int_{E_{min}}^{E_{e_i}} E_p \, \frac{\mu_{en}}{\rho} \, N_{br}(E_{e_i}, E_p) \, B \, e^{-\mu x} \, dE_p,$$ Equation [2-13]

where, similar to Equation [2-2], k equals

$$k = \frac{10^9 \left[\frac{\text{nt}}{\text{s GBq}}\right] \cdot 3{,}600 \left[\frac{\text{s}}{\text{h}}\right] \cdot 1.602 \times 10^{-10} \left[\frac{\text{mSv kg}}{\text{MeV}}\right]}{4\pi} = 45.9 \left[\frac{\text{mSv kg nt}}{\text{GBq MeV h}}\right].$$

The bremsstrahlung dose-rate kernel for all monoenergetic electron emissions of a given radionuclide is therefore,

$$\Delta_{pr}^{e} \left[\frac{mSv\ m^2}{GBq\ h}\right] = k \sum_i f_i \int_{E_{min}}^{E_{e_i}} E_p \, \frac{\mu_{en}}{\rho} \, N_{br}^{e_i}(E_{e_i}, E_p) \, B \, e^{-\mu x} \, dE_p.$$ Equation [2-14]

For beta-particle emitters with a continuous distribution of electron energies $N_\beta(E_\text{e})$, the energy distribution of the resulting bremsstrahlung photons is

$$N_{br}^{\beta}(E_\text{p}) = \int_{E_\text{p}}^{E_\text{max}} N_\beta(E_\text{e}) \, N_\text{br}(E_\text{e}, E_\text{p}) \, dE_\text{e}.$$ Equation [2-15]

The energy-normalized bremsstrahlung spectrum reported by Shultis and Faw (2000) has a shape identical to that shown in **Figure *2-3*** of this document for ^{32}P. Similar to the reasoning for monoenergetic electron emissions above, and for each beta endpoint energy, i, the dose-rate kernel for bremsstrahlung photons due to positron and negatron decay emissions by a given radionuclide becomes,

$$\Delta_{pr}^{\beta} \left[\frac{mSv\ m^2}{GBq\ h}\right] = k \sum_i f_i \int_{E_{min}}^{E_{max_i}} E_p \, \frac{\mu_\text{en}}{\rho} \, N_{br}^{\beta_i}(E_\text{p}) \, B \, e^{-\mu x} \, dE_p.$$ Equation [2-16]

Shultis and Faw (2000) compared CSDA bremsstrahlung predictions for lead to results from the methods of Wyard (1952) and showed similar results for the bremsstrahlung photon distribution over a wide range of energies.

Bremsstrahlung dose-rate kernels calculated for single-transition beta emitters (ICRP 2008) over a range of maximum energies (39.4 keV to 2.86 MeV) are tabulated in

Table 2-3 *and plotted in* **Figure 2-4** *as a function of maximum beta energy. Bremsstrahlung results are presented for: (1) tissue with no attenuation (blue); (2) tissue with attenuation and buildup in 20 mm tissue (green); (3) titanium with attenuation and buildup in 0.05 mm titanium (light blue); and (4) titanium with attenuation and buildup in 0.05 mm titanium followed by attenuation and buildup in 20 mm tissue (red). Many radionuclides listed in*

Table *2-3* are not used in nuclear medicine and are not encapsulated, but their results show higher-Z material (titanium) effects on bremsstrahlung production over a broad range of electron energies. Radionuclides of interest to nuclear medicine are addressed later in this chapter.

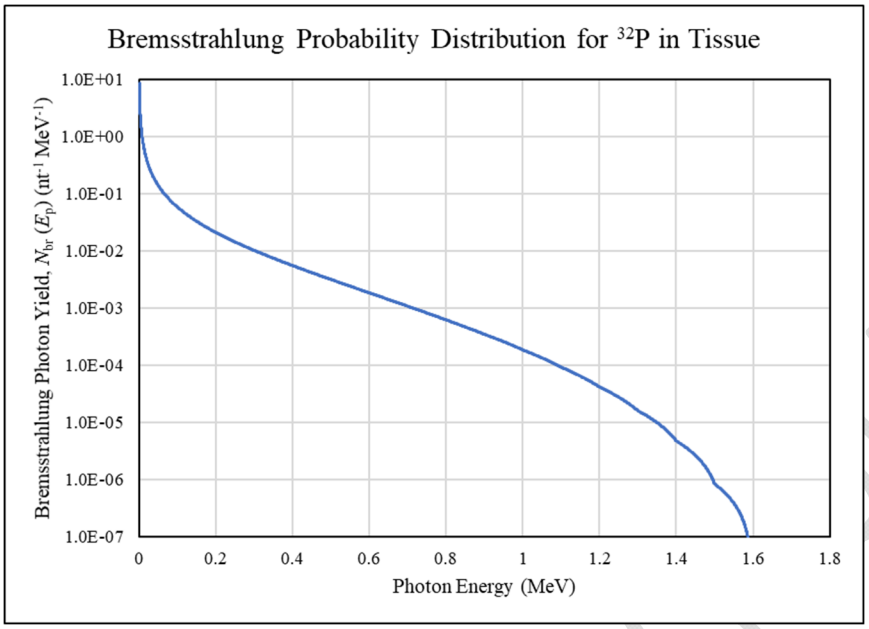

Figure 2-3 Bremsstrahlung photon spectrum calculated according to Equation [2-16] for ^{32}P in tissue

Table 2-3 Dose-rate kernels for bremsstrahlung in tissue and titanium for single beta transition radionuclides

Radionuclide	Max Energy (MeV)	None[a] Δ_{pr}^{β}	20-mm tissue[a] Δ_{pr}^{β}	0.05-mm Ti[a] Δ_{pr}^{β}	Ti + tissue[a] Δ_{pr}^{β}	Zanzonico[b] G_g
Ru-106	0.0393	2.12×10^{-6}	6.54×10^{-8}	1.88×10^{-6}	1.43×10^{-7}	
Zr-93	0.0615	1.03×10^{-5}	6.97×10^{-7}	1.14×10^{-5}	1.83×10^{-6}	
Ni-63	0.0669	8.70×10^{-6}	5.91×10^{-7}	9.64×10^{-6}	1.56×10^{-6}	
Sm-151[c]	0.0767	1.14×10^{-5}	8.85×10^{-7}	1.31×10^{-5}	2.40×10^{-6}	
Tm-171[c]	0.0963	1.71×10^{-5}	1.65×10^{-6}	2.11×10^{-5}	4.69×10^{-6}	
Bk-249	0.1239	2.74×10^{-5}	3.18×10^{-6}	3.58×10^{-5}	9.49×10^{-6}	
Os-191	0.1424	3.46×10^{-5}	4.43×10^{-6}	4.67×10^{-5}	1.34×10^{-5}	
Se-79	0.1509	5.51×10^{-5}	8.00×10^{-6}	7.76×10^{-5}	2.47×10^{-5}	
I-129	0.1544	5.16×10^{-5}	7.46×10^{-6}	7.26×10^{-5}	2.30×10^{-5}	
C-14	0.1564	5.02×10^{-5}	7.11×10^{-6}	7.00×10^{-5}	2.19×10^{-5}	
S-35	0.1671	4.96×10^{-5}	7.20×10^{-6}	6.97×10^{-5}	2.23×10^{-5}	3.02×10^{-5}
P-33	0.2484	8.87×10^{-5}	1.61×10^{-5}	1.33×10^{-4}	5.16×10^{-5}	1.78×10^{-5}
Ca-45	0.2567	8.99×10^{-5}	1.65×10^{-5}	1.35×10^{-4}	5.30×10^{-5}	1.85×10^{-5}
Sc-46	0.3570	1.39×10^{-4}	2.99×10^{-5}	2.19×10^{-4}	9.84×10^{-5}	
In-115	0.4959	1.95×10^{-4}	4.84×10^{-5}	3.21×10^{-4}	1.61×10^{-4}	
Sr-90	0.5460	2.55×10^{-4}	6.91×10^{-5}	4.30×10^{-4}	2.32×10^{-4}	
Pb-209	0.6443	2.57×10^{-4}	7.12×10^{-5}	4.37×10^{-4}	2.39×10^{-4}	
Zn-69	0.9060	4.34×10^{-4}	1.44×10^{-4}	7.83×10^{-4}	4.87×10^{-4}	
Pr-143	0.9338	4.25×10^{-4}	1.42×10^{-4}	7.67×10^{-4}	4.78×10^{-4}	2.97×10^{-5}
Bi-210	1.161	5.39×10^{-4}	1.97×10^{-4}	1.01×10^{-3}	6.64×10^{-4}	4.13×10^{-5}
Sr-89	1.495	8.62×10^{-4}	3.69×10^{-4}	1.71×10^{-3}	1.24×10^{-3}	8.48×10^{-5}
P-32	1.711	1.05×10^{-3}	4.73×10^{-4}	2.13×10^{-3}	1.58×10^{-3}	1.09×10^{-4}
Tl-209	1.825	1.00×10^{-3}	4.50×10^{-4}	2.03×10^{-3}	1.51×10^{-3}	
Y-90	2.280	1.56×10^{-3}	7.97×10^{-4}	3.34×10^{-3}	2.64×10^{-3}	1.52×10^{-4}
Al-28	2.863	2.26×10^{-3}	1.26×10^{-3}	5.03×10^{-3}	4.13×10^{-3}	

[a]all values presented in units of [mSv m^2 / GBq h]

[b]Zanzonico et al. 1999; values from their Table 1 converted by 0.027 [mSv m^2 mCi / R GBq cm^2]

[c]beta yield is 0.978 (^{151}Sm) and 0.991 (^{171}Tm); included here due to their maximum energy

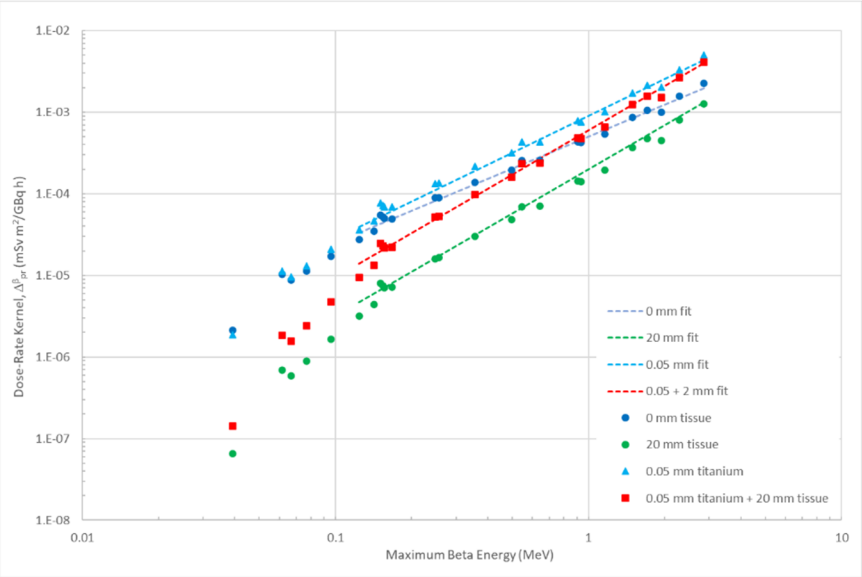

Figure 2-4 Dose-rate kernel for bremsstrahlung generated in tissue or titanium as a function of maximum beta energy for single-transition beta emitters listed in Table 2-3. Curve fitting is displayed for beta emitters with maximum energies exceeding 0.125 MeV

Figure *2-5* compares the dose-rate kernel for bremsstrahlung to the results of Zanzonico et al. (1999), which were calculated for exposure in air from beta-particles slowing in tissue. Dose-rate kernels for tissue generation and tissue absorption without attenuation and buildup are shown by blue circles; red squares denote radionuclide-specific exposure-rate constants from Zanzonico et al. (1999) with their generalization curve as a function of maximum electron energy shown by the dashed red line. The bremsstrahlung dose-rate kernels for patient release exhibit a monotonic increasing trend with maximum beta energy.

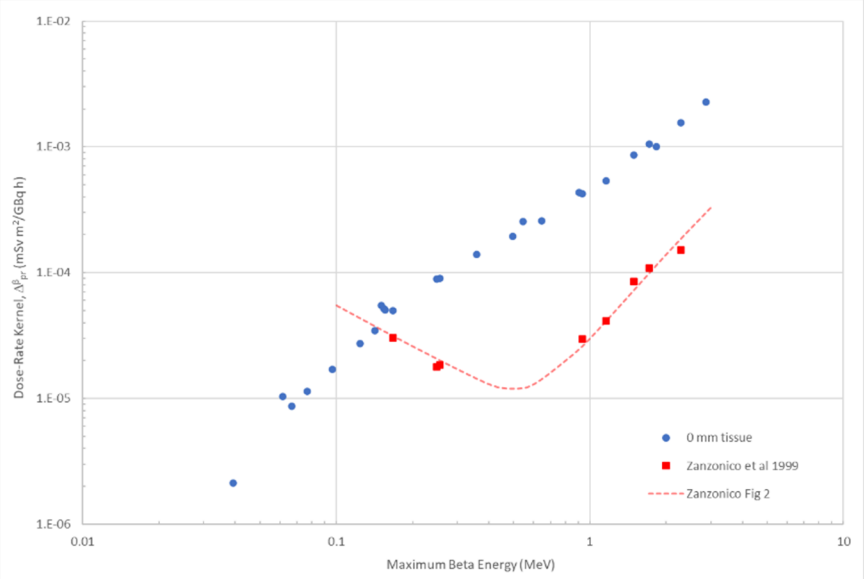

Figure 2-5 Comparison of the bremsstrahlung dose-rate kernel for tissue generation and tissue receptor without buildup and attenuation to the bremsstrahlung exposure-rate constant (Γ_g) from Zanzonico et al. (1999)

As shown in **Figure *2-6***, bremsstrahlung dose-rate kernels were also compared to Monte Carlo (MCNP6) simulation results using the F5 tally for photons with 20 mm of attenuating tissue. The dose-rate kernels for primary photons shown in **Figure *2-6***(A) compare very well with Monte Carlo simulation. In **Figure *2-6***(B) and (C), the comparison is very good except for the case of encapsulated sources (0.05 mm titanium) when the kernel calculation overestimates dose rate at high charged particle emission energies. Both figures demonstrate that the bremsstrahlung dose-rate kernel for patient release is overpredicted, increasingly so as the dose-rate kernel increases. This difference relates to our assumption and simplification of complete electron absorption in the titanium encapsulation with complete bremsstrahlung production in titanium for patient release calculations. The Monte Carlo simulation, however, allows electrons to deposit a fraction of their energy in titanium with a consistent fraction of bremsstrahlung production in titanium compared to tissue. As shown in **Figure *2-6***(C), differences associated with the simplifying assumption of complete bremsstrahlung production in titanium are greatest for high-energy electrons with ranges in excess of the encapsulation material thickness.

Although not implemented in the formulations for patient release, the bremsstrahlung dose-rate kernel for single beta-emitters with maximum energy greater than 125 keV can be approximated with a power function,

$$\Delta_{pr}^{\beta} \approx a\left(E_{\beta}^{max}\right)^{b}, \qquad \text{Equation [2-17]}$$

where the coefficients a and b are presented in **Table *2-4***. **Figure *2-4*** shows that the power functions fail at lower energies, most likely due to the 10-keV threshold applied to prevent overestimations in bystander dose for patient release scenarios. As the maximum beta-transition energy decreases, bremsstrahlung photons at energies less than 10 keV take on more importance relative to the total number of bremsstrahlung photons generated. From a patient release perspective, these low-energy photons lack the range in tissue to escape the patient and deliver dose to sensitive internal organs of the bystander. The bremsstrahlung dose-rate kernel for radionuclides with multiple beta-transition energy levels can be approximated with the equation above, but with less confidence.

Table 2-4 Power function coefficients to estimate patient release dose-rate kernels in four materials

Materials	a	b
No attenuation	0.0005	1.3
20 mm tissue	0.0002	1.8
0.05 mm Ti	0.0009	1.5
Ti + tissue	0.0006	1.8

Total Dose-Rate Kernel for Patient Release

Table 2-5 lists the dose-rate constants, Δ_{pr}, for 33 radionuclides and 4 implants using nuclear decay data from Publication 38 (ICRP 1983) and Publication 107 (ICRP 2008). Additional nuclides historically used in nuclear medicine are listed at the end of this chapter. All dose-rate constants including those for brachytherapy sources were assumed to originate as points, and dose was calculated to a tissue point at 1 meter. Values for the exposure rate constants from Revision 1 of Regulatory Guide 8.39 (NRC 2020; Table A-1) are included for comparison.

Dose-rate kernels specific to patient release calculated using the ICRP-107 (2008) database are presented in **Table *2-6*** alongside recent estimates of exposure rate in air without tissue attenuation by Smith and Stabin (2012) and Peplow (2020). Three nuclides in the list have vastly different values compared to Peplow (2020); these relate to constants based on primary photon emissions without consideration of bremsstrahlung.

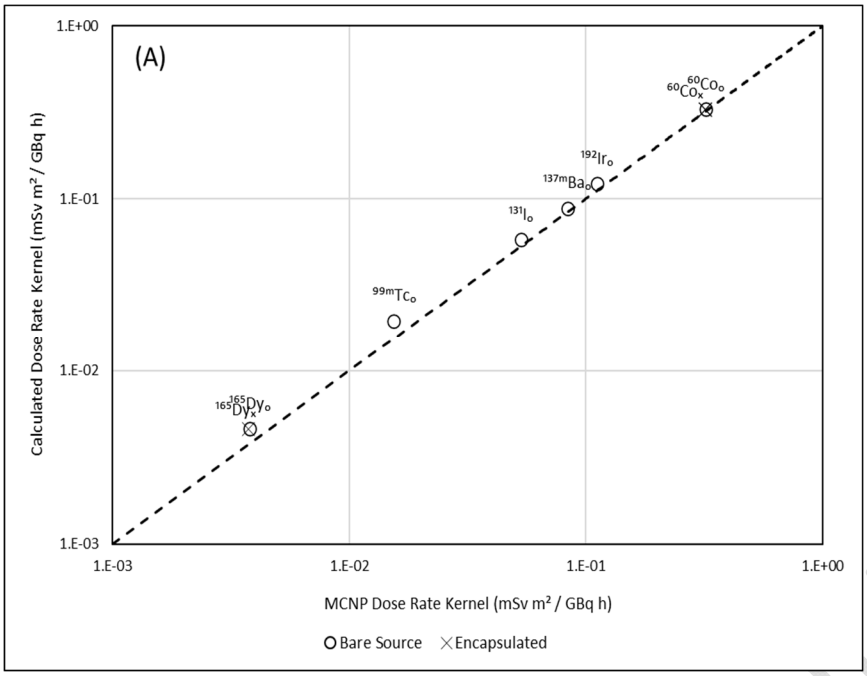

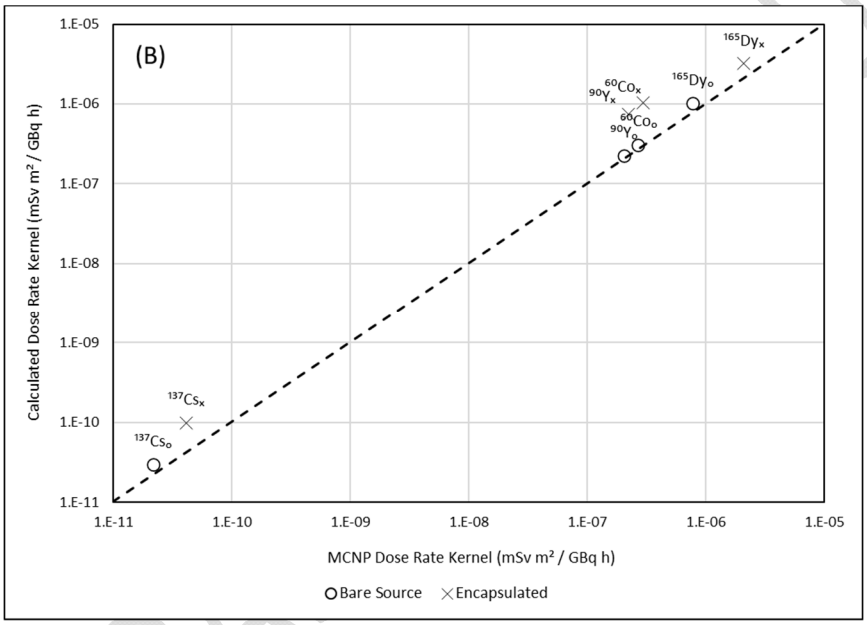

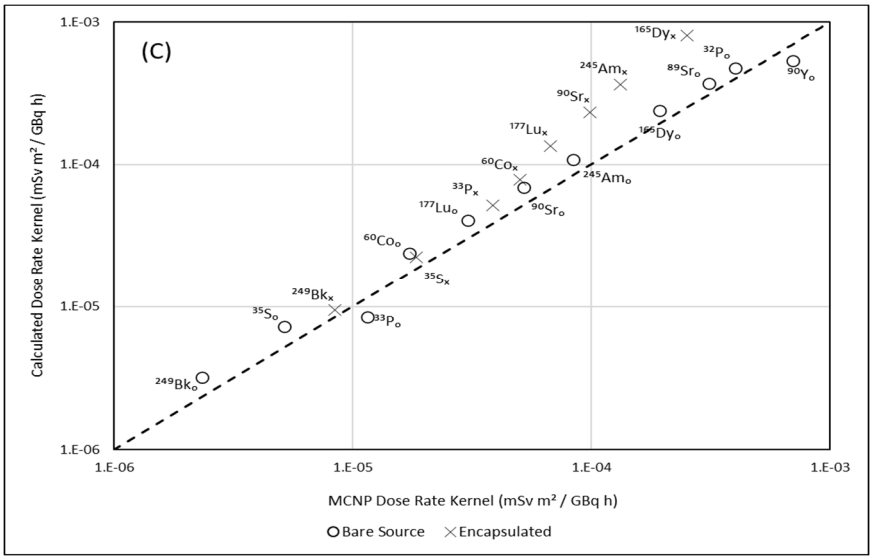

Figure 2-6 Comparison of dose-rate kernels for patient release with MCNP6 results for emissions of (A) primary photons, Δ_{pr}^{γ}, (B) monoenergetic electrons, Δ_{pr}^{e}, and (C) beta-particle distributions, Δ_{pr}^{β}. Radioactive sources are either bare (open circles) or encapsulated in 0.05 mm of titanium (X) with 20 mm of overlying tissue

Table 2-5 Photon dose-rate kernels compared to gamma-ray constants from NRC (2020)

Radionuclide	Half-Life (d)	Δ_{pr} ICRP-38 (1983) (mSv m^2 / GBq h)	Δ_{pr} ICRP-107 (2008) (mSv m^2 / GBq h)	RG 8.39, Rev 1 (NRC 2020) (mSv m^2 / GBq h) [a]
C-11	0.0142	0.154	0.154	
Cr-51	27.703	0.00461	0.00465	0.00432
Cs-131	9.689	0.0143	0.0144	
Cs-131 implant[b]	9.689	0.0129	0.0130	
Cu-64	0.5292	0.0284	0.0277	0.0324
Cu-67	2.576	0.0150	0.0150	0.0157
Er-169[c]	9.4	0.000122	0.000121	
F-18	0.0762	0.154	0.148	
Ga-67	3.261	0.0206	0.0207	0.0203
Ga-68	0.04702	0.143	0.143	
I-123	0.553	0.0387	0.0390	0.0435
I-124	4.176	0.165	0.167	
I-125	59.4	0.0328	0.0332	0.0383
I-125 eye plaque[b]	59.4	0.0287	0.0291	0.0300
I-131	8.0207	0.0574	0.0576	0.0594
In-111	2.8047	0.0794	0.0798	0.0867
Ir-192	73.827	0.125	0.125	
Ir-192 implant[b]	73.827	0.121	0.121	0.124
Kr-81m	0.000152	0.0387	0.0385	
Lu-177	6.647	0.00525	0.00527	
N-13	0.00692	0.154	0.154	
O-15	0.00141	0.154	0.154	
P-32[c]	14.263	0.00105	0.00105	
P-33[c]	25.4	0.0000890	0.0000887	
Pd-103	16.991	0.0304	0.0306	
Pd-103 implant[b]	16.991	0.0219	0.0220	0.0232
Ra-223	11.43	0.0444	0.0475	
Rb-82	0.000884	0.170	0.172	
Sm-153	1.938	0.0112	0.0115	0.0115
Sr-89[c]	50.53	0.000872	0.000875	
Sr-90[c]	10,508	0.000255	0.000255	
Tc-99m	0.2506	0.0194	0.0194	0.0204
Tl-201	3.038	0.0413	0.0405	0.0121
Xe-133	5.243	0.0124	0.0128	
Y-90[c]	2.67	0.00157	0.00157	
Yb-169	32.026	0.0445	0.0477	0.0494
Zr-89	3.267	0.208	0.207	

[a]units adjusted to be consistent with new dose-rate kernels

[b]implants and eye plaques are assumed to be encapsulated in 0.05 mm of titanium

[c]greater than 5% of Δ_{pr} due to bremsstrahlung production

Table 2-6 Photon dose-rate kernels compared to exposure constants in the recent literature

Radionuclide	Δ_{pr} ICRP-107 (2008) (mSv m^2 / GBq h)	Smith & Stabin (2012) (mSv m^2 / GBq h)	Peplow (2020) (mSv m^2 / GBq h)
C-11	0.154	0.158	0.144
Cr-51	0.00465	0.00481	0.00457
Cs-131	0.0144	0.0183	-
Cs-131 implant[a]	0.0130	-	-
Cu-64	0.0277	0.0284	0.0259
Cu-67	0.0150	0.0155	0.0166
Er-169[b]	0.000121	-	0.000000501
F-18	0.148	0.153	-
Ga-67	0.0207	0.0217	0.0225
Ga-68	0.143	0.147	0.133
I-123	0.0390	0.0481	0.0285
I-124	0.167	0.178	0.147
I-125	0.0332	0.0473	0.0125
I-125 eye plaque[a]	0.0291	-	-
I-131	0.0576	0.0594	0.0548
In-111	0.0798	0.0934	0.0615
Ir-192	0.125	0.124	0.117
Ir-192 implant[a]	0.121	-	-
Kr-81m	0.0385	0.0178	0.0190
Lu-177	0.00527	0.00489	0.00518
N-13	0.154	0.158	0.144
O-15	0.154	0.158	0.144
P-32[b]	0.00105	-	-
P-33[b]	0.0000887	-	-
Pd-103	0.0306	0.0381	0.00458
Pd-103 implant[a]	0.0220	-	-
Ra-223	0.0475	0.0208	0.0211
Rb-82	0.172	0.171	0.155
Sm-153	0.0115	0.0130	0.0119
Sr-89[b]	0.000875	-	0.0000114
Sr-90[b]	0.000255	-	-
Tc-99m	0.0194	0.0215	0.0184
Tl-201	0.0405	0.0122	0.0149
Xe-133	0.0128	0.0153	0.00950
Y-90[b]	0.00157	-	0.000000362
Yb-169	0.0477	0.0524	0.0545
Zr-89	0.207	0.178	0.155

[a]implants and eye plaques are assumed to be encapsulated in 0.05 mm of titanium

[b]greater than 5% of Δ_{pr} due to bremsstrahlung production

Basic Activity Threshold

Consistent with the total dose-rate kernel for a point geometry, the radionuclide-specific *basic activity thresholds* for patient release, Q_{rel}, and issuing dose-minimizing instructions, Q_{ins}, are defined at a distance of 1 meter. Activity thresholds calculated here differ from those in Tables 2-1 and 2-2 of previous versions of Regulatory Guide 8.39, Revision 1 (NRC 2020) and Revision 0 (NRC 1997a), because the formulation intentionally does not consider occupancy at this stage. These thresholds for radionuclide activity are conservative because a bystander is assumed to be continuously present at a distance of 1 meter from the patient for all radioactive decays in the original administration without reductions due to natural biological clearance of radiopharmaceutical from the patient, periods of time when the bystander is not near the patient, separation distances greater than 1 m, and tissue attenuation and buildup effects that may result in lower dose rates. Basic thresholds are calculated for the dose limits of 5 mSv (basic activity threshold for patient release, Q_{rel}) and 1 mSv (basic activity threshold for issuing instructions, Q_{ins}).

The basic activity threshold originates from the calculation of time-integrated dose, $\widetilde{D}(\infty)$, which represents the maximum potential dose to a bystander from all radioactive disintegrations in a patient receiving an administration of radioactive material, A_0. This maximum potential time-integrated dose is calculated as

$$\widetilde{D}(\infty) = \frac{1.44 \cdot T_r \cdot A_0 \cdot \Delta_{pr}}{r^2}, \qquad \text{Equation [2-18]}$$

where

T_r radiological (physical) half-life of the administered nuclide [h];

A_0 administered activity [GBq];

Δ_{pr} dose-rate kernel specific to patient release $\left[\frac{mSv\ m^2}{GBq\ h}\right]$; and

r source-to-bystander distance [m].

This equation can be rearranged by replacing the administered activity with the activity threshold, Q_{rel} or Q_{ins}, for respective dose limits of 5 mSv for patient release and 1 mSv for issuing instructions. Assuming exposure at the standard distance of 1 m for close contact, the conservative basic activity threshold for patient release becomes

$$Q_{rel} = \frac{5\ [mSv] \cdot 1\ [m^2]}{\Delta_{pr} \cdot 1.44 \cdot T_r}. \qquad \text{Equation [2-19]}$$

A dose equivalent of 5 mSv is inferred for a hypothetical bystander who is continuously present at a distance of 1 meter from a patient administered an activity equaling Q_{rel} without biological losses. The basic activity threshold for patient release is convenient because it is highly conservative and patients receiving activities less than Q_{rel} can be released by the licensee without further dosimetric evaluation. The assessment also considers when dose-minimizing instructions should be issued to the patient, and Q_{ins} is calculated in similar fashion with

$$Q_{ins} = \frac{1\ [mSv] \cdot 1\ [m^2]}{\Delta_{pr} \cdot 1.44 \cdot T_r}. \qquad \text{Equation [2-20]}$$

Likewise, the basic activity threshold for issuing instructions is convenient because patients receiving activities less than Q_{ins} can be released by the licensee without dose-minimizing instructions.

Table ***2-7*** provides basic activity thresholds for patient release (5 mSv) and dose-minimizing instruction (1 mSv). Basic activity thresholds involve integration from the time of administration (t = 0) to the time of radionuclide depletion (infinity), without factors for more realistic exposure considerations. Basic activity thresholds represent the most conservative calculations for patient release. In other words, at a defined distance between the patient and bystander of 1 meter, the basic activity thresholds exemplify theoretical maximums for demonstrating compliance (i.e., the minimum activity corresponding to a maximum limiting dose).

If desired, the maximum integrated dose to a bystander, $\widetilde{D}(\infty)$, can be estimated from an administration, A_0, other than the threshold with a simple ratio calculation as

$$\widetilde{D}(\infty) = \frac{A_0}{Q_{rel}}\ 5\ [mSv]. \qquad \text{Equation [2-21]}$$

Most implants and eye plaques do not remain in place for their full radiological lifetime, and encapsulated implants do not experience biological loss. Nevertheless, tabulated basic activity and measurement thresholds assume infinite time-integration. Therefore, for implants that remain in the body for a limited time, the infinite time-integration factor for radiological decay $\left(\frac{1}{\lambda_r} = 1.44\ T_r\right)$ would be inappropriate. When the implantation time is known and reliable from the perspective of medical follow-up to assure regulatory compliance, the factor

$$\frac{1 - e^{-\lambda_r t}}{\lambda_r} = 1.44\ T_r\left(1 - e^{-\lambda_r t}\right) \qquad \text{Equation [2-22]}$$

can be used for calculating basic thresholds or time-integrated doses, where t is the time between implant administration and removal. A patient release determination based on implanted activity is not necessary for patients who remain in the medical facility for the full duration of the implant procedure and are released without the implant.

Table 2-7 Basic activity thresholds for bystander exposures at 1 meter

Radionuclide	Patient Release Threshold, Q_{rel} (GBq)	Patient Release Threshold, Q_{rel} (mCi)	Instruction Threshold, Q_{ins} (GBq)	Instruction Threshold, Q_{ins} (mCi)
C-11	68	1,800	14	380
Cr-51	1.1	30	0.23	6.2
Cs-131	1.1	30	0.21	5.7
Cs-131 implant[a]	1.1	30	0.23	6.2
Cu-64	9.7	260	1.9	51
Cu-67	3.7	100	0.75	20
Er-169[b]	130	3,500	26	700
F-18	13	350	2.5	68
Ga-67	2.1	57	0.42	11
Ga-68	22	590	4.4	120
I-123	6.7	180	1.3	35
I-124	0.20	5.4	0.041	1.1
I-125	0.074	2.0	0.015	0.41
I-125 eye plaque[a]	0.084	2.3	0.017	0.46
I-131	0.32	8.6	0.063	1.7
In-111	0.64	17	0.13	3.5
Ir-192	0.015	0.41	0.0030	0.081
Ir-192 implant[a]	0.016	0.43	0.0033	0.089
Kr-81m	25,000	680,000	5,000	140,000
Lu-177	4.1	110	0.82	22
N-13	140	3,800	28	760
O-15	680	18,000	140	3,800
P-32[b]	9.2	250	1.8	49
P-33[b]	64	1,700	13	350
Pd-103	0.27	7.3	0.055	1.5
Pd-103 implant[a]	0.39	11	0.077	2.1
Ra-223	0.27	7.3	0.054	1.5
Rb-82	960	26,000	190	5,100
Sm-153	6.8	180	1.4	38
Sr-89[b]	3.3	89	0.66	18
Sr-90[b]	0.055	1.5	0.011	0.30
Tc-99m	30	810	6.1	160
Tl-201	1.2	32	0.23	6.2
Xe-133	2.1	57	0.42	11
Y-90[b]	34	920	6.8	180
Yb-169	0.094	2.5	0.019	0.51
Zr-89	0.21	5.7	0.042	1.1

[a]implants and eye plaques are assumed to be encapsulated in 0.05 mm of titanium
[b]greater than 5% of Δ_{pr} due to bremsstrahlung production

Basic Measurement Threshold

Measurement thresholds facilitate patient release decision-making according to a measured dose rate at a given distance from the patient. For the standard measurement distance of 1 meter, the *basic measurement threshold* for patient release, M_{rel}, is related to the dose-rate constant and basic activity threshold

$$M_{rel} = \frac{\Delta_{pr} \cdot Q_{rel}}{1\ [m^2]}. \qquad \text{Equation [2-23]}$$

By inspection, the basic measurement threshold is also equal to

$$M_{rel} = \frac{5\ [mSv]}{1.44 \cdot T_r\ [h]} \qquad \text{Equation [2-24]}$$

or

$$M_{ins} = \frac{1\ [mSv]}{1.44 \cdot T_r\ [h]}$$

where the factor of $1.44 \cdot T_r$ accounts for the time-integration of activity. For basic screening, the dose rate measured at a distance of 1 m from the patient after radionuclide administration can be compared to the measurement thresholds. When a bystander is assumed to be continuously present until the radionuclide in the patient is entirely depleted due to radioactive decay, the basic measurement threshold is the dose rate that yields a time-integrated dose of either 5 or 1 mSv. Because theoretical dose accumulation continues until the radionuclide is completely depleted, exposure durations for long-lived radionuclides are much longer than for short-lived radionuclides. Intrinsic to the kinetics of decay and time-integrated dose shown in Equation [2-24], radiological half-life becomes the fundamental radionuclide-dependent parameter for converting time-integrated dose into the basic measurement threshold, M_0.

Table ***2-8*** provides basic measurement thresholds for patient release (5 mSv) and issuing instructions (1 mSv). Due to assumptions for continuous bystander presence and dose accumulation until complete radioactive decay, some basic measurement thresholds are associated with very low dose rates at the time of measurement. When measurement thresholds for some radionuclides are associated with dose rate contributions less than typical ambient dose rates from natural background, they become difficult to measure and, thus, have less practical value.

As previously described, external exposure formulations for patient release account for primary photon emissions and bremsstrahlung production from the administered radionuclide in the patient's body. Kim et al. (2010) noted the absence of dose-rate guidelines for determining patient release following the administration of ^{90}Y. International guidance (ARPANSA 2002; IAEA 2009) states a measured exposure-rate limit of 2.5 mR/h (25 µSv/h) for patient release.

Table ***2-8*** indicates ^{90}Y measurement thresholds of 54 and 11 µSv/h for dose limits of 5 and 1 mSv, respectively. These measurement thresholds, therefore, are reasonably consistent with international guidance and associated perspectives. Additionally, the package insert for ^{90}Y microspheres from Sirtex Medical (2020) provides an average measured dose rate (using TLDs) of 1.5 µSv/h at 1 meter from the abdomen of patients containing about 2.0 GBq of ^{90}Y. Bremsstrahlung calculations in this chapter yield an estimate of 1.6 µSv/h for similar exposure conditions.

Table 2-8 Basic measurement thresholds for bystander exposures at 1 meter

Radionuclide	Patient Release Threshold, M_{rel} (mSv/h)	(mrem/h)	Instruction Threshold, M_{ins} (mSv/h)	(mrem/h)
C-11	10	1,000	2.1	210
Cr-51	0.0051	0.51	0.0011	0.11
Cs-131	0.015	1.5	0.0029	0.29
Cs-131 implant[a]	0.014	1.4	0.0030	0.30
Cu-64	0.27	27	0.053	5.3
Cu-67	0.056	5.6	0.011	1.1
Er-169[b]	0.016	1.6	0.0031	0.31
F-18	2.0	200	0.38	38
Ga-67	0.044	4.4	0.0088	0.88
Ga-68	3.1	310	0.62	62
I-123	0.26	26	0.051	5.1
I-124	0.034	3.4	0.0070	0.70
I-125	0.0024	0.24	0.00050	0.050
I-125 eye plaque[a]	0.0024	0.24	0.00049	0.049
I-131	0.018	1.8	0.0036	0.36
In-111	0.051	5.1	0.010	1.0
Ir-192	0.0020	0.20	0.00039	0.039
Ir-192 implant[a]	0.0019	0.19	0.00040	0.040
Kr-81m	950	95,000	190	19,000
Lu-177	0.022	2.2	0.0043	0.43
N-13	21	2,100	4.2	420
O-15	100	10,000	21	2,100
P-32[b]	0.010	1.0	0.0020	0.20
P-33[b]	0.0057	0.57	0.0012	0.12
Pd-103	0.0084	0.84	0.0017	0.17
Pd-103 implant[a]	0.0086	0.86	0.0017	0.17
Ra-223	0.013	1.3	0.0025	0.25
Rb-82	160	16,000	32	3,200
Sm-153	0.075	7.5	0.015	1.5
Sr-89[b]	0.0029	0.29	0.00057	0.057
Sr-90[b]	0.000014	0.0014	0.0000028	0.00028
Tc-99m	0.57	57	0.12	12
Tl-201	0.049	4.9	0.0094	0.94
Xe-133	0.027	2.7	0.0055	0.55
Y-90[b]	0.054	5.4	0.011	1.1

Radionuclide	Patient Release Threshold, M_{rel} (mSv/h)	(mrem/h)	Instruction Threshold, M_{ins} (mSv/h)	(mrem/h)
Yb-169	0.0045	0.45	0.00091	0.091
Zr-89	0.044	4.4	0.0088	0.88

[a]implants and eye plaques are assumed to be encapsulated in 0.05 mm of titanium
[b]greater than 5% of Δ_{pr} due to bremsstrahlung production

Supplemental Material for Basic Thresholds

Table *2-9*, **Table *2-10***, **Table *2-11***, and **Table *2-12*** present information for additional radionuclides. These radionuclides were either historically used in nuclear medicine or listed in Regulatory Guide 8.39, Revision 1 (NRC 2020) and not included in the main tabulations above.

Table 2-9 Additional photon dose-rate kernels compared to gamma-ray exposure constants in NRC (2020)

Radionuclide	Half-Life (d)	Δ_{pr} ICRP-38 (1983) (mSv m^2 / GBq h)	Δ_{pr} ICRP-107 (2008) (mSv m^2 / GBq h)	RG 8.39, Rev 1 (NRC 2020) Exposure constant[a] (mSv m^2 / GBq h)
Ag-111	7.45	0.00440	0.00442	0.00405
At-211	0.3006	0.0287	0.0288	
Au-198	2.696	0.0618	0.0615	0.0621
Bi-213	0.0317	0.0225	0.0218	
C-14[b]	2,080,000	0.00000502	0.00000502	
Dy-165	0.09725	0.00455	0.00464	
Ho-166[b]	1.117	0.00497	0.00507	0.00540
Re-186	3.7183	0.00603	0.00631	0.00702
Re-188[b]	0.7085	0.0121	0.0127	
Ru-106[b]	373.59	0.00000212	0.00000212	
Ru-106[b] implant[c]	373.59	0.00000188	0.00000188	0.0151
Sc-47	3.3492	0.0140	0.0140	0.0540
Se-75	119.78	0.155	0.153	0.0400
Sn-117m	13.76	0.0363	0.0364	
Xe-127	36.41	0.0534	0.0535	

[a]units adjusted to be consistent with new dose-rate kernels
[b]greater than 5% of Δ_{pr} due to bremsstrahlung production
[c]implants are assumed to be encapsulated in 0.05 mm of titanium

Table 2-10 Additional photon dose-rate kernels compared to exposure rate constants in recent literature

Radionuclide	Δ_{pr} ICRP-107 (2008) (mSv m^2 / GBq h)	Smith/Stabin (2012) (mSv m^2 / GBq h)	Peplow (2020) (mSv m^2 / GBq h)
Ag-111	0.00442	0.00405	0.00381
At-211	0.0288	0.00578	0.00591
Au-198	0.0615	0.0621	0.0576
Bi-213	0.0218	0.0197	0.0182
C-14	0.00000502	-	-
Dy-165	0.00464	0.00427	0.00407
Ho-166[a]	0.00507	0.00432	0.00417
Re-186	0.00631	0.00278	0.00318
Re-188[a]	0.0127	0.00853	0.00849
Ru-106[a]	0.00000212	-	-
Ru-106[a] implant[b]	0.00000188	-	-
Sc-47	0.0140	0.0144	0.0155
Se-75	0.153	0.0548	0.0564
Sn-117m	0.0364	0.0456	0.0254
Xe-127	0.0535	0.0616	0.0442

[a]greater than 5% of Δ_{pr} due to bremsstrahlung production

[b]implants are assumed to be encapsulated in 0.05 mm of titanium

Table 2-11 Additional basic activity thresholds for bystander exposures at 1 meter

Radionuclide	Release Threshold, Q_{rel}		Instruction Threshold, Q_{ins}	
	(GBq)	(mCi)	(GBq)	(mCi)
Ag-111	4.4	120	0.88	24
At-211	17	460	3.3	89
Au-198	0.88	24	0.18	4.9
Bi-213	210	5,700	41	1,100
C-14[b]	0.0014	0.038	0.00028	0.0076
Dy-165	320	8,600	65	1,800
Ho-166[a]	26	700	5.2	140
Re-186	6.2	170	1.2	32
Re-188[a]	16	430	3.1	84
Ru-106[a]	180	4,900	37	1,000
Ru-106[a] implant[b]	200	5,400	550	15,000
Sc-47	3.1	84	0.62	17
Se-75	0.0080	0.22	0.0016	0.043
Sn-117m	0.29	7.8	0.058	1.6
Xe-127	0.073	2.0	0.015	0.41

[a]greater than 5% of Δ_{pr} due to bremsstrahlung production
[b]implants are assumed to be encapsulated in 0.05 mm of titanium

Table 2-12 Additional basic measurement thresholds for bystander exposures at 1 meter

Radionuclide	Release Threshold, M_{rel}		Instruction Threshold, M_{ins}	
	(mSv/h)	(mrem/h)	(mSv/h)	(mrem/h)
Ag-111	0.019	1.9	0.0039	0.39
At-211	0.49	49	0.096	9.6
Au-198	0.054	5.4	0.011	1.1
Bi-213	4.6	460	0.90	90
C-14[b]	0.000000070	0.0000070	0.000000014	0.0000014
Dy-165	1.5	150	0.30	30
Ho-166[a]	0.13	13	0.026	2.6
Re-186	0.039	3.9	0.0076	0.76
Re-188[a]	0.21	21	0.040	4.0
Ru-106[a]	0.00038	0.038	0.000078	0.0078
Ru-106[a] implant[b]	0.00038	0.038	0.000077	0.0077
Sc-47	0.043	4.3	0.0087	0.87
Se-75	0.0012	0.12	0.00024	0.024
Sn-117m	0.010	1.0	0.0021	0.21
Xe-127	0.0039	0.39	0.00081	0.081

[a]greater than 5% of Δ_{pr} due to bremsstrahlung production
[b]implants are assumed to be encapsulated in 0.05 mm of titanium

3. INTERNAL DOSE ASSESSMENT

Regulatory Guide 8.39 Rev 1 (2020) addresses potential contributions to total effective dose equivalent (TEDE) from the ingestion/inhalation of iodine-131 by the maximum bystander. The review in the regulatory guide provides an estimate of the maximum likely committed effective dose equivalent (CEDE) from internal exposure by applying an assumed intake fraction of $1x10^{-5}$ as the fraction of administered activity that could be taken in by the maximum bystander. This factor considers a common rule-of-thumb supported by intake data (Buchanan and Brindle 1971; Jacobson et al. 1978; Brodsky 1981) combined with a safety factor of 10 and is assumed to account for the most highly exposed individual while adding a degree of conservatism to the CEDE dose calculation. The potential intake of ^{131}I and its subsequent contribution to CEDE is shown to be insignificant compared with the external dose potential.

To further ensure that members of the public are protected by 10 CFR 35.75, the potential contributions to total effective dose equivalent from internally deposited lutetium-177 is considered. Patients administered ^{177}Lu are typically held for 4-5 hours after administration (Nelson and Sheetz 2019), but then can be released under 10 CFR 35.75 with instructions on how to minimize dose to others. The assessment that follows addresses whether there is the potential for significant internal dose to others from patients released after medical administration of ^{177}Lu.

The Regulatory Guide 8.39 Rev 1 (NRC 2020) states that, "… the [internal] dose from intake by other individuals is expected to be small for most radiopharmaceuticals (less than a few percent) relative to the external gamma-ray dose." Given the high administration activity of 7.4 GBq of ^{177}Lu-dotatate (AAA 2019) and the reported contamination detected in the bathrooms used by ^{177}Lu patients (Calais and Turner 2014; Nelson and Sheetz 2019), the possibility for the spread of ^{177}Lu contamination exists. Because of this potential, a conservative internal pathway analysis was conducted to determine whether the radiation dose from an internal intake of ^{177}Lu was greater than a "few percent" of the projected external dose to the maximum bystander.

Since a large fraction of activity (about 50%) is lost within the first few hours after administration through urination (Nelson and Sheetz 2019; Calais and Turner 2014), a major pathway for the potential uptake of ^{177}Lu intake is likely via this route. The literature indicates a common theme that urine contamination in the bathroom can be problematic. Because ^{177}Lu is present in the sweat and saliva of patients (Nelson and Sheetz 2019), there also exists additional pathways for uptake by others namely kissing, hugging, and the potential for activity transfer through open wounds. This assessment looks at each of these pathways to determine its significance compared to the expected external effective dose equivalent. Additionally, contamination of ^{177}Lu with ^{177m}Lu is possible, therefore internal and external dose from that nuclide will be assessed as well to determine its relative contribution and whether it is a nuclide of concern.

External Bystander Dosimetry

The calculated ^{177}Lu activity threshold for instruction (i.e., 1 mSv) is 0.82 GBq (refer to

Table *2-7*), meaning that with an administration of 7.4 GBq the maximum conceivable (i.e., highly conservative) bystander dose is 9.0 mSv.

$$D = \frac{7.4\ [GBq]}{0.82\ [GBq]} \cdot 1\ [mSv] = 9.0\ [mSv]$$ Equation [3-1]

This estimate, however, assumes 100% occupancy, point/point geometry, no biological loss, and no attenuating tissue. With patient-specific modifiers (F_B = 0.5; F_O = 0.6; F_A = 0.8; F_G = 0.8; see Chapter 4; only assumed for this example), a reasonably conservative patient-specific activity threshold of 4.3 GBq can be calculated, resulting in a more realistic dose to the maximum bystander of about 1.7 mSv from external exposure to the ^{177}Lu patient.

$$D = \frac{7.4\ [GBq]}{4.3\ [GBq]} \cdot 1\ [mSv] = 1.7\ [mSv]$$ Equation [3-2]

Therefore, if a conservative estimate of internal dose to the maximum bystander is less than an assessment level of about 50 µSv (i.e., 3%), the test of "less than a few percent" is met, and routine internal dosimetry can be deemed unnecessary.

Contributions from ^{177m}Lu. If the supply of ^{177}Lu is obtained by the neutron activation of ^{176}Lu, the potential for long-lived ^{177m}Lu contamination exists. Lutetium-177 dotatate is produced by this method (Calais and Turner 2019; Webb 2021). The contamination of ^{177m}Lu at the end of generation is reported to be about 0.05% (atom %) of ^{177}Lu (Calais and Turner 2019). Thus, for an administration of 7.4 GBq of ^{177}Lu-dotatate, approximately 150 kBq of ^{177m}Lu is produced.

$$A_m = \frac{T}{T_m} A\ (0.05\%) = \frac{6.7\ [d]}{161\ [d]} 7.4x10^6\ [kBq]\ (0.0005) = 154\ kB$$ Equation [3-3]

The external dose-rate constant for ^{177}Lu is 0.00527 (Table 2-6) and the constant for ^{177m}Lu (calculated in the same manner as above) is 0.147, both in units of [mSv m^2 GBq^{-1} h^{-1}]. The external dose rate at 1 meter on administration of 7.4 GBq is 39 µSv/h and 0.023 µSv/h, respectively, for the two nuclides. Therefore, at administration, the contribution from ^{177m}Lu contamination to external dose is insignificant at a factor of about 1,700 times less than that from ^{177}Lu. At two months post-administration (i.e., 60 days) the dose-rate contribution from ^{177m}Lu has increased, to a factor that is now only 4.4 times less than the dose rate from ^{177}Lu, but still considered insignificant at 0.018 µSv/h.

Internal Pathway Analysis

Internal dose pathways of potential significance are identified as the unwitting intake of ^{177}Lu (and possibly ^{177m}Lu) by exposure to contamination due to urine, sweat, and saliva. The likelihood (probability) of each pathway is not estimated, rather reasonably conservative transfer fractions are provided to result in a conservative estimate of intake activity. The internal dose coefficient for the ingestion of free ^{177}Lu is 530 mSv/GBq and the dose coefficient for ^{177m}Lu is 1,700 mSv/GBq (ICRP 1994). The dose coefficient for the contaminant (^{177m}Lu) is three times larger, but the associated activity is thousands of times smaller. The contaminant nuclide is insignificant from an internal dose perspective and is not considered further.

It is unclear as to chemical form of the lutetium when ingested/absorbed/etc. by the bystander. Collections of dose coefficients specific to radiopharmaceuticals (ICRP 1987; ICRP 2008a; ICRP 2015) do not list factors for any pharmaceutical containing ^{177}Lu. This assessment assumes that when the lutetium is ingested by the bystander,

it is dissociated from the pharmaceutical. If, however introduced directly into the blood stream (open wound), an EDE dose coefficient (86 mSv/GBq) derived from the manufacturer's data for ^{177}Lu-dotatate is used (AAA 2019).

Transfer via Urine. Given that 7.4 GBq of ^{177}Lu is administered, approximately half (Nelson and Sheetz 2019; Levart et al. 2019; Calais and Turner 2014) is excreted in urine before the patient leaves the hospital (within 6 hours). If it is conservatively assumed that 0.1% of the void activity of ^{177}Lu does not flush down the toilet (i.e., contaminates the bathroom) and 0.1% of the activity contaminating the bathroom is ingested by another person, suggesting an oral intake of 3.7 kBq ^{177}Lu could occur. This intake results in a CEDE of 2 µSv, or about 0.12% of the dose from external exposure.

Transfer via Sweat. Nelson and Sheetz (2019) report that between 7 and 2,300 Bq (n = 110) of ^{177}Lu appeared in saliva samples and alcohol swabs of the skin of treated patients soon after administration (no other detail was presented). For this assessment, with both saliva and skin, a maximum intake of 5 kBq per contact (at administration and decayed thereafter) is deemed conservative. Thus, on transfer of a single bolus of 5 kBq from patient sweat into an open wound of the caregiver, the committed effective dose would be 0.43 µSv, less than 0.03% of the predicted external dose.

Transfer via Saliva. Again, using the data from Nelson and Sheetz (2019), with an upper-bound transfer of 5 kBq per kiss, assuming 2 kisses per day starting one week after administration, the total intake is about 44 kBq (through 10 physical half-lives) and the committed effective dose would be 23 µSv, or about 1.4% of the external dose estimate. If the interruption were not adhered to, and kissing began immediately after release, a total intake of about 102 kBq could be realized resulting in a dose to the patient's partner of about 54 µSv. These upper-bound screening values overestimate potential activities available for transfer because biological reductions in the source activity are neglected.

Intimacy is an activity that should be restricted within some timeframe after administration (Nelson and Sheetz 2019). However, assuming intimacy on the day of administration, a transfer of 5 kBq per kiss, and a 20x factor for intimate contact, an intake of 100 kBq could occur with a resulting internal dose of about 53 µSv. Internal uptake by a spouse or partner of a recently released patient through kissing or intimate activity can be reduced by providing instructions to avoid such activity within the first several weeks after administration. Even without those instructed interruptions, the internal dose is "less than a few percent" of the dose received via external exposure.

Table *3-1* summarizes the internal pathway dosimetric analysis.

Table 3-1 Internal pathways

Pathway	Intake (kBq)	DC (µSv/kBq)	Dose (µSv)	% of External
External			1,700	
Urine	3.7	0.53	2	0.12
Open wound	5.0	0.086	0.43	0.03
Kissing (1 wk interruption)	44	0.53	23	1.4
Kissing (no interruption)	102	0.53	54	3.2
Intimacy	100	0.53	53	3.1

Conclusions

This assessment suggests that internal uptake by the caregiver, spouse, or other individual exposed to someone having had a medical administration of ^{177}Lu is less than a few percent of the potential radiation dose received through external exposure. Consistent with the findings expressed in Regulatory Guide 8.39 for ^{131}I uptake (NRC 2020), the potential internal dose to the maximum bystander is not likely to reach a level of significance compared to the likely external dose received by that same individual. Kissing could be problematic for internal dose of a spouse or partner, but with instruction to refrain from kissing and proper following of those instructions, this pathway can be eliminated.

It is further concluded that ^{177m}Lu, a potential contaminant of ^{177}Lu is of such low activity that it does not rise to a level of concern except for potential long-term contamination of restroom facilities used by ^{177}Lu patients. From a single administration, although contamination is detectable, exposure rates in the bathroom from ^{177}Lu (and ^{177m}Lu) would not necessarily be cause for concern, but the buildup over time of ^{177m}Lu contamination with multiple administrations is a possibility and may become problematic if radiation safety protocol is not implemented to minimize contamination. Mehmedovic (2021) even suggests outfitting bathrooms with stainless steel rather than porcelain to make decontamination easier.

4. PATIENT-SPECIFIC MODIFYING FACTORS

Patient-specific modifying factors facilitate additional realism. While the regulatory guide adopts simplified terminology, greater mathematical detail in this document can influence descriptions, such as time-integrated biokinetics compared to biokinetics. Nevertheless, consistency is intended for parameters sharing the same symbol. Basic activity thresholds and basic measurement thresholds developed in Chapter 2 provide an initial technical basis for releasing patients with no restrictions, for releasing patients with dose-minimizing instructions, or for holding patients in the administering facility for some time prior to release. Methods in Chapter 5 address potential internal doses if the patient is breastfeeding an infant or child.

Dosimetry Methods

Bystanders are externally exposed to radiation emitted by radionuclides in the patient when in close contact with the patient. External dose rates primarily depend on distance from the patient, radionuclide activity remaining in the patient, tissue attenuation, and emission characteristics of the radionuclide. External dose equivalent to an individual can be estimated from a combination of factors for administered activity, activity-to-dose-rate conversion, geometry, attenuation, and time-integrated effects from bystander occupancy and radionuclide retention:

$$D_{ext}(r,\tau_1,\tau_2) = A_0 \cdot \Delta_{pr} \cdot F_G(r) \cdot F_A \cdot \int_0^{\infty} [F_O(\tau_1,\tau_2) \cdot R(t)]dt \qquad \text{Equation [4-1]}$$

where

$D_{ext}(r,\tau_1,\tau_2)$ external dose equivalent to an individual exposed to the patient at a distance r between times τ_1 and τ_2 after radionuclide administration [mSv];

A_0 radionuclide activity in the administered radiopharmaceutical [GBq];

Δ_{pr} dose-rate constant for a point source of the administered radionuclide at a distance of 1 m $\left[\frac{\text{mSv}}{\text{GBq h}}\right]$;

$F_G(r)$ geometric factor for the radionuclide distribution in the patient and sensitive organs in the bystander at a distance r [unitless];

F_A attenuation factor for photon scatter, buildup, and absorption [unitless];

$F_O(\tau_1,\tau_2)$ occupancy function that assigns a value of unity (1) when the bystander is exposed to the patient between times τ_1 and τ_2 and a value of zero (0) when the bystander is not exposed to the patient [unitless];

$R(t)$ radiopharmaceutical retention in the patient at time t after administration [unitless];

τ_1 time representing the beginning of bystander exposure to the patient [h];

τ_2 time representing the end of bystander exposure to the patient [h]; and

dt time differential used in integration $[\mathrm{h}]$.

It is assumed in Equation [4-1] that one representative distance is adequate for calculating dose accumulated over time. Multiple exposure geometries and distances, however, can be accommodated by a summation with different bystander occupancy, geometric and attenuation effects, and time integration limits:

$$D_{ext} = \left(A_0 \cdot \Delta_{pr}\right) \sum_{i=1}^{n} \left[F_G(r_i) \cdot F_A \cdot \int_0^{\infty} F_O(\tau_{1i}, \tau_{2i}) \cdot R(t)\, dt \right] \quad \text{Equation [4-2]}$$

where

i index for multiple exposure geometries with no overlap in time intervals (τ_{1i}, τ_{2i}) and
n total number of exposure geometries for the bystander.

The accumulated dose for an infinite time equals $1.44 \cdot \mathrm{T_r} \cdot \mathrm{A_0} \cdot \Delta_{\mathrm{pr}}$ for the basic assumptions of point-source and point-target geometries, exposure at the standard distance of 1 m, 100% occupancy beginning immediately after administration $(\tau_1 = 0)$ and lasting through complete radionuclide depletion in the patient $(\tau_2 = \infty)$, and radionuclide retention controlled solely by radiological decay (i.e., neglecting biological clearance). The same result of $1.44 \cdot \mathrm{T_r} \cdot \mathrm{A_0} \cdot \Delta_{\mathrm{pr}}$ is obtained when these assumptions are applied to Equation [4-1] and Equation [4-2]. Refer to the "Application of Thresholds" section for additional information. The dose rate at a distance r and time t simply equals $\mathrm{A_0} \cdot \Delta_{\mathrm{pr}} \cdot \mathrm{F_G(r)} \cdot \mathrm{F_A} \cdot \mathrm{R(t)}$, where the radiopharmaceutical retention function accounts for changes over time.

Equation [4-1] and Equation [4-2] calculate the external dose equivalent to a bystander from time-integrated exposure to the patient. The integrals explicitly address effects from patient biokinetics and bystander occupancy together in a single integrand. To account for patient-specific biological clearance of the radiopharmaceutical, a modifying factor for biokinetics and time integration, $\mathrm{F_B}$, is introduced relative to the basic assumption of no biological clearance:

$$F_B \equiv \frac{\int_0^{\infty} R(t) dt}{\int_0^{\infty} e^{-\lambda_r t}\, dt} = \lambda_r \int_0^{\infty} R(t)\, dt = \frac{\int_0^{\infty} R(t)\, dt}{1.44 \cdot T_r} \quad \text{Equation [4-3]}$$

For biokinetics, $\mathrm{F_B}$ equals the number of disintegrations occurring in the patient with biological and radiological removal relative to the number of disintegrations assuming no biological removal. In other words, $\mathrm{F_B}$ equals the fraction of disintegrations in the patient available for the exposure of bystanders. It is important to note that this definition of $\mathrm{F_B}$ provides a quantitative estimate of time-integrated biokinetics solely based on patient-specific information. $\mathrm{F_B}$ does not depend on bystander behaviors.

A similar ratio is computed in the definition of a modifying factor for occupancy:

$$F_O \equiv \frac{\int_0^{\infty} F_O(\tau_1, \tau_2) \cdot R(t) dt}{\int_0^{\infty} R(t) dt} = \frac{\int_{\tau_1}^{\tau_2} R(t) dt}{\int_0^{\infty} R(t) dt} \quad \text{Equation [4-4]}$$

For occupancy, $\mathrm{F_O}$ equals the disintegrations during bystander exposure relative to the total number of disintegrations occurring in the patient. In other words, $\mathrm{F_O}$ represents the fraction of available disintegrations

associated with a specific bystander's exposure. F_O depends on when and for how long the bystander is exposed to the patient relative to the time of radiopharmaceutical administration.

For geometry and attenuation, the $F_G \cdot F_A$ product equals the dose rate to the bystander at a distance r relative to the dose rate calculated from point-source and point-target irradiation assumptions at 1 m in the definition of the dose rate kernels. For details, refer to the upcoming sections on the modifying factors for geometry and attenuation.

Substituting Equation [4-3] and Equation [4-4] into Equation [4-1] yields an expression with modifying factors for time-integrated biokinetics, occupancy, geometry, and attenuation:

$$D_{ext} = 1.44 \cdot T_r \cdot \Delta_{pr} \cdot A_0 \cdot F_B \cdot F_O \cdot F_G \cdot F_A \qquad \text{Equation [4-5]}$$

Retention functions are typically defined with t = 0 h when the radiopharmaceutical is administered. This time origin appears in the definitions for the modifying factors F_B and F_O. Bystander exposure after patient release implies $\tau_1 > 0$ h for times no earlier than the time of patient release. Bystander exposure at various times after administration are addressed in the modifying factor for occupancy shown in Equation [4-4].

Retention Functions

A double-exponential retention function provides flexibility to model rapid biological clearance rates at times shortly after administration as well as transitions to slower clearance rates at longer times. The general form of this retention function is $R(t) = f_1 e^{-\lambda_{e_1} t} + f_2 e^{-\lambda_{e_2} t}$. To ensure 100% retention at the time of administration, a common constraint of $f_2 = 1 - f_1$ results in the following simplification:

$$R(t) = f e^{-\lambda_{e_1} t} + (1 - f) e^{-\lambda_{e_2} t} \qquad \text{Equation [4-6]}$$

where

f fraction of activity exhibiting rapid clearance [unitless];

λ_{e_1} effective removal rate for rapid clearance [h^{-1}]; and

λ_{e_2} effective removal rate for slower clearance [h^{-1}].

Time integration returns a result with units of time and, with this simplification, becomes

$$\int_{\tau_1}^{\tau_2} R(t)\ dt = \int_{\tau_1}^{\tau_2} \left[f e^{-\lambda_{e_1} t} + (1 - f) e^{-\lambda_{e_2} t} \right] dt = \frac{f}{\lambda_{e_1}} \left(e^{-\lambda_{e_1} \tau_1} - e^{-\lambda_{e_1} \tau_2} \right) + \frac{1 - f}{\lambda_{e_2}} \left(e^{-\lambda_{e_2} \tau_1} - e^{-\lambda_{e_2} \tau_2} \right) \qquad \text{Equation [4-7]}$$

For radiopharmaceuticals that can be approximated by a single exponential, Equation [4-7] reduces to

$$\int_{\tau_1}^{\tau_2} R(t)\ dt = \int_{\tau_1}^{\tau_2} e^{-\lambda_e t} dt = \frac{1}{\lambda_e} \left(e^{-\lambda_e \tau_2} - e^{-\lambda_e \tau_1} \right) \qquad \text{Equation [4-8]}$$

where

λ_e effective removal rate for the radiopharmaceutical including radiological decay and biological clearance [h^{-1}] and

$\lambda_e = \lambda_e + \lambda_r$ effective removal rate equals the summation of the biological clearance rate and radiological decay constant.

Because the occupancy factor accounts for the fraction of time that the bystander is in close contact with the patient, the time-integrated biokinetic factor is addressed with full integration limits (i.e., $\tau_1 = 0$ and $\tau_2 = \infty$), as originally defined in Equation [4-3].

- For double-exponential retention,

$$F_B = \frac{fT_{e1}+(1-f)T_{e2}}{T_r} = f\frac{\lambda_r}{\lambda_{e1}} + (1-f)\frac{\lambda_r}{\lambda_{e2}}.$$

- For single-exponential retention,

$$F_B = \frac{T_e}{T_r} = \frac{\lambda_r}{\lambda_e}.$$

When there are multiple exposure geometries, distances, and/or time intervals, a summation is necessary

$$D_{ext} = \left(1.44 \cdot T_r \cdot \Delta_{pr} \cdot A_0 \cdot F_B \cdot F_A\right) \sum_{i=1}^{n} \left[F_{O,i} \cdot F_G(r_i)\right] \quad \text{Equation [4-9]}$$

such that

$$F_{O,i} = \frac{\int_{\tau_{1i}}^{\tau_{2i}} R(t)dt}{\int_0^{\infty} R(t)dt} \quad \text{Equation [4-10]}$$

Effective half-life is an important parameter. When the effective half-life of the radiopharmaceutical exceeds 1 day, determinations of the occupancy factor for repeated exposures (e.g., on a daily basis) can be simplified in Equation [4-9] and Equation [4-10] and replaced with a single occupancy factor F_O equal to the fraction of time that the bystander is exposed to the patient (such as 40 hours per week = $\frac{40}{168} = 0.24$ or 6 hours per day = $\frac{6}{24} = 0.25$). Breastfeeding a child is one example of repeated exposure. Details on internal and external doses to breastfeeding children are discussed in Chapter 5.

In this report, F_A has been defined based on attenuation by the patient, so that calculated dose rates will be patient specific and analogous to survey instrument measurements at potential bystander locations (e.g., 1 m). As shown in Equation [4-9], aspects of bystander exposure are addressed by modifying factors for occupancy and geometry. This approach is considered to be protective and flexible. When very specific details on bystander position relative to the patient are known, such as greater tissue thicknesses for side-by-side (i.e., shoulder-to-shoulder) exposure compared to face-to-face exposure, the attenuation factor F_A can be adjusted for that irradiation geometry.

Application of Thresholds

The basic activity threshold Q and basic measurement threshold M were introduced in Chapter 2 for the limits of 5 mSv for patient release and 1 mSv for issuing instructions. Activity and measurement thresholds are operational quantities that provide a convenient means for demonstrating compliance with requirements for patient release and issuing instructions. Basic activity and basic measurement thresholds for a given radionuclide are denoted as Q_{rel} and M_{rel} for patient release and Q_{ins} and M_{ins} for issuing instructions. These basic thresholds are calculated by methods described in Chapter 2 with several nominal assumptions: 100% occupancy beginning immediately after administration and lasting through complete radionuclide depletion; attenuation and buildup for 20 mm of tissue; exposure at the standard distance of 1 m; and radionuclide retention controlled solely by radiological decay (i.e., intentionally neglecting biological clearance).

For a standard measurement distance of 1 m, the basic measurement threshold is closely related to the basic activity threshold, $\mathrm{M} = \Delta_{\mathrm{pr}} \cdot \mathrm{Q}$. To define the basic activity threshold, replacing A_0 with Q in Equation [4-1] according to the nominal assumptions of $\mathrm{D}_{\mathrm{ext}} = 5\ \mathrm{mSv}$; $\mathrm{F_O} = 1$; $\mathrm{F_G}(1\ \mathrm{m}) = 1$ to match the point-point geometry of the Δ_{pr} dose-rate kernel; $\mathrm{R(t)} = \mathrm{e}^{-\lambda_{\mathrm{r}} \mathrm{t}}$; $\tau_1 = 0$ h; and $\tau_2 = \infty$ yields:

$$5\ \mathrm{mSv} = \Delta_{\mathrm{pr}} \cdot \mathrm{Q} \cdot \int_0^{\infty} \mathrm{e}^{-\lambda_{\mathrm{r}} \mathrm{t}}\, \mathrm{dt} = \frac{\Delta_{\mathrm{pr}} \cdot \mathrm{Q}}{\lambda_{\mathrm{r}}} = 1.44 \cdot \mathrm{T_r} \cdot \Delta_{\mathrm{pr}} \cdot \mathrm{Q} \qquad \text{Equation [4-11]}$$

where

λ_{r} radiological decay constant for the radionuclide [h^{-1}] and

$\mathrm{T_r}$ radiological half-life for the radionuclide [h].

Equation [4-11] is identical to Equation [2-21] for the standard distance of 1 m. To streamline the equations, only thresholds for patient release corresponding to a hypothetical bystander dose equivalent of 5 mSv are explicitly addressed in the remainder of this Chapter. To minimize repetition, thresholds for issuing instructions are intentionally not introduced into the equations because they are simply a factor of 5 lower than the thresholds for patient release.

As described in Chapter 2, the basic activity thresholds (Q) provide the foundation for guidance and further calculation. By combining Equation [4-5] and Equation [4-11], introducing a modified activity threshold Q' to replace A_0, and simplifying, a new expression emerges with four modifying factors. The modified activity threshold is calculated directly from the basic activity threshold and patient-specific factors for biokinetics, occupancy, geometry, and attenuation:

$$\mathrm{Q}' = \frac{\mathrm{Q}}{\mathrm{F_B} \cdot \mathrm{F_O} \cdot \mathrm{F_G} \cdot \mathrm{F_A}} \qquad \text{Equation [4-12]}$$

Additionally, for a standard measurement distance of 1 m, a modified measurement threshold can be calculated from the product of the dose-rate kernel and modified activity threshold:

$$\mathrm{M}' = \Delta_{\mathrm{pr}} \cdot \mathrm{Q}' \qquad \text{Equation [4-13]}$$

The modified measurement threshold represents the dose rate at 1 m at the time of administration anticipated to result in a 5-mSv bystander dose equivalent according to patient- and bystander-specific exposure conditions reflected by the four modifying factors.

Modifying Factors

Time-integrated Biokinetics, F_B

The modifying factor for time-integrated biokinetics can be determined directly from patient-specific radiopharmaceutical retention data. F_B values are greater than zero and less than or equal to unity. F_B is strictly dependent on radiopharmaceutical retention in the patient and independent of bystander behaviors. Radionuclide retention over time can be estimated from either (i) several dose rate measurements at the same distance from the patient after the therapeutic administration or (ii) retention data from a prior dosimetric evaluation for the same patient and radiopharmaceutical. Slower biological clearance increases the value of F_B. Radionuclide retention fractions (or percentages) can be determined from retained radioactivity in the patient or results of dose rate measurements over time. **Figure *4-1*** provides a generalized template for any administered radionuclide and allows F_B to be determined from patient retention data in three simple steps: (1) divide times after administration by radiological half-life; (2) plot percentages from radiopharmaceutical retention; and (3) assign F_B to the smallest single-digit value intercepted by the data. An example for Lu-177 in Figure 4-1(d) illustrates a challenge to the generalized curves from rapid biological clearance shortly after administration (e.g., first plotted data point approaches the next lower curve for 0.2 but does not intercept it). To avoid underestimation of F_B, data plotting beyond 0.1 radiological half-lives after administration is recommended. When patient retention data are not available, it can be assumed that the patient exhibits the slowest biological clearance according to the manufacturer excretion information. Without any knowledge of biological clearance rates, assign $F_B = 1$. Note: $F_B = 1$ for encapsulated radionuclide implants or seeds.

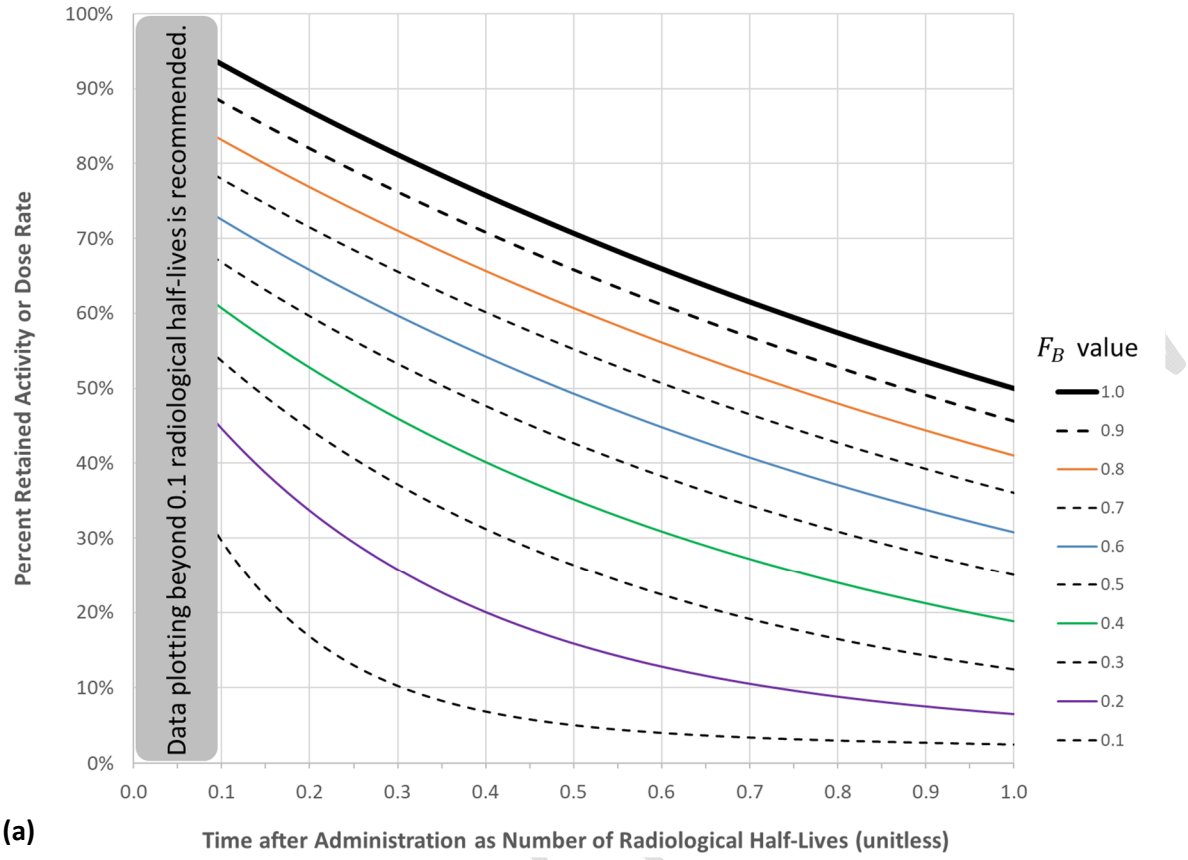

(a)

Figure 4-1 (a) Generalized graphical template to determine F_B from patient retention data. The generalized template is produced from averaging two bounding cases.

FAST BOUNDING CASE: For fast clearance, instantaneous biological removal from the fast component is coupled with no biological removal from the slow component. In terms of two effective half-lives, $T_{e1} = 0$ and $T_{e2} = T_r$. With instantaneous biological loss, each curve starts at its respective percentage.

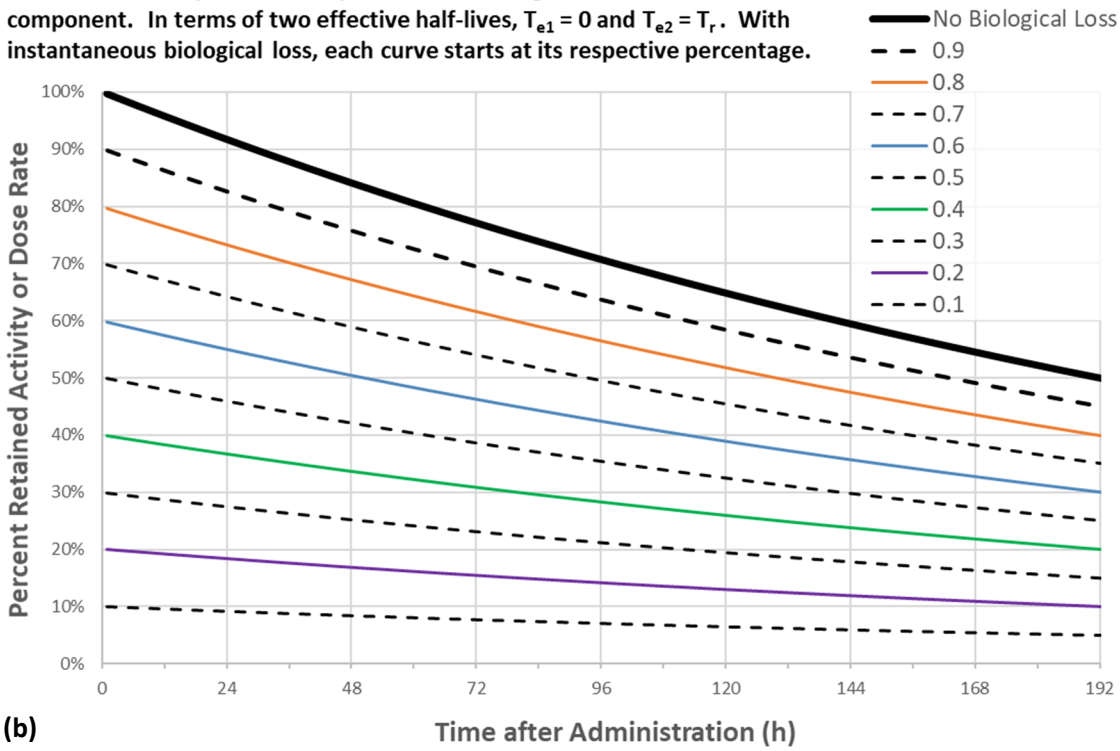

(b)

SLOW BOUNDING CASE: The bounding case for slow clearance features no biological removal from the fast component ($f_1 = 0$). The general model with two effective half-lives simplifies to a single effective half-life to represent the most gradual biological removal over time.

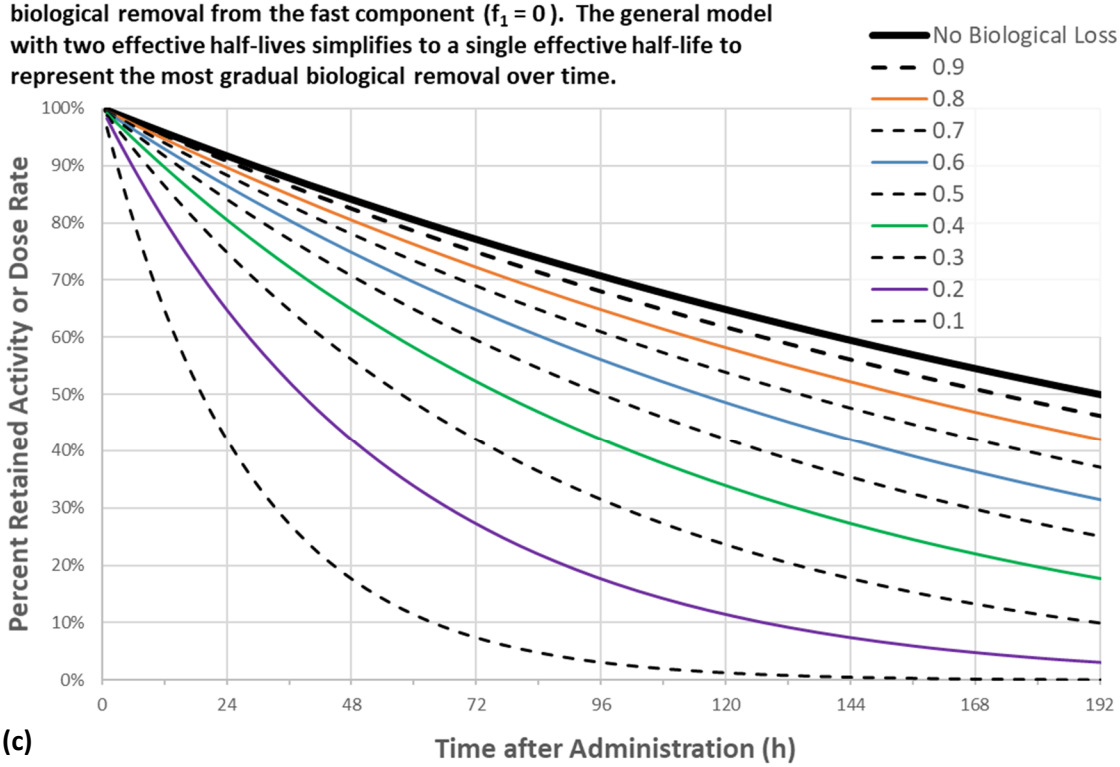

(c)

Figure 4-1 cont'd (b) I-131 example fast bounding case vs. time and (c) I-131 example slow bounding case for I-131 vs. time, shown before converting time after administration into radiological half-lives.

Example patient retention from dose rate measurements at 1 m

Time (h)	Measured Dose Rate ($\frac{\mu Sv}{h}$)
t_1 = 0	m_1 = 41
t_2 = 5	m_2 = 23
t_3 = 24	m_3 = 17
t_3 = 48	m_3 = 13

Divide time by 160 h
Divide dose rate by 41 $\frac{\mu Sv}{h}$

Number of Half-Lives	Percent Retention
0	100%
0.031	56%
0.15	41%
0.30	32%

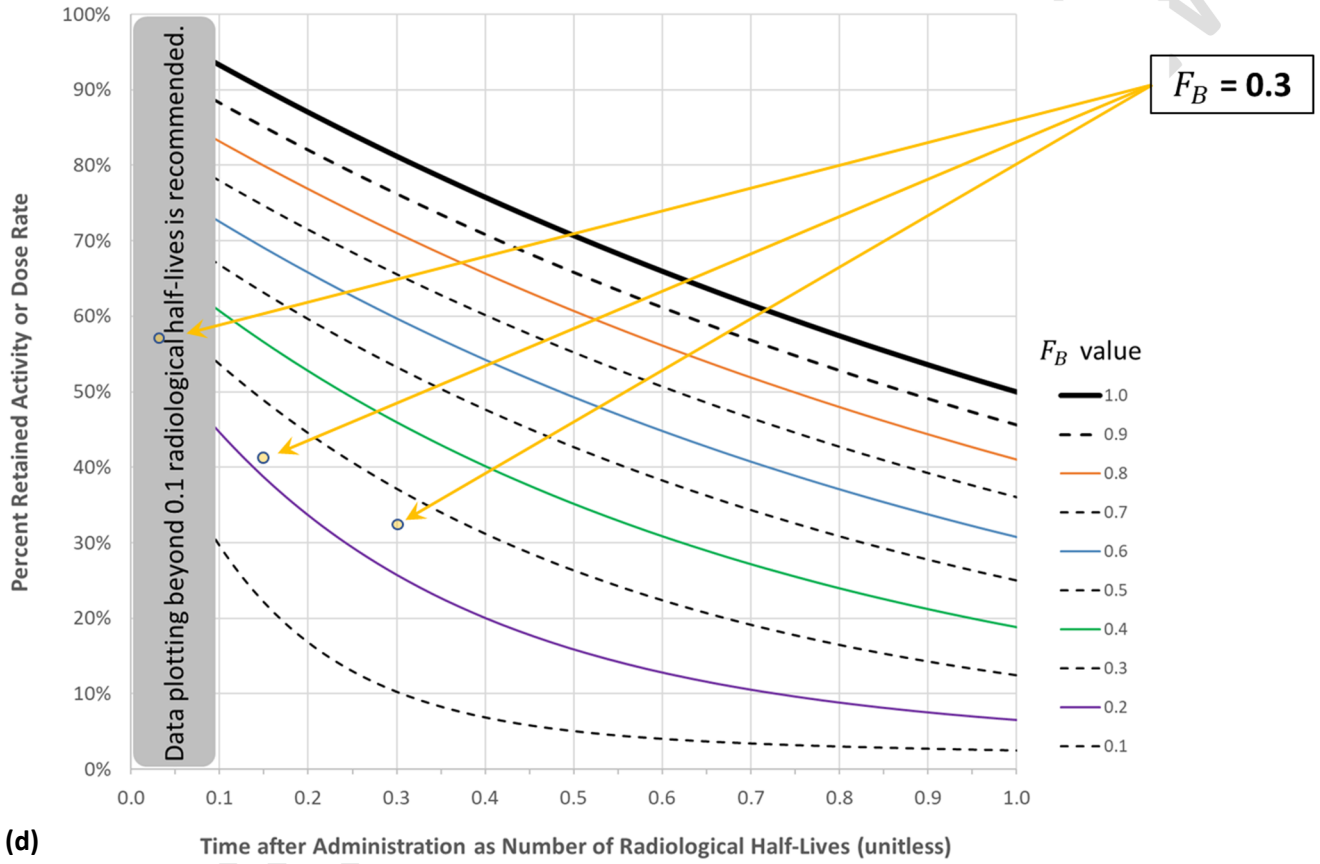

(d)

Figure 4-1 cont'd (d) Test of the generalized template with example patient retention data for Lu-177.

When exponential retention with a single effective half-life is assumed and fitted to patient retention data at long times after administration, the resulting retention curve will tend to overestimate F_B. The overestimation is visually apparent in **Figure *4-2*** by comparing the areas under the curve for the dashed line (single-exponential assumption) and solid blue line (double-exponential retention). An advantage of this simplification is that F_B can be determined from a single long-term retention data point and a few straightforward mathematical relationships. With this approach, R_n [unitless] is the retention fraction in the patient at the "latest" time t_n [h] after administration. Note, $t_n > 48$ h is preferred for radionuclides with $T_r > 24$ h. Following a basic conversion $\lambda_r = \frac{1}{1.44 \cdot T_r}$, the time-integrated biokinetic factor equals

$$F_B = -\frac{\lambda_r \, t_n}{\ln(R_n)} \qquad \text{Equation [4-14]}$$

Figure *4-2* also illustrates the interrelationship of biokinetics and occupancy. Methods presented in this chapter allow the biokinetic modifying factor to be determined relative to radiological removal and the occupancy factor to be determined according to the effective half-life of the radiopharmaceutical as described in the next section.

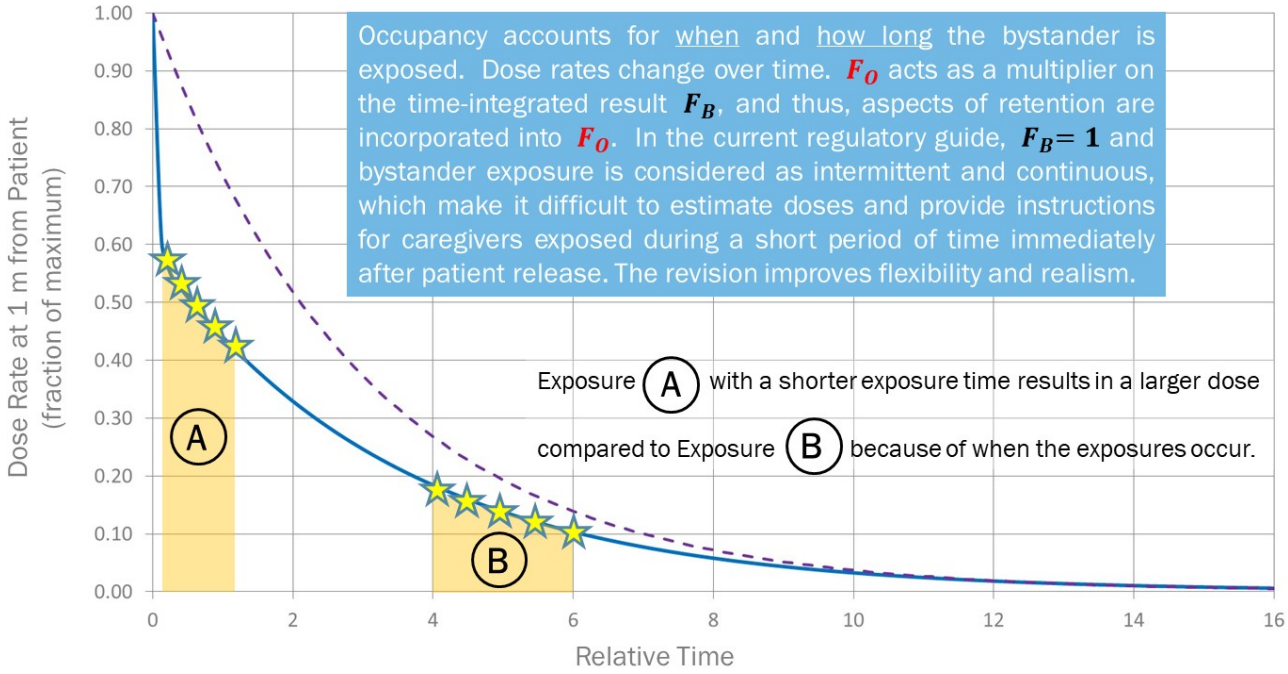

Figure 4-2 Overview depicting radionuclide retention and bystander exposure in two time intervals

Occupancy, F_O

This section presents background information and supplemental examples on occupancy to support revisions to Regulatory Guide 8.39 (NRC 2020). The methodology for occupancy described in the revision represents the primary implementation of Equation [4-4] for occupancy, and it is not repeated in this section. Example calculations for occupancy include calculations as well as tabulated values for F_O based on the effective half-life of the radiopharmaceutical and bystander exposure behavior. Patient-specific information for bystander exposure, which may include a patient questionnaire is described in Section 0.

The modifying factor for occupancy, $F_O(\tau_1, \tau_2)$, is defined for a known time interval of bystander exposure and takes values greater than zero and less than or equal to 1. In Equation [4-1], $F_O = 1$ when the bystander is exposed for the entire time between τ_1 and τ_2. When bystander exposure only represents a fraction of time within the integration limits, F_O equals the fraction of radioactive emissions in the patient to which the bystander is exposed. When the time interval is unknown or characterized by repeated exposures during the first few effective half-lives of the radiopharmaceutical, the modifying factor for occupancy can be assigned to the fraction of time that the bystander is expected to be in close contact with the patient.

Example Calculation for Double Exponential Retention. As shown in the visual overview of **Figure *4-2***, F_O equals the area under the retention curve for the given time interval of exposure divided by the total area under the curve. Areas under the curve are obtained by integrating the retention function within specific time intervals. Integrated solutions are presented for a specific time interval within the first 2 days after release to increase fidelity during travel and repeated exposure thereafter (after 48 h). The integrated solution in the first 2 days

requires beginning and ending times for bystander exposure (τ_1 & τ_2) in that 48-h period. Selecting 2 days for the first time period is convenient for radiopharmaceuticals with effective half-lives of 1 day or longer (e.g., most therapeutic procedures). Under these conditions, the integrals in Equation [4-4] for occupancy can be written as

$$F_O = \left[\frac{\int_{\tau_1}^{\tau_2}\left(f_1 e^{-\lambda_{e1} t} + f_2 e^{-\lambda_{e2} t}\right) dt}{\frac{f_1}{\lambda_{e1}} + \frac{f_2}{\lambda_{e2}}}\right] + \left(\frac{E_w}{168}\right)\left[\frac{\int_{48h}^{\infty}\left(f_1 e^{-\lambda_{e1} t} + f_2 e^{-\lambda_{e2} t}\right) dt}{\frac{f_1}{\lambda_{e1}} + \frac{f_2}{\lambda_{e2}}}\right] \quad \text{Equation [4-15]}$$

$$= \left[\frac{\frac{f_1}{\lambda_{e1}}\left(e^{-\lambda_{e1}\tau_1} - e^{-\lambda_{e1}\tau_2}\right) + \frac{f_2}{\lambda_{e2}}\left(e^{-\lambda_{e2}\tau_1} - e^{-\lambda_{e2}\tau_2}\right)}{\frac{f_1}{\lambda_{e1}} + \frac{f_2}{\lambda_{e2}}}\right] + \left(\frac{E_w}{168}\right)\left[\frac{\frac{f_1}{\lambda_{e1}}\left(e^{-\lambda_{e1}\,48h}\right) + \frac{f_2}{\lambda_{e2}}\left(e^{-\lambda_{e2}\,48h}\right)}{\frac{f_1}{\lambda_{e1}} + \frac{f_2}{\lambda_{e2}}}\right]$$

where

E_w estimated weekly bystander exposure time after the first 2 days [h].

For situations in which definite time limits for bystander exposure are not known within the first 2 days, a simplification is suggested that involves evaluating the first integral over its full-time interval and including a term for the fraction of time within the first 48 h that the bystander is exposed to the patient.

$$F_O = \left(\frac{E_2}{48}\right)\left[\frac{\int_0^{48h}\left(f_1 e^{-\lambda_{e1} t} + f_2 e^{-\lambda_{e2} t}\right) dt}{\frac{f_1}{\lambda_{e1}} + \frac{f_2}{\lambda_{e2}}}\right] + \left(\frac{E_w}{168}\right)\left[\frac{\int_{48h}^{\infty}\left(f_1 e^{-\lambda_{e1} t} + f_2 e^{-\lambda_{e2} t}\right) dt}{\frac{f_1}{\lambda_{e1}} + \frac{f_2}{\lambda_{e2}}}\right] \quad \text{Equation [4-16]}$$

$$= \left(\frac{E_2}{48}\right)\left[\frac{\frac{f_1}{\lambda_{e1}}\left(1 - e^{-\lambda_{e1}\,48h}\right) + \frac{f_2}{\lambda_{e2}}\left(1 - e^{-\lambda_{e2}\,48h}\right)}{\frac{f_1}{\lambda_{e1}} + \frac{f_2}{\lambda_{e2}}}\right] + \left(\frac{E_w}{168}\right)\left[\frac{\frac{f_1}{\lambda_{e1}}\left(e^{-\lambda_{e1}\,48h}\right) + \frac{f_2}{\lambda_{e2}}\left(e^{-\lambda_{e2}\,48h}\right)}{\frac{f_1}{\lambda_{e1}} + \frac{f_2}{\lambda_{e2}}}\right]$$

where

E_2 estimated bystander exposure time within the first 2 days [h].

Although the separate $\left(\frac{E_2}{48}\right)$ term is unnecessary in Equation [4-15] due to exposure only within the time limits of the first integral, it accounts for bystander exposure during only a fraction of the first 48 hours in Equation [4-16]. By not specifying the starting and ending times, Equation [4-16] effectively applies an average value for each hour of exposure in the two respective time periods. When bystander exposure is known to occur only during the early part of the first 48 hours, Equation [4-15] is recommended. In so far as E_2 and E_w are not underestimated, Equation [4-16] is expected to provide a reasonably good estimate or slightly conservative estimate of F_O when bystander exposure occurs in the middle or latter part of, or in a distribution throughout, the 48-h period.

Example Simplification for Effective Removal Modeled by a Single Exponential. When bystander exposure can be adequately described by the two periods shown in Equation [4-16] with a single effective half-life implied in Equation [4-13], the calculation for the occupancy modifying factor reduces to

$$F_o = 0.02\ E_2\ (1 - R_2) + 0.006\ E_w\ R_2$$ Equation [4-17]

where $R_2 = (R_n)^x$ and $x = \frac{48}{t_n}$ with R_n and t_n previously defined in Section 4.4.1.

As effective half-life falls below 1 d, R_2 becomes small, and the last term in Equation [4-17] provides diminished contributions. Equation [4-16] and Equation [4-17] shown for a 2-d initial time period are not recommended for radiopharmaceuticals with effective half-lives less than 6 h because occupancy considerations tend to be important only during the first few effective half-lives after administration. This point is illustrated in **Figure *4-3***.

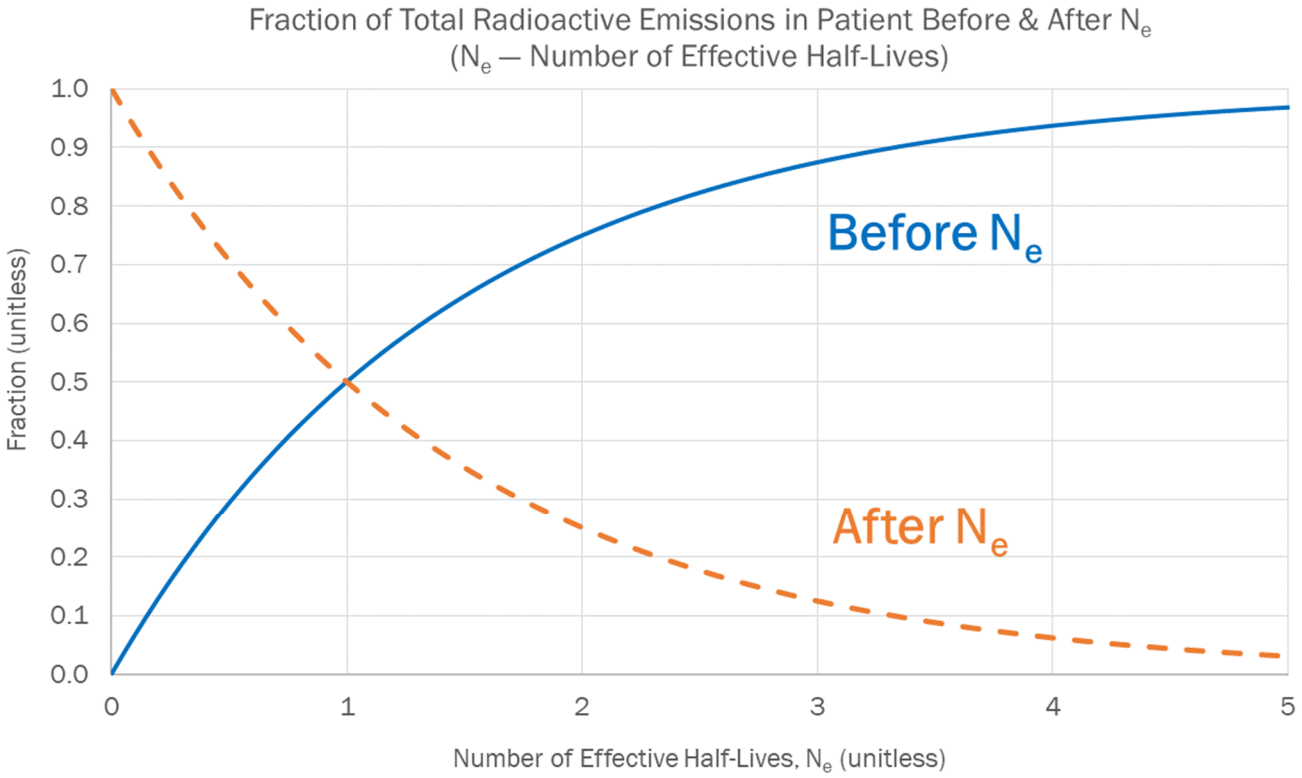

Figure 4-3 Fraction of Radioactive Emissions Generalized to the Number of Effective Half Lives

The combined effect of exposure delay and duration on the occupancy factor is illustrated in **Figure *4-3*** for a single effective half-life with the bystander exposed between the times τ_1 and τ_2. Both the delay and exposure duration were generalized and converted into the number of effective half-lives (T_e). Exposure delays greater than 2 T_e result in $F_O < 0.2$. Bystander exposure durations greater than 1 T_e are required with minimal delays to yield $F_O \sim 0.5$. Figure 4-4 only displays five numerical regions with increments of 0.2. Subdivision of multiple potential occupancy values below 0.2 are not shown. When lower occupancy values ($F_O < 0.2$) are justified, calculation of the occupancy factor is recommended according to Equation [4-18].

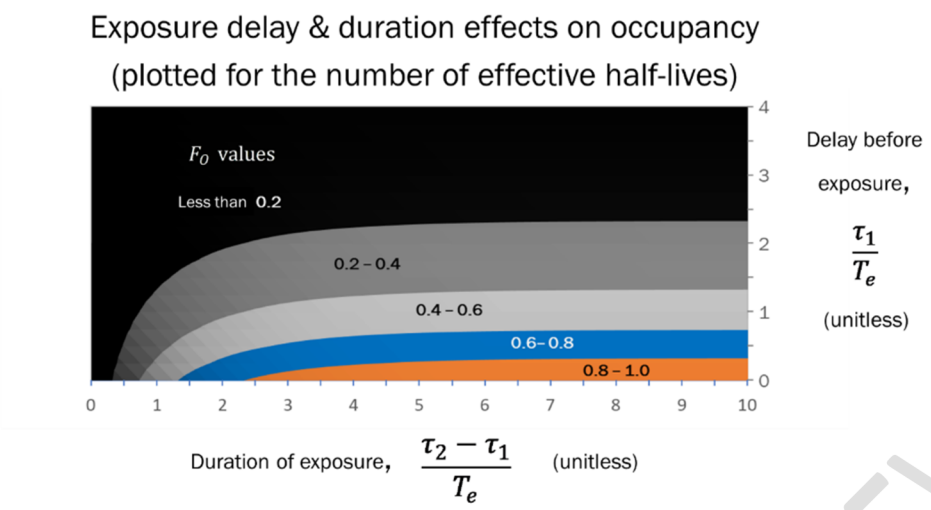

Figure 4-4 Generalized Effects from Exposure Delay (vertical axis) and Duration (horizontal axis)

For generalized parameters in effective half-lives, the occupancy factor for a single exposure between the times τ_1 and τ_2 reduces to

$$F_O = \left(\frac{1}{2}\right)^{\tau_1'} - \left(\frac{1}{2}\right)^{\tau_2'} \quad \text{Equation [4-18]}$$

where

$\tau_1' = \frac{\tau_1}{T_e}$ delay time before exposure in effective half-lives (unitless)

$\tau_2' = \frac{\tau_2}{T_e}$ exposure end time in effective half-lives (unitless)

Example Table of F_O Values. As an alternative to equations and calculations, **Table *4-1*** provides example occupancy factors for a range of exposure durations and timings. For multiple bystanders who may be exposed to the patient, decisions on patient release can be based on the largest F_O value when very close contact (e.g., holding another person) does not occur. When holding another person is expected, decisions can be made according to the bystander with the largest multiplicative product, $F_O \cdot F_G$. It is assumed that the patient is given and follows discharge instructions to prevent bystander exposure at distances of less than 1 m (e.g., being held). The effective half-life for the radiopharmaceutical can be approximated as $T_e = T_r \times F_B$ or calculated directly from the data point for the patient's retention as

$$T_e = -\frac{\ln(2)}{\ln(R_n)} t_n \quad \text{Equation [4-19]}$$

This report does not establish generic guidance on recommended time periods for following instructions; however, when dose-minimizing instructions are required, following instructions for at least 2 T_e can represent a good starting point for patient-specific considerations.

Table 4-1. Example occupancy factors for effective half-life and exposure characteristics

Instructions:

1. **Consider multiple bystanders with anticipated exposure to the patient after release.**
2. **Assign an F_O value to each bystander according to the patient behavior and exposure descriptions below.**
3. **Select the largest F_O value to demonstrate compliance.**

Effective Half-Life* of Radiopharmaceutical	Early Exposure to Patient	Patient Isolates	Longer Term Exposure to Patient	Recommended Occupancy F_O
$T_e \leq 6$ h	Travel or immediately after release			0.8
	Travel on public transportation			0.5
		6 h	< 18 h per day	0.25
		12 h	< 18 h per day	0.125
6 h < $T_e \leq$ 1 d	First 6 h			0.4
	First 12 h			0.6
	> 18 h in first day		> 18 h per day	0.85
	12 - 18 h in first day		12 - 18 h per day	0.65
	6 - 12 h in first day		6 - 12 h per day	0.45
	< 6 h in first day		< 6 h per day	0.25
		1 d	< 18 h per day	0.3
		2 d	< 18 h per day	0.2
1 d < $T_e \leq$ 6 d	> 36 h in first 2 days			0.6
	24 - 36 h in first 2 days			0.45
	12 - 24 h in first 2 days			0.3
		2 d	12 - 18 h per day	0.5
		2 d	6-12 h per day	0.35
		2 d	< 6 h per day	0.2
6 d < T_e	12 - 18 h per day in first week			0.3
	6 - 12 h per day in first week			0.2
	> 36 h in first 2 days			0.2
	< 9 h per day in first week		> 18 h per day	0.75
	< 6 h per day in first week		12 - 18 h per day	0.55
	< 6 h per day in first week		6 - 12 h per day	0.4

* Use radioactive half-life for sealed implants or seeds. For unsealed radiopharmaceuticals, T_e can be estimated by $T_r \times F_B$.

Additional Example Illustrating Incremental Exposure. When bystander exposure is converted into the number of effective half-lives, the occupancy factor can be estimated from **Figure *4-5*** by selecting each incremental exposure (vertical bars) pertaining to the bystander's exposure timeframe and summing F_O for those increments. **Figure *4-5*** facilitates estimation of the occupancy factor for a broad range of radiopharmaceuticals and allows for exposures at various times after administration. The summation of incremental exposures shown equals 0.97, because the total fraction of radioactive emissions in the patient after 5 effective half-lives equals 0.03 (not plotted).

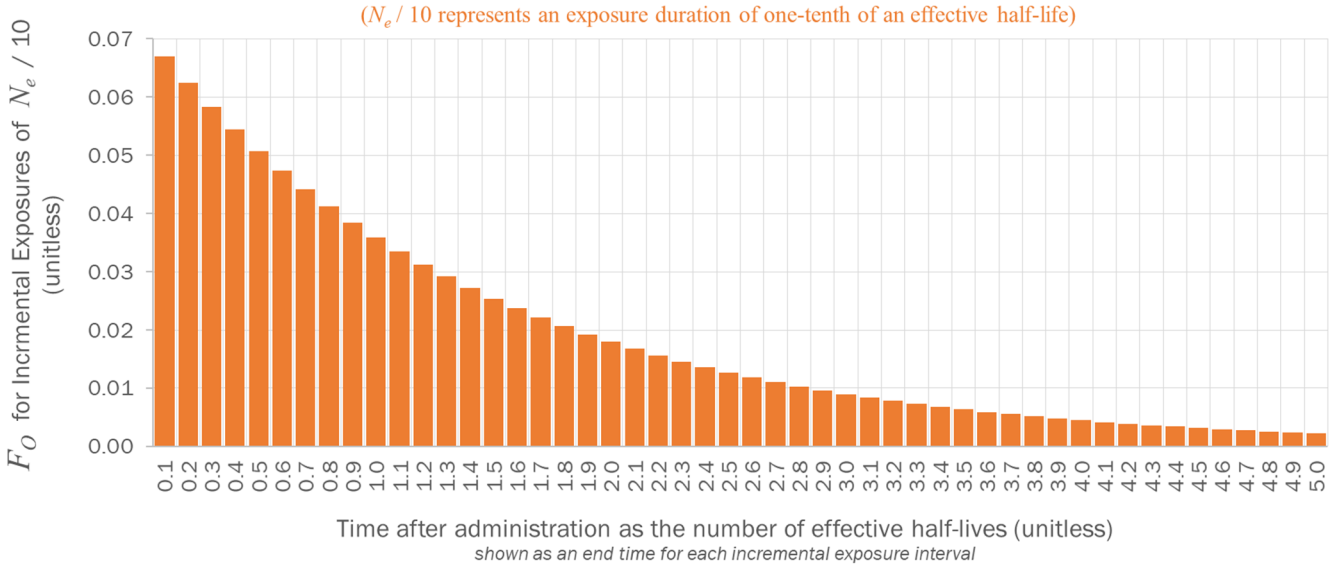

Figure 4-5 Occupancy values for 50 time intervals of equal duration immediately after administration for a single effective half-life. Time intervals are generalized for one-tenth of an effective half-life. When bystander exposure occurs over multiple time intervals, F_O values for those time intervals are summed

Methodology for Occupancy in the Revised Regulatory Guide. The previous examples reinforce concepts germane to occupancy. To accommodate a large range of potential patient-specific factors, bystander behaviors, and occupancy values, the methodology in the revision to Regulatory Guide 8.39 (NRC 2020) calculates F_O according to the effective half-life of the radiopharmaceutical in two parts: (1) bystander exposure during the patient's travel from the medical facility and (2) bystander exposure to the patient after travel. Times (typically in hours) are intentionally converted into the number of effective half-lives (unitless) so that a single set of tabulated values will apply to a broad range of radiopharmaceuticals.

Geometry, F_G

External dose rates, such as scattered radiation buildup and attenuation by intervening materials and tissue masses in the patient and bystander, depend on physical attributes and geometric positioning. As described in Chapter 2, the detailed development of dose-rate kernels resulted in basic activity thresholds and measurement thresholds for numerous radionuclides relevant to patient release based on point-to-point geometric assumptions at a nominal distance ($r = 1$ m). The modifying factor for geometry, $F_G(r)$, facilitates additional realism and can be supported by other models for external dose rate. To directly incorporate other modeling results into the presented methodology, the modeling result should be normalized by an additional calculation for a point-point geometry at the standard 1-m separation distance. The geometric modification factor takes the form of

$$F_G(r) = \frac{Result\ for\ realistic\ geometry\ with\ separation\ distance\ r}{Result\ for\ point\text{-}point\ geometry\ with\ 1\text{-}m\ separation} \qquad \text{Equation [4-20]}$$

Units for the numerator and dominator of Equation [4-20] can be user defined but should be the same. For example, the detailed calculation of bystander dose rate for a realistic geometry would be normalized by a similar calculation of bystander dose rate for the simplified point-point geometry with a nominal separation of 1 m. The nominal separation distance effectively scales the standardized dose-rate kernel in the proposed methodology to account for realistic geometric effects in the numerator. Detailed three-dimensional modeling (e.g., Monte Carlo

simulation) can be used to account for attenuation and buildup by tissue, air, or other materials between the patient and bystander. Those aspects are accounted for in the numerator of Equation [4-20]. When the $\mathrm{F_G} \cdot \mathrm{F_A}$ product is calculated from three-dimensional modeling for use with the dose-rate kernels or thresholds presented in Chapter 2, as shown in Equation [4-1], Equation [4-2], Equation [4-5], or Equation [4-9] through Equation [4-13], the same geometric assumptions for tissue attenuation and buildup used during kernel development should be included in the denominator of Equation [4-20]. These are a point source surrounded by no tissue for unsealed radionuclides and a point source surrounded by 0.05 mm titanium spherical encapsulation for implanted radionuclides. When bystander dose is calculated directly from three-dimensional modeling, the dose-rate kernel and Equation [4-20] are unnecessary.

Equation [4-1] also includes a single geometric factor as representative for the entire duration of bystander exposure. Because geometric effects are strongly dependent on distance, Equation [4-1] can be used directly when the bystander is primarily exposed at the standard patient-to-bystander distance of 1 meter. Although this may not be strictly accurate for prolonged human interactions, selecting a closer distance within a range of distances during close contact between 1 m and several meters can provide a reasonably conservative estimate. The nominal distance for close contact is 1 m, and it provides a convenient option for assigning time spent in close contact to the patient that includes distances within a few meters of the patient. When a bystander is known to spend most of the exposure time at a distance greater than 1 m from the patient, determining the geometric factor for the correct distance is advised. Due to the strong sensitivity of geometric influences on distance, it is recommended that separate geometric factors and exposure time frames be determined for distances closer than 1 m. For example, a centerline-to-centerline distance of 0.3 m is recommended for time spent holding another person.

Bystander irradiation at separation distances closer than 1 m is very important to consider because the $F_G(r)$ modifying factor can take values greater than 1. At very close distances, the effect of extended geometries is magnified, and point-point assumptions become overly conservative compared to more realistic nonpoint source and nonpoint target geometries. For these reasons, the presented methodology is based on simplified source and target irradiation geometries (e.g., full 1.7-m height for an adult patient and partial 0.7-m height for the most sensitive organs of an adult bystander). **Figure *4-6*** shows that at distances of 2 m or more, the point-point approximation (i.e., $\frac{1}{\mathrm{r}^2}$ relationship) can be applied due to expected overestimations of less than 10 percent compared to line-line irradiation results. In other words, $F_G(r) \approx \frac{1}{\mathrm{r}^2}$ when $\mathrm{r} \geq 2$ m, with r in units of m while F_G remains unitless. For example, $F_G \approx \frac{1}{4^2} = 0.063$ for a bystander at 4 m.

$F_G(r)$ has the potential to accommodate a broad range of patient-to-bystander geometries. Although this flexibility can be convenient in principle, the National Council on Radiation Protection and Measurements (NCRP) suggests index distances of 1 m and 0.3 m in its recommendations on patient-release criteria (NCRP 2006). An index distance of 1 m is recommended for the exposure of family members and members of the public who are "specifically in the company of" the patient.

Each index distance corresponds to a new $F_G(r)$ value. Most exposure calculations will utilize the standard distance of 1 m or greater distances when justified. The distance of 0.3 m is appropriate when the patient is being held or holding another person. Sharing the same bed as the patient, does not automatically imply the act of holding while sleeping. A closer distance of 0.2 m is proposed for a nursing child being held during breastfeeding. Accordingly, $\mathrm{F_G}$ values are presented for the separation distances of 0.1 and 0.2 m for a breastfeeding child externally exposed to the patient's breastmilk and body, respectively.

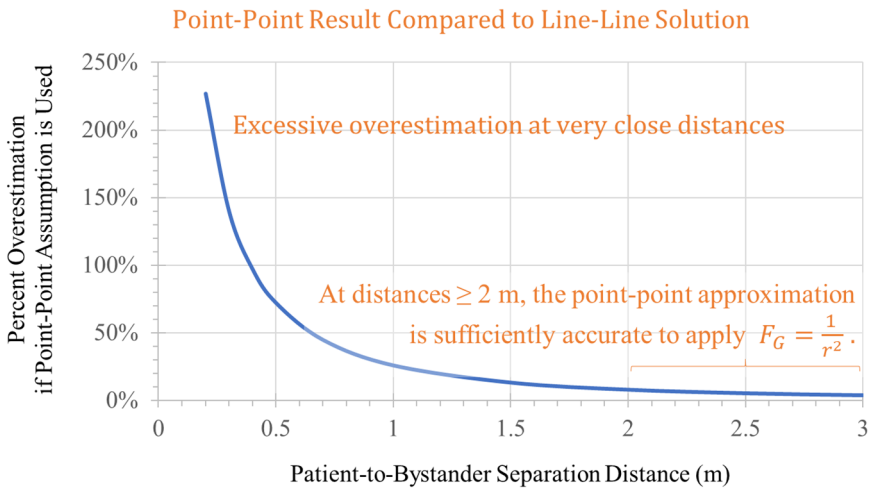

Figure 4-6 Reconciling geometric assumptions for calculating the modifying factor

Precalculated values for $F_G(r)$ are presented for a specific bystander separation distance, r. $F_G(r)$ values less than 1 are typical for patient-to-bystander distances ≥ 1 m. $F_G(r)$ can exceed 1 for patient-to-bystander distances closer than 1 m. **Figure *4-7*** displays geometric factors for adult exposure geometries as well as additional factors for external exposure to a breastfeeding child.

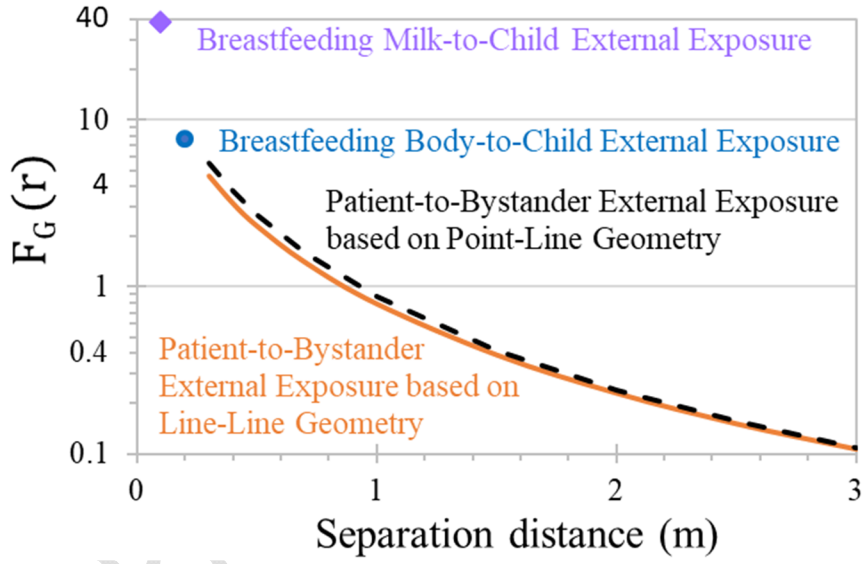

Figure 4-7 Geometric modifying factors for external exposure. Line-Line geometry refers to a 1.7-m source length and 0.7-m length for critical organs. Point-Line refers to a point source at the end of the 0.7-m length for critical organs

Suggested $F_G(r)$ values for two-dimensional geometries (e.g., point-point, point-line, line-line) are based on uncollided photon fluxes for various simplified source-target orientations. Similar to the dose-rate constants in Chapter 2, these simplified irradiation geometries do not include attenuation and buildup. Without attenuation and buildup from material interactions, these simplified irradiation calculations become energy independent, radionuclide independent, and patient independent. In other words, one table of $F_G(r)$ values can accommodate

a wide range of medical procedures, radionuclides, patients, and potential bystander exposure geometries. Details and derivations of the equations for uncollided photon flux are presented in Section 0.

A point-like source representation was considered for radioactive implants (e.g., prostate seeds) or significant source activity concentrated in one region of the body (e.g., thyroid uptake of radioiodine) and compared to line-line solutions for radioactivity widely distributed within the patient's body. Slightly higher modification factors were found for these point-line source geometries, decreasing from +20 percent to +2 percent at separation distances of less than 0.5 m to 3 m, respectively. These differences are shown by the dashed and solid lines in **Figure *4-7***.

Attenuation, F_A

The attenuation modifying factor adjusts the dose-rate kernel for patient-specific tissue thicknesses. F_A takes values greater than zero and generally less than or equal to one (1), except in situations when the energy distribution of photon emissions corresponds to the greatest enhancements from photon buildup and results in F_A values greater than 1. Attenuation and buildup effects were calculated for pertinent radionuclides with physical half-lives greater than 1 hour. As described in Chapter 2, the point-kernel dose rate constant for patient release, Δ_{pr}, is calculated with an assumption of no overlying tissue. A nominal tissue thickness, such as 20 mm, allows for a small amount of patient self-absorption and removes very low-energy photons from contributing dose to a bystander. It also allows for the slowing of electron emissions and subsequent creation of bremsstrahlung. Thus, a 20-mm thickness may be appropriate in certain circumstances, e.g., tissue overlying the thyroid or thickness of the eyeball when considering an eye plaque. For other instances, emissions from radionuclides distributed inside the chest wall or beneath excessive body fat, for example, would experience greater self-absorption by the patient's tissues. For this reason, relative dose kernels are plotted in Section 0 as a function of tissue thickness for selected radionuclides.

Determining the Maximally Exposed Individual

The maximally exposed individual is the bystander with the greatest $F_O \cdot F_G$ product because other factors of the dose calculation in Equation [4-5] are independent of bystander characteristics and behaviors. An example is presented with a graphical template for comparing anticipated dose implications to multiple bystanders.

The example calculation considers a patient who receives a radiopharmaceutical for cancer therapy on Friday and intends to rest and recover at home, mainly in isolation for three days before returning to work. A friend drives the patient home after the procedure, which takes 4 hours. The patient's family is planning a visit during the weekend of less than 4 hours. One of the visiting family members is a grandchild. In this example, the occupancy factor is calculated for three individuals: the driver, the grandchild, and a coworker. Based on manufacturer information for the radiopharmaceutical, the patient's retention is estimated to be 5% (or less) at 96 hours post-administration. As shown in **Figure *4-8***, the graphical template accepts three inputs (T_e, τ_1, and τ_2 or τ_{wk}) for each bystander.

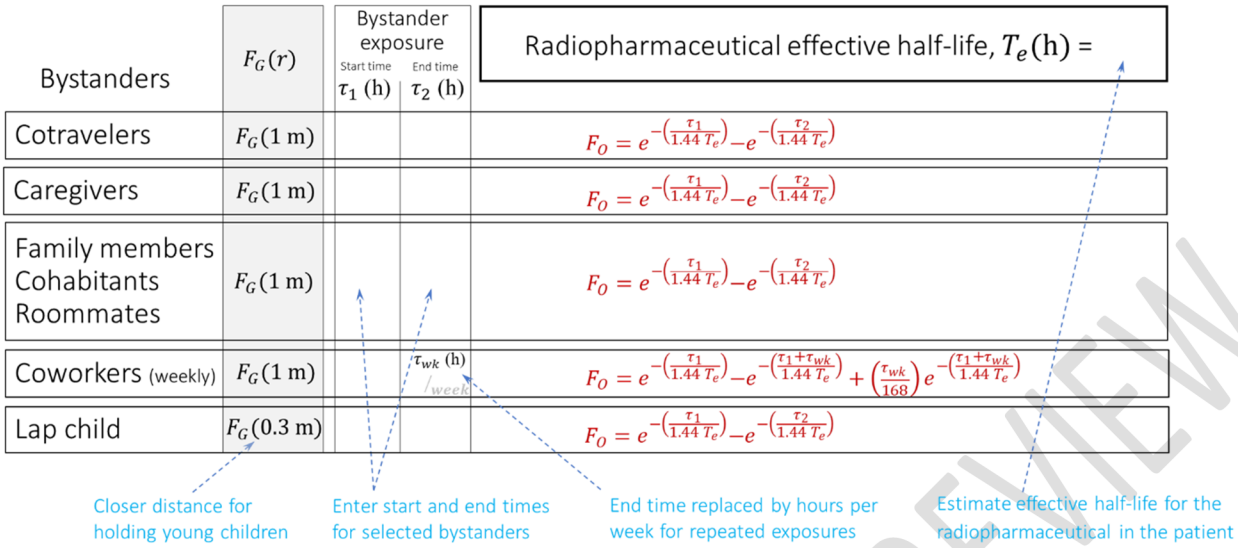

Figure 4-8 Graphical Survey Template for Bystander Occupancy

Main steps for the graphical survey for occupancy are presented below. **Figure *4-9*** illustrates example data.

1. Determine effective half-life of the radiopharmaceutical for the patient's retention using Equation [4-19]

$$T_e = -\frac{\ln(2)}{\ln(0.05)}(96\text{ h}) = 22\text{ h}$$

2. Identify potential maximum bystanders (e.g., driver, grandchild, and coworker)
3. Enter exposure start and end times (or repetitive exposure durations) for each bystander
4. Calculate the occupancy factor for each bystander

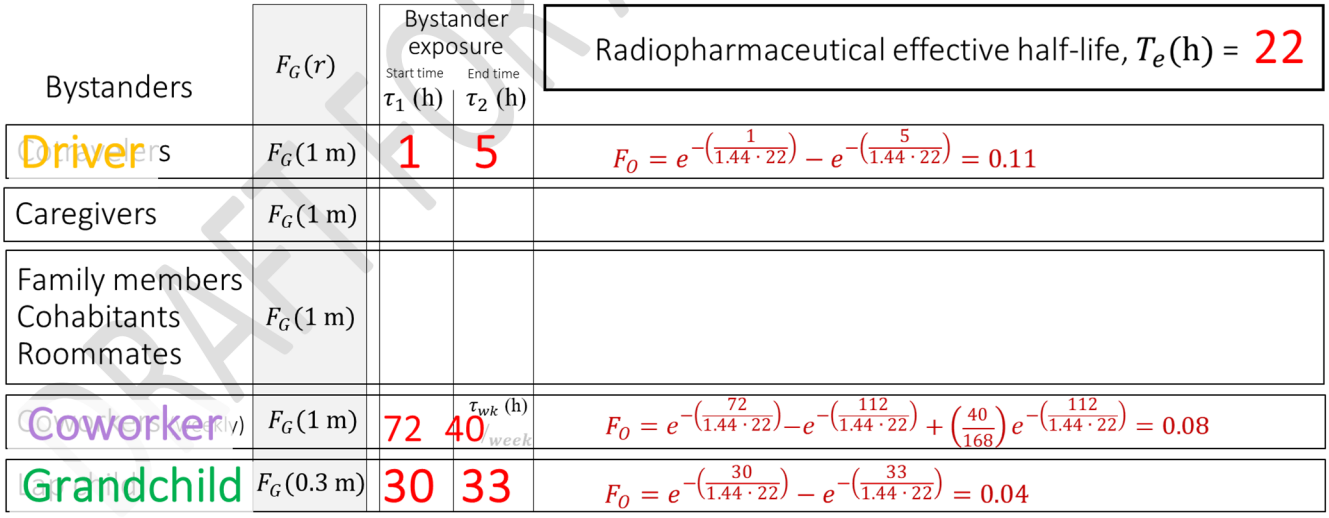

Figure 4-9 Example occupancy determination for multiple bystanders using the graphical template

Prior guidance (NRC 2020) allowed a value of 0.125 for occupancy with additional instructions. All three F_O values from this example are below 0.125; occupancy factors less than 0.125 can occur for realistic exposures when dose minimizing instructions are followed. The occupancy assessment should include bystander exposure characteristics for all potential maximally exposed individuals.

From **Figure *4-9*** for F_O and **Figure *4-7*** for F_G, the $F_O \cdot F_G$ products for the three bystanders are

- Driver: $F_O \cdot F_G(1\text{ m}) = 0.11 \cdot\ 0.79\ = 0.09$
- Coworker: $F_O \cdot F_G(1\text{ m}) = 0.08 \cdot\ 0.79 = 0.06$
- Grandchild: $F_O \cdot F_G(0.3\text{ m}) = 0.04 \cdot\ 4.6 = 0.18$

With the previously stated simplifications, the grandchild is determined to be the maximally exposed individual. This is largely due to the added realism of a larger geometric modification factor when the grandchild is being held by the patient. Timing of the exposure is accurately reflected in this prospective assessment with the graphical template and found to significantly influence the results. With these formulations, the occupancy modifying factor depends on the number of radioactive emissions when the bystander is in close contact with the patient. This is more realistic than estimations based primarily on time spent near the patient. If fact, the coworker spends the largest amount of time near the patient but yields the lowest expected dose in this example because the exposure occurs later in time. If the driver is also a family member who is exposed to the patient after travel, additional terms with different start and end times can be added to the calculation.

Patient Questionnaire as Supporting Information

Survey information can be collected from individual patients to inform the determination of modifying factors for occupancy, geometry, and attenuation. Answers to some questions could indicate uncertainty exists with the patient's ability to understand and ultimately follow discharge instructions, including restrictions for radiological protection. For example, the patient may (i) depend on others, (ii) indicate assistance is needed to read and understand instructions, or (iii) take medications to mitigate confusion. In these situations, cautious modifying factor assumptions or communicating instructions to individuals who are present to assist the patient can increase confidence in patient release decisions.

Table 4-2 Example Patient Questionnaire for Determining Patient-Specific Modifying Factors

To Be Completed by the Licensee						
Patient Identification Number						
Patient is capable and plans to follow discharge instructions including behavior restrictions?					yes	no
Estimate the patient's overlying tissue for attenuation and buildup: _____ cm						
Is a patient-to-bystander distance less than 1 m expected with a geometric modifying factor greater than 1?					yes	no
To Be Completed with Patient Input						
How long is the return trip home?						
Will someone accompany you on the return trip home?	yes / no	How will you be returning home?	my vehicle	bus	taxi	
			train	plane	other	
When will you return to work?		Do you spend more than 10 hours per week closer than 10 feet from the same person at work?			yes	no
Who do you see in person on a routine basis?						
Do you anticipate spending more than an hour a day closer than arm's length (1 meter) from another individual?	yes / no	If yes, at what distance and for how long?				
Do you/have you ever needed help with the following tasks?	getting on and off chairs	walking	using the restroom	bathing		
	getting in and out of vehicles	cooking/ eating	reading/understanding instructions	none of the above		
Do you live in an apartment or facility with other people in adjacent rooms/on adjacent floors?					yes	no
Are you currently nursing (breastfeeding) a child?	yes / no	Could you be pregnant?	yes / no	Do you share a bed with anyone?	yes	no
Are you able to sleep in your own bed without another person for some length of time after the procedure?					yes	no
Are you willing to change your behavior as directed by posttreatment instructions to minimize exposure to other individuals?					yes	no

Flux Calculations for the Geometric Modifying Factor

Geometric flux relationships are presented for radiation transport without attenuation and buildup. Three basic irradiation geometries are investigated: Point-Point, Point-Line, and Line-Line. Differences among the results for Point-Point and Line-Line assumptions are shown to be large at distances less than 1 m.

Point Source & Point Target

$$\phi_{\text{Point-Point}} = \frac{S}{4\pi r^2}$$ Equation [4-21]

where

S source emission rate $\left(\frac{\gamma}{s}\right)$ and

r distance between the source and target.

Point Source & Line Target

$$\phi_{\text{Point-Line}} = \frac{S}{4\pi L r}\left[\tan^{-1}\left(\frac{h}{r}\right) + \tan^{-1}\left(\frac{L-h}{r}\right)\right]$$ Equation [4-22]

where

L length of the line target and

h vertical position of the source point ($0 \le h \le L$).

Equation [4-22] can be rewritten for the minimum and maximum heights of the target line

$$\phi_{\text{Point-Line}} = \frac{S}{4\pi (h_{max}-h_{min}) r}\left[\tan^{-1}\left(\frac{h_{max}-h^*}{r}\right) + \tan^{-1}\left(\frac{h^*-h_{min}}{r}\right)\right]$$ Equation [4-23]

where

h^* height of the point source

h_{max} maximum vertical position of the target line, and

h_{min} minimum vertical position of the target line.

Figure 4-10 illustrates the point-line irradiation geometries for the parameterization shown in Equation [4-22] and Equation [4-23]. Point-Line irradiation geometries can be representative for bystander irradiation by a patient with prostate seed implants or a patient with substantial radionuclide uptake by the thyroid and minimal redistribution to other parts of the body. **Figure *4-11*** presents dimensions in the calculation of the geometric modifying factor for these irradiation scenarios. Because parameter definitions in Equation [4-22] and Equation [4-23] can be inverted for an analogous geometry with a line source and point target, inverted geometries for Line-Point irradiation are not presented further.

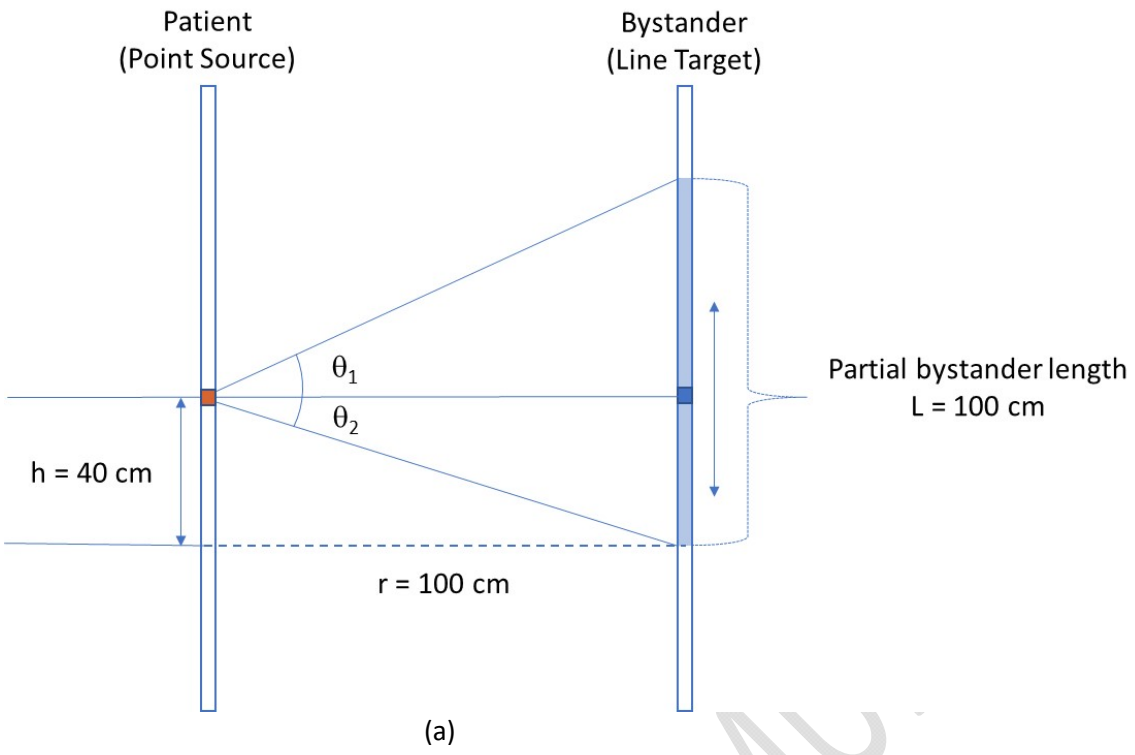

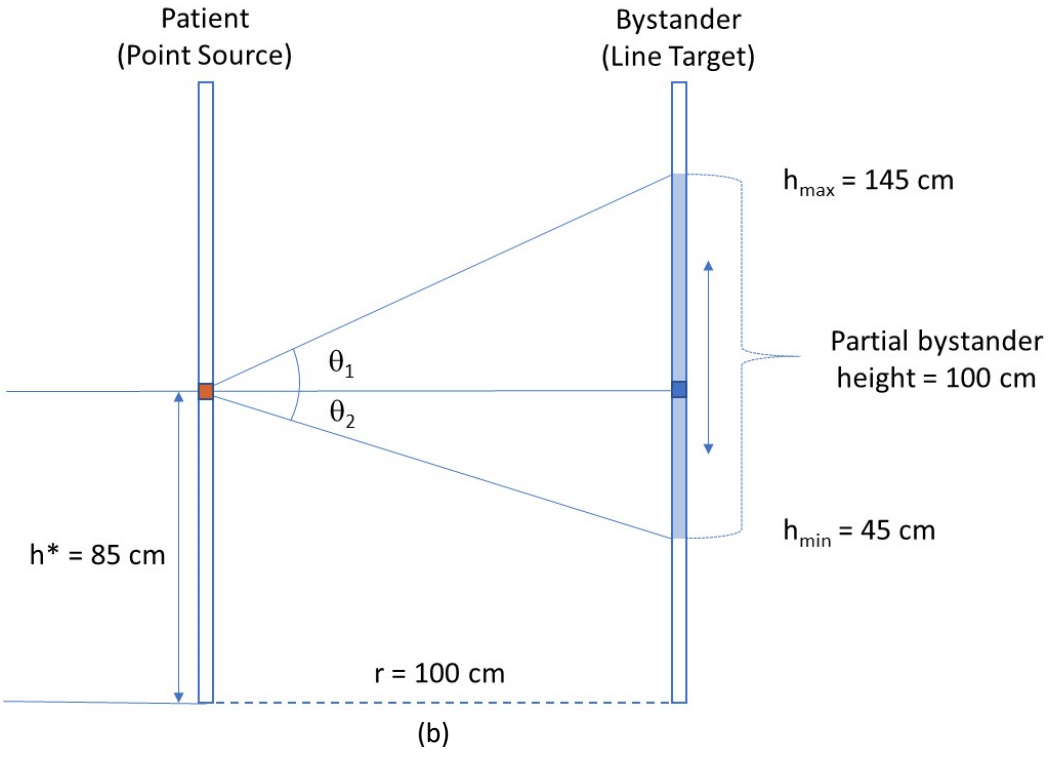

Figure 4-10 Point-Line geometries with parameterization for (a) Equation [4-22] and (b) Equation [4-23]

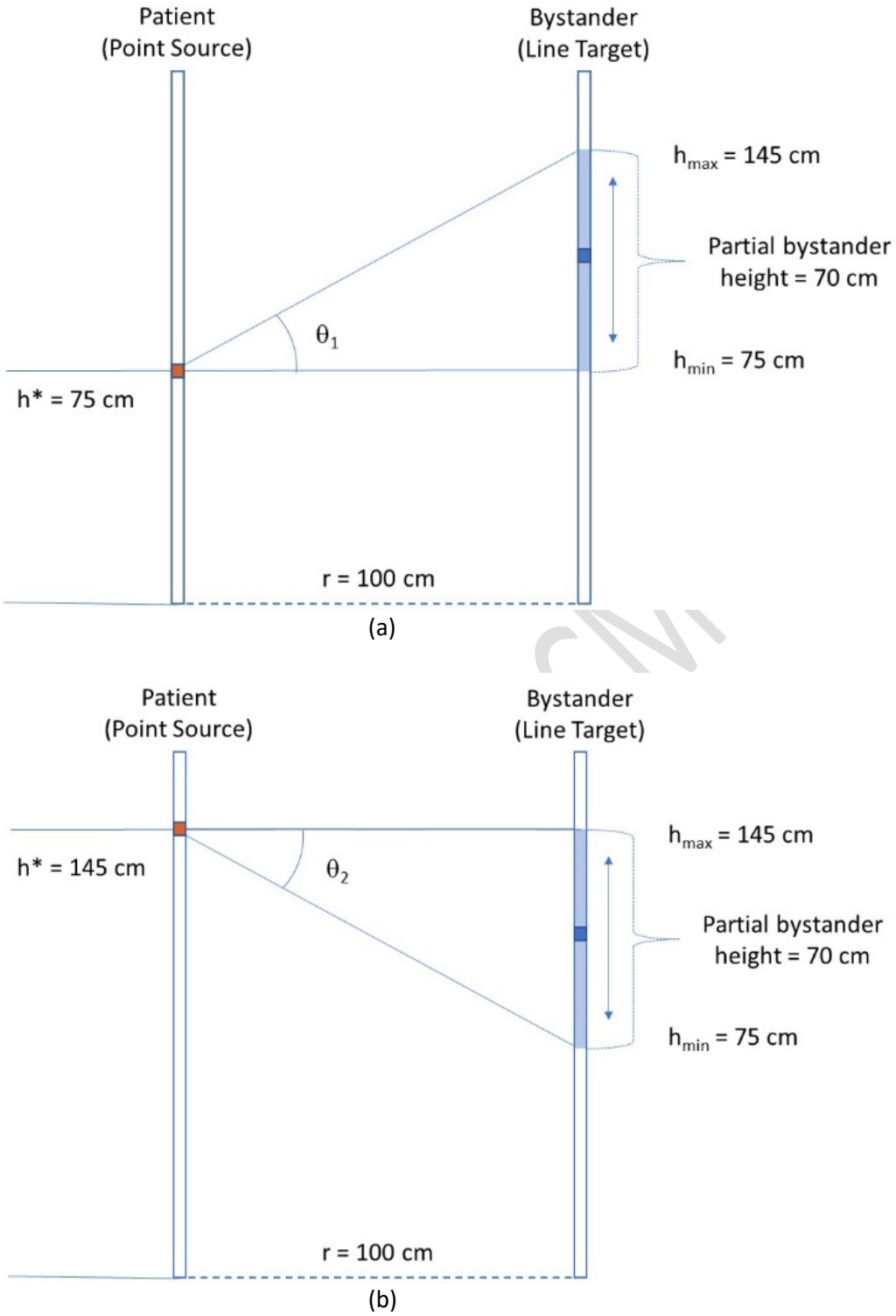

Figure 4-11 Point-Line irradiation geometries for calculating the geometric modifying factor representing (a) prostate seed implants and (b) radionuclide uptake by the thyroid. Both shown with a separation distance of 1 m

Line Source & Line Bystander

To extend Point-Line results for a line-line irradiation geometry, the point-line relationship in Equation [4-22] is integrated over a range of source points

$$\Phi_{\text{Line-Line}} = \frac{S}{4\pi\, L\, r} \frac{\int_{h_{min}}^{h_{max}} \left[\tan^{-1}\left(\frac{h}{r}\right) + \tan^{-1}\left(\frac{L-h}{r}\right)\right] dh}{\int_{h_{min}}^{h_{max}} dh} \qquad \text{Equation [4-24]}$$

with minimum and maximum vertical positions of the source point, denoted by h_{min} and h_{max} as the limits of integration.

Applying substitution for $x = L - h$ and $dx = -dh$, the second term of numerator can be written as

$$\int_{h_{min}}^{h_{max}} \tan^{-1}\left(\frac{L-h}{r}\right) dh = -\int_{L-h_{min}}^{L-h_{max}} \tan^{-1}\left(\frac{x}{r}\right) dx = \int_{L-h_{max}}^{L-h_{min}} \tan^{-1}\left(\frac{x}{r}\right) dx$$

Performing the integration in the denominator, the general expression becomes

$$\Phi_{\text{Line-Line}} = \frac{S}{4\pi\, L\, r} \frac{\int_{h_{min}}^{h_{max}} \tan^{-1}\left(\frac{h}{r}\right) dh + \int_{L-h_{max}}^{L-h_{min}} \tan^{-1}\left(\frac{x}{r}\right) dx}{h_{max} - h_{min}} \qquad \text{Equation [4-25]}$$

For a full-length bystander with h_{min}= 0 cm and h_{max} = L, symmetry allows for further simplifications

$$\Phi_{\text{Line-Line}} = \frac{S}{2\pi\, L^2\, r} \int_0^L \tan^{-1}\left(\frac{h}{r}\right) dh$$

Applying the generic solution $\int \tan^{-1}\left(\frac{h}{r}\right) dh = h \tan^{-1}\left(\frac{h}{r}\right) - \frac{r}{2} \ln\left(\frac{r^2+h^2}{r^2}\right)$ with the limits of integration for a full-length bystander yields

$$\Phi_{\text{Line-Line}} = \frac{S}{2\pi\, L^2\, r} \left[L \tan^{-1}\left(\frac{L}{r}\right) - \frac{r}{2} \ln\left(\frac{r^2+L^2}{r^2}\right)\right] \qquad \text{Equation [4-26]}$$

Figure *4-12* highlights the line-source and line-target irradiation geometry for a full-length source and full-length target shown in Equation [4-26].

To account for sensitive organs of the bystander distributed within a partial height, **Figure *4-13*** illustrates this line-line geometry with a partial target height of 0.7 m (70 cm). Compared to a full-length target line, shortening the length of target line results in a higher average radiation flux because ends of the target line are not included in the average. Ends of the target line experience lower radiation fluxes compared to points on the target line near its midpoint. Therefore, averaging the radiation flux over a shorter target line across from the midpoint of the source line will yield an increased result compared to averaging over the entire height of the bystander. The sensitivity of the average flux to this length reduction and its dependency on the dimensions of the irradiation geometry are investigated further.

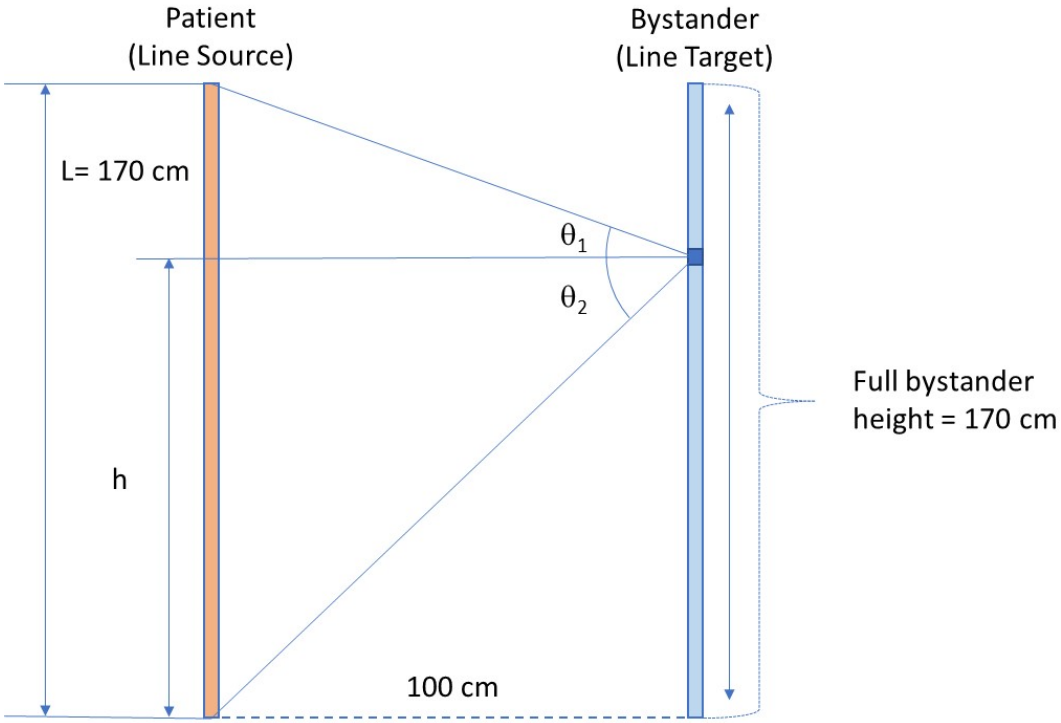

Figure 4-12 Line-Line irradiation geometries for a full-length patient and full-length bystander

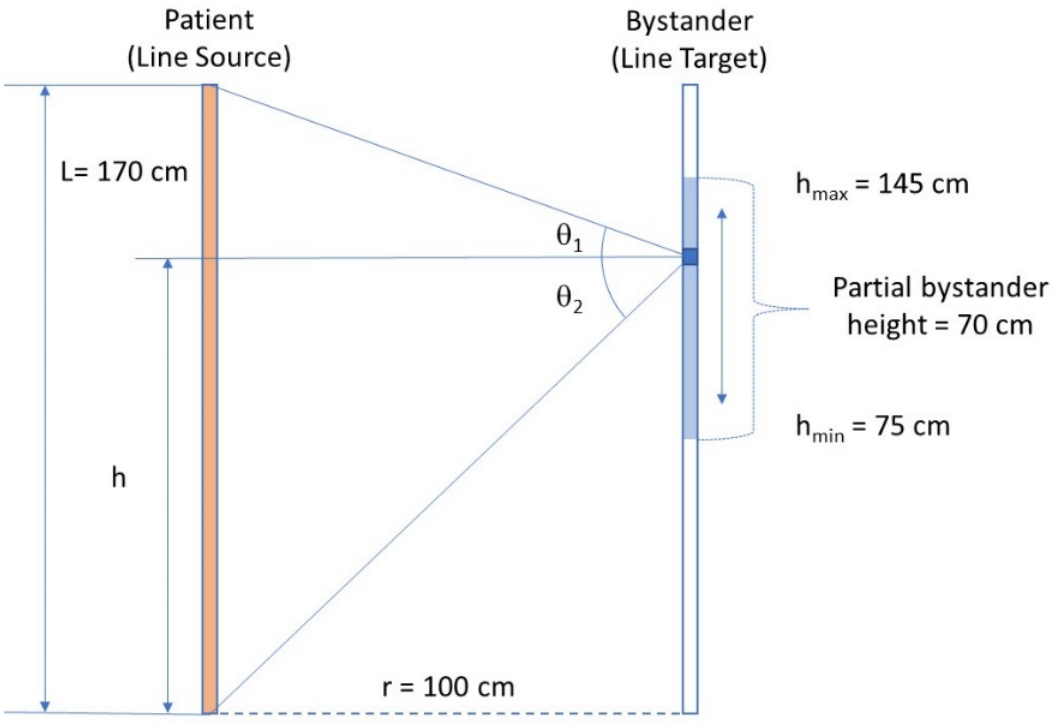

Figure 4-13 Line-Line irradiation geometries for calculating the geometric modifying factor with a partial bystander height representing a distribution of sensitive organs in the bystander

To avoid underestimating the geometric modifying factor, the 0.7-m partial height for target organs is adopted for an adult bystander. However, the previous symmetry resulting in Equation [4-26] does not apply to the partial bystander height. Therefore, Equation [4-25] evaluated according to its integration limits yields

$$\phi_{Line-Line} = \frac{S}{2\pi L\,(h_{max}-h_{min})r}\left\{\begin{array}{c}\left[h_{max}\tan^{-1}\left(\frac{h_{max}}{r}\right)-h_{max}\tan^{-1}\left(\frac{h_{min}}{r}\right)\right]\\ -\left[\frac{r}{2}\ln\left(\frac{r^2+{h_{max}}^2}{r^2}\right)-\frac{r}{2}\ln\left(\frac{r^2+{h_{min}}^2}{r^2}\right)\right]\\ +\left[(L-h_{min})\tan^{-1}\left(\frac{L-h_{min}}{r}\right)-(L-h_{max})\tan^{-1}\left(\frac{L-h_{max}}{r}\right)\right]\\ -\left[\frac{r}{2}\ln\left(\frac{r^2+(L-h_{min})^2}{r^2}\right)-\frac{r}{2}\ln\left(\frac{r^2+(L-h_{max})^2}{r^2}\right)\right]\end{array}\right\} \quad \text{Equation [4-27]}$$

For a range of separation distances, **Figure *4-14*** compares average flux results for point-point and line-line irradiation geometries, as calculated by Equation [4-21] and Equation [4-27] respectively. Differences in the average flux for point-point and line-line assumptions become large as the separation distance decreases below 1 m. At very close distances, point-point irradiation geometries become unrealistic and overly conservative. This sensitivity highlights a need to exercise caution when modeling bystander exposures to a patient at distances considerably closer than 1 m. Therefore, the line-line and point-line irradiation geometries were considered further for calculating the geometric modifying factor.

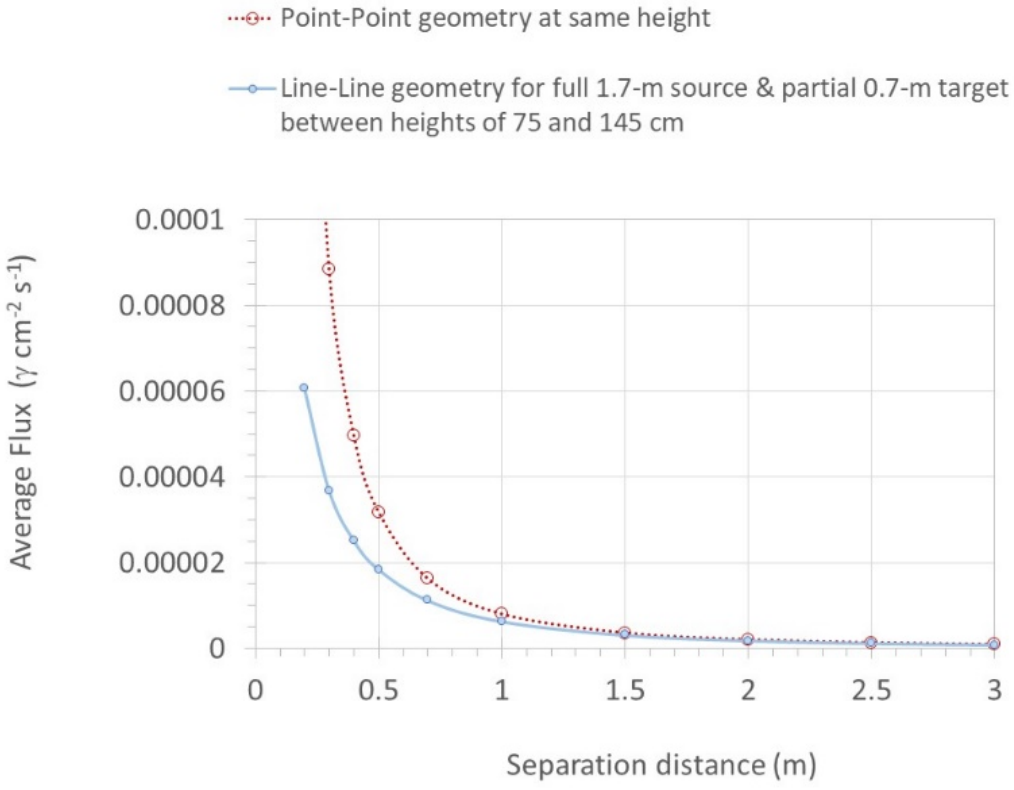

Figure 4-14 Comparison of the average flux without attenuation and buildup

Figure 4-15 compares geometric modifying factors for various irradiation geometries and distances, based on the average radiation flux without considering attenuation and buildup. According to the dimensions in Figure 4-13, results for line-line irradiation were calculated from Eq [4-27]. For comparative purposes, the point-line irradiation geometry shown in **Figure *4-15*** was included to represent radionuclide concentrations in either the prostate or thyroid. Average radiation fluxes were slightly higher for the point-line irradiation geometry compared to the

line-line irradiation geometry over a broad range of separation distances. Differences shown in **Figure *4-15*** were deemed small enough to not require a separate tabulation of geometric modifying factors because the results do not include larger potential influences from the combined effects of unmodeled attenuation and buildup as well as unmodeled lateral distributions of the source and target organs that tend to reduce the average radiation flux. Equations in this appendix enable future calculations, approximations, and comparisons for alternative irradiation dimensions.

As previously demonstrated by **Figure *4-14***, extended source and target dimensions have a limited influence on the average radiation flux at separation distances greater than 2 m. This geometric insensitivity at distances greater than 2 m is also supported by **Figure *4-14*** and **Figure *4-15***. **Figure *4-15*** includes an irradiation geometry for a mother holding a child. The irradiation geometry for a child being held is shown in **Figure *4-16*** with the child's body length parallel to the patient, because holding the child horizontal across the patient's chest (**Figure *4-17***) resulted in a 13-percent-lower average flux. For simplicity, this alternative horizontal irradiation position is not included in **Figure *4-15***.

Figure *4-17* displays breastmilk as two circular sources. Because the average flux is calculated along the target line without attenuation and buildup from radiation interactions in tissue, it is permissible to simplify breastmilk irradiation by replacing each circular source with a point source.

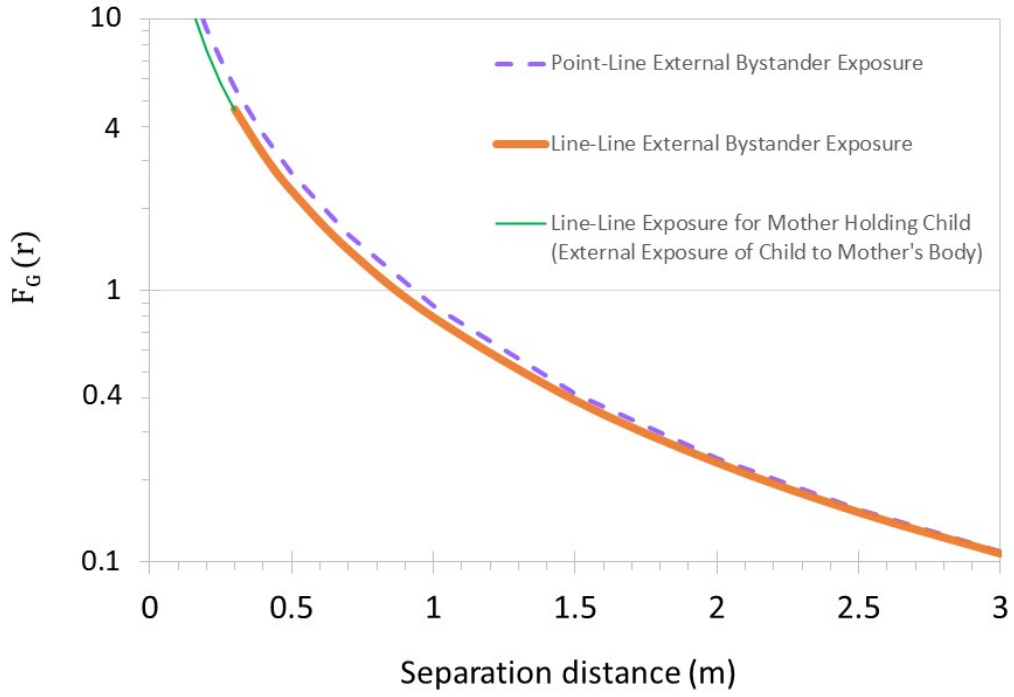

Figure 4-15 Geometric modifying factors for external exposure

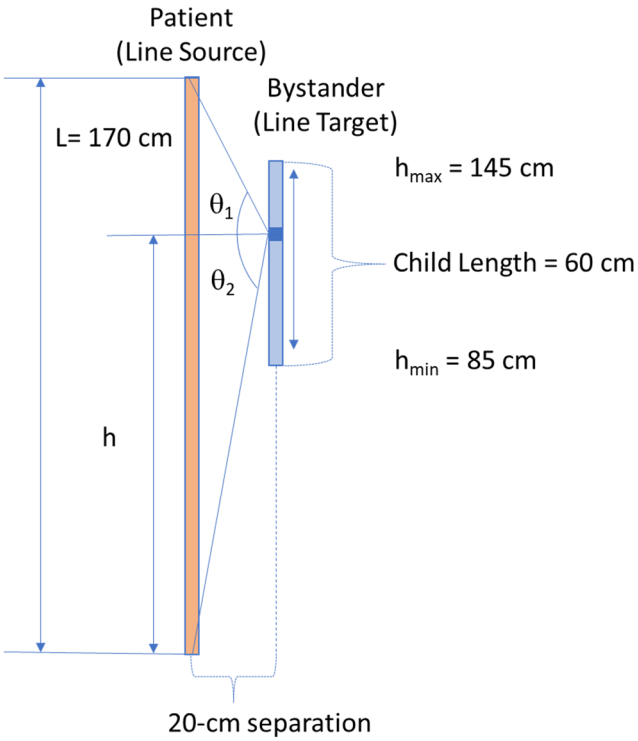

Figure 4-16 Line-Line irradiation geometry for a child being held during breastfeeding

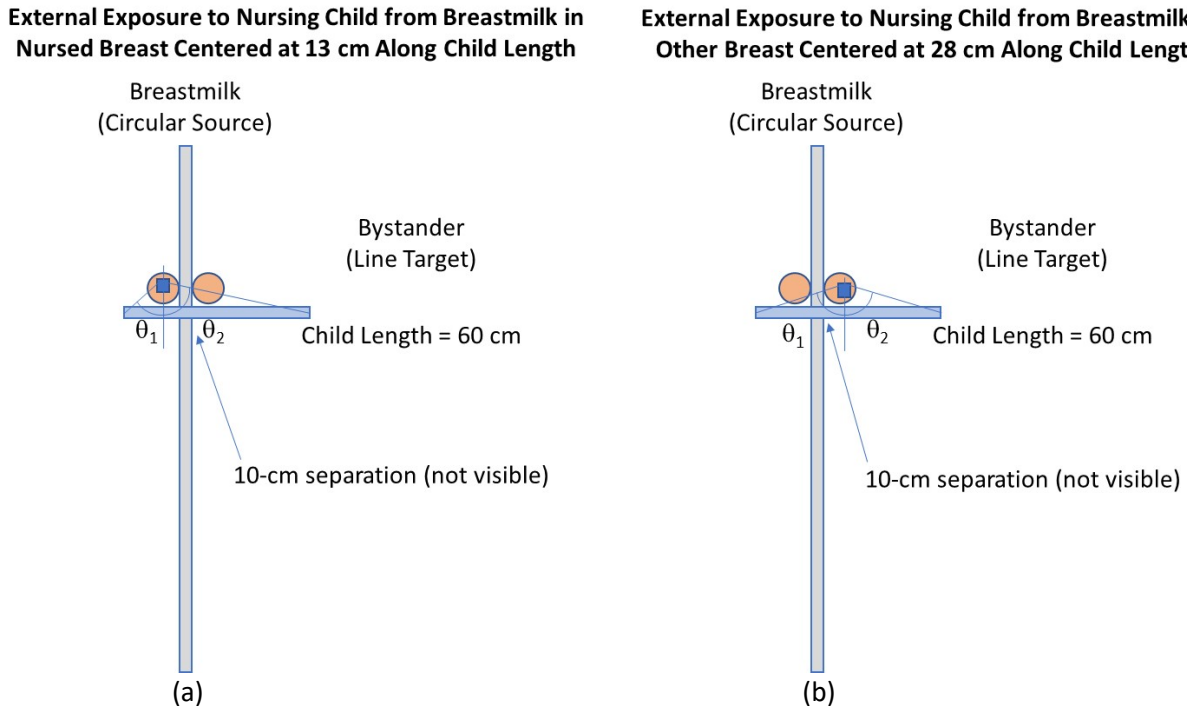

Figure 4-17 Irradiation geometries for external exposure of the child's body to breastmilk radioactivity in the (a) nursed breast and (b) other breast. One geometric modifying factor for breastmilk exposure is developed from averaging results of two irradiation geometries

Compared to a simplified point-line geometry, the effective separation distance to the target line from all points on the circular source would be slightly greater. Changes to the linear extent of the target line, as viewed from all points on each circle compared to its center, also imply a reasonable but slightly conservative point-line simplification for breastmilk irradiation. Specifically, modeling breastmilk as a point source overestimated the average flux by less than 5 percent for a target length of 60 cm. For the point-line simplification of breastmilk irradiation, Equation [4-22] is applied twice—once for a vertical position of 13 cm and once for a vertical position of 28 cm—and averaged.

Attenuation Factors for Various Tissue Thicknesses

Figure 4-18 features 40 plots for attenuation and buildup effects in the modifying factor F_A. By noting the location of the source in the patient's body and the average tissue thickness between the source and the body surface, the appropriate thickness of tissue (x-axis) can be selected for the exposure scenario. The "Attenuation Factor" (y-axis) represents the point-kernel dose constant for a given attenuation/buildup thickness relative to the point-kernel dose constant for no tissue thickness. In all plots, the attenuation factor equals one (1) at a tissue thickness of zero. The attenuation factor, F_A, generally takes values between zero and one, but values greater than one are possible.

For example, the standard assumption of no attenuating tissue results in Δ_{pr} = 0.0194 [mSv m^2 GBq^{-1} h^{-1}] for ^{99m}Tc. When ^{99m}Tc is administered to a patient with only a few cm of overlying tissue (e.g., 5 cm in this example), the dose-rate kernel increases due to photon buildup such that Δ_{pr} = 0.0229 [mSv m^2 GBq^{-1} h^{-1}]. The ratio of these dose-rate kernels for a specific tissue thickness determines the attenuation factor F_A:

$$F_A = \text{Relative dose kernel} = \frac{\Delta_{pr} \text{ for 5 cm}}{\Delta_{pr} \text{for 0 cm}} = \frac{0.0229}{0.0194} = 1.18. \quad \text{Equation [4-28]}$$

This section contains plots for the attenuation factor as a function of tissue thickness. The calculated value for F_A with 5 cm of tissue—shown above and in the plot for ^{99m}Tc—is greater than one (1) because the buildup of photons through 5 cm of tissue is greater than the loss due to attenuation in that same thickness. In general, buildup is most important in the photon energy range of 60 – 80 keV, and therefore, nuclides with an abundance of these low-energy photon emissions, or those with high contributions from bremsstrahlung photons, may exhibit F_A values greater than one (1) within 5 – 15 cm of tissue.

Examining the plot for ^{18}F for example, it is noted that F_A does not exceed one (1) because buildup and attenuation offset equally until attenuation dominates at tissue thickness greater than about 5 cm. Users should estimate the minimum amount of tissue through which the photons would pass or use the radius of the patient's torso if the activity is uniformly distributed throughout the body. In contrast, differences in metal encasements of implants have very little impact on the attenuation/buildup factors and are not considered further.

As an additional illustration, a patient is assumed to have a uniform distribution of ^{67}Ga throughout their torso following the administration of ^{67}Ga-citrate. For a patient torso girth of 160 cm, the average radius is

$$r = \frac{G}{2\pi} = \frac{160 \text{ [cm]}}{2\pi} = 25 \text{ [cm]}. \quad \text{Equation [4-29]}$$

For a 25-cm thickness, $F_A = 0.7$ for ^{67}Ga implies a 30% reduction in bystander dose due to tissue attenuation.

Figure 4-18 Attenuation modifying factors versus tissue thickness for 40 radionuclides: C-14, F-18, P-32, P-33, Sc-47, Cr-51, Cu-64, Cu-67, Ga-67, Se-75, Zr-89, Sr-89, Sr-90, Y-90, Tc-99m, Pd-103, Ru-106, Ag-111, In-111, Sn-177m, I-123, I-124, I-125, Xe-127, I-131, Cs-131, Xe-133, Sm-153, Dy-165, Ho-166, Er-169, Yb-169, Lu-177, Re-186, Re-188 Ir-192, Au-198, Tl-201, At-211, and Ra-223

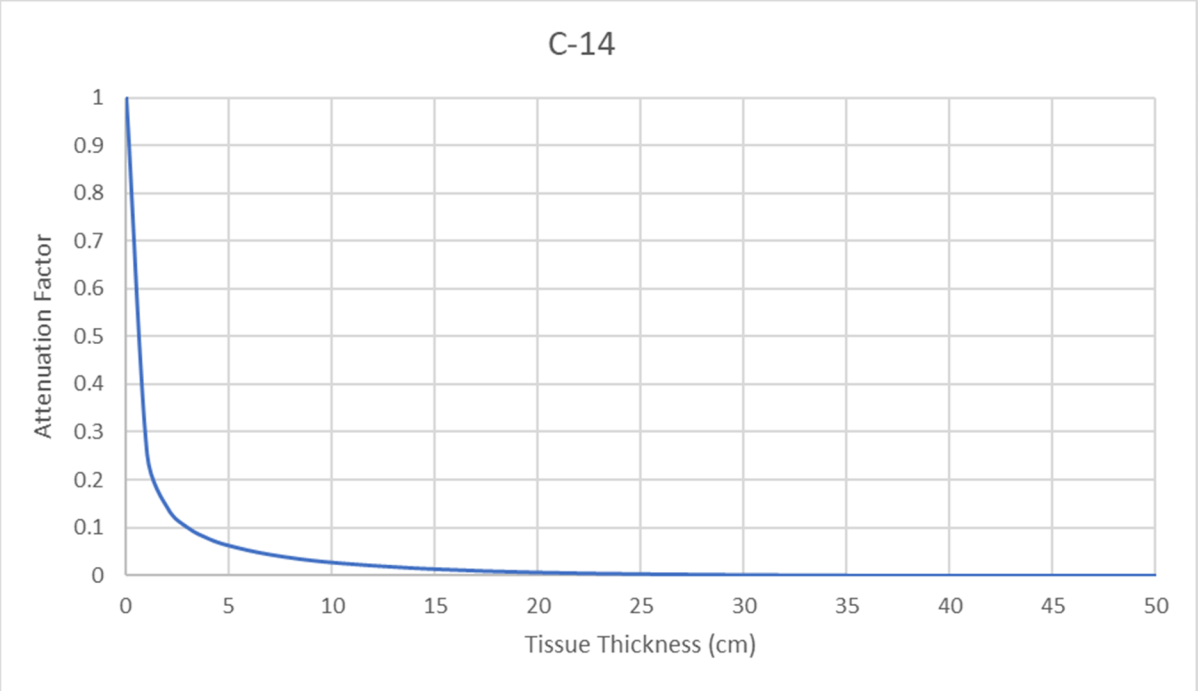

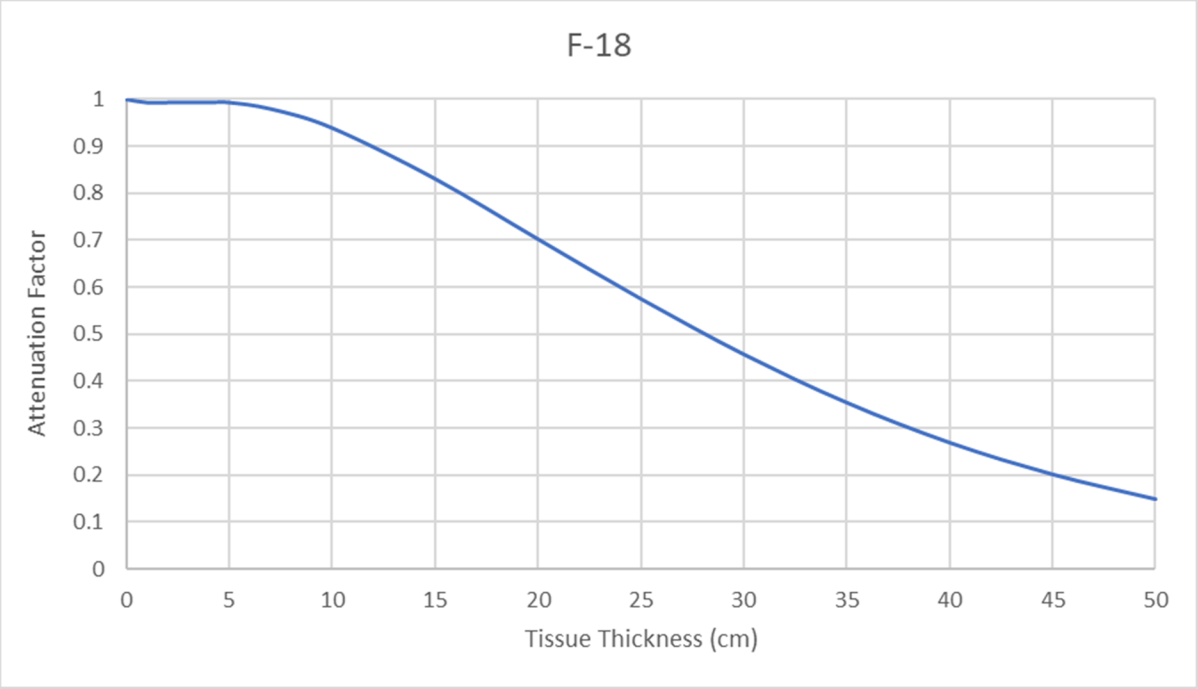

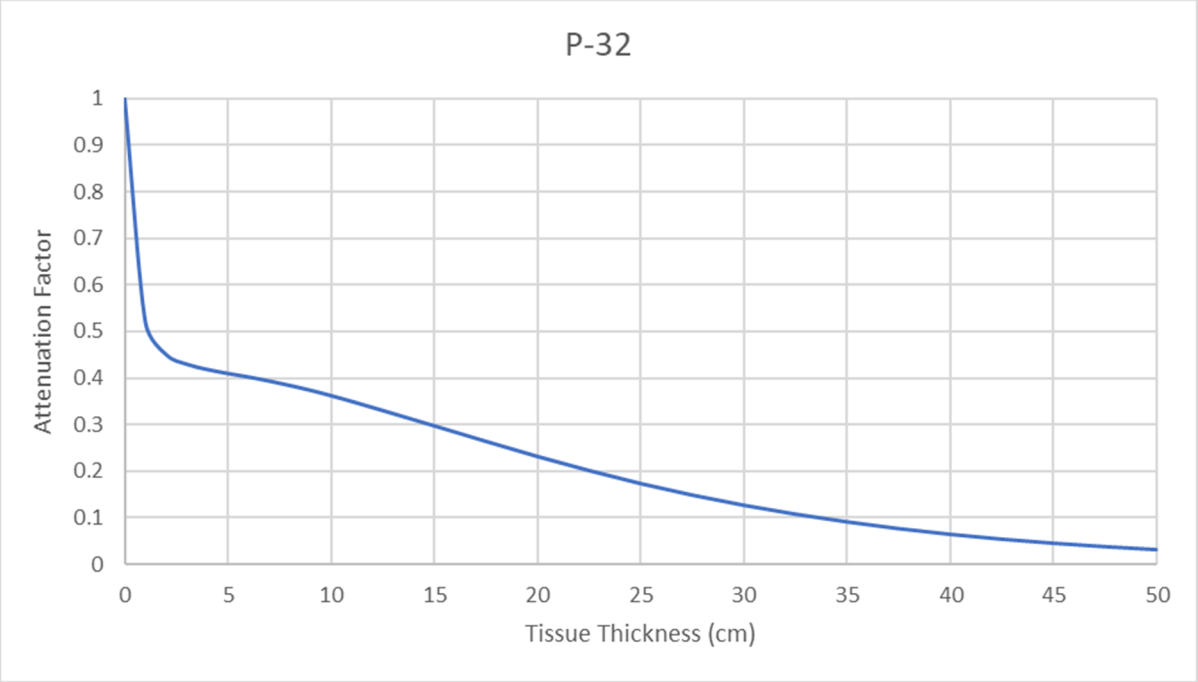
P-32
Attenuation Factor
1
0.9
0.8
0.7
0.6
0.5
0.4
0.3
0.2
0.1
0
0
5
10
15
20
25
30
35
40
45
50
Tissue Thickness (cm)

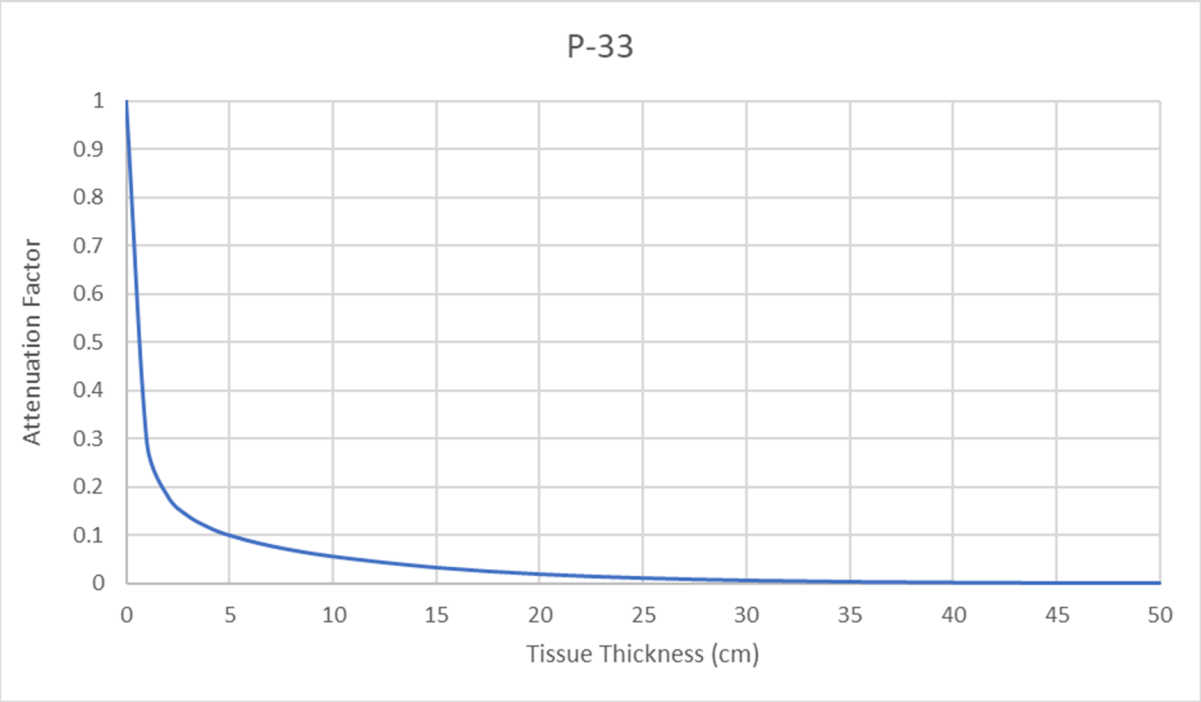
P-33
Attenuation Factor
1
0.9
0.8
0.7
0.6
0.5
0.4
0.3
0.2
0.1
0
0
5
10
15
20
25
30
35
40
45
50
Tissue Thickness (cm)

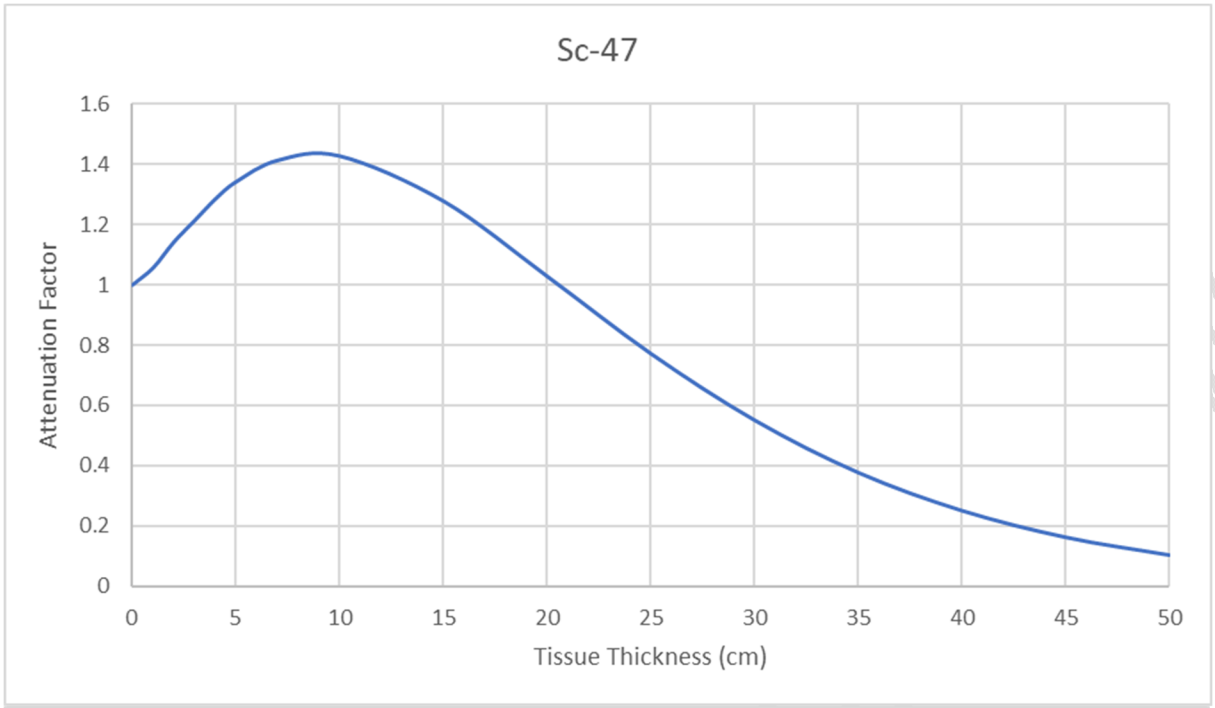
Sc-47
Attenuation Factor
1.6
1.4
1.2
1
0.8
0.6
0.4
0.2
0
0
5
10
15
20
25
30
35
40
45
50
Tissue Thickness (cm)

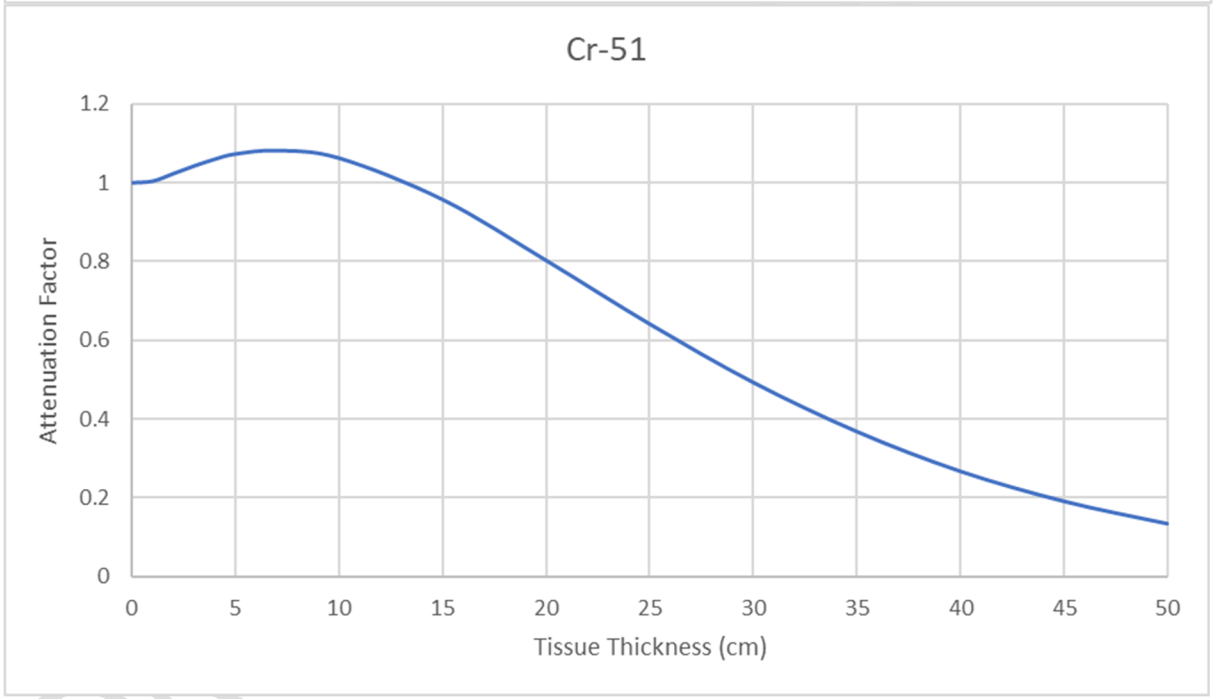
Cr-51
Attenuation Factor
1.2
1
0.8
0.6
0.4
0.2
0
0
5
10
15
20
25
30
35
40
45
50
Tissue Thickness (cm)


Cu-64
Attenuation Factor
1
0.9
0.8
0.7
0.6
0.5
0.4
0.3
0.2
0.1
0
0
5
10
15
20
25
30
35
40
45
50
Tissue Thickness (cm)


Cu-67
Attenuation Factor
1.6
1.4
1.2
1
0.8
0.6
0.4
0.2
0
0
5
10
15
20
25
30
35
40
45
50
Tissue Thickness (cm)

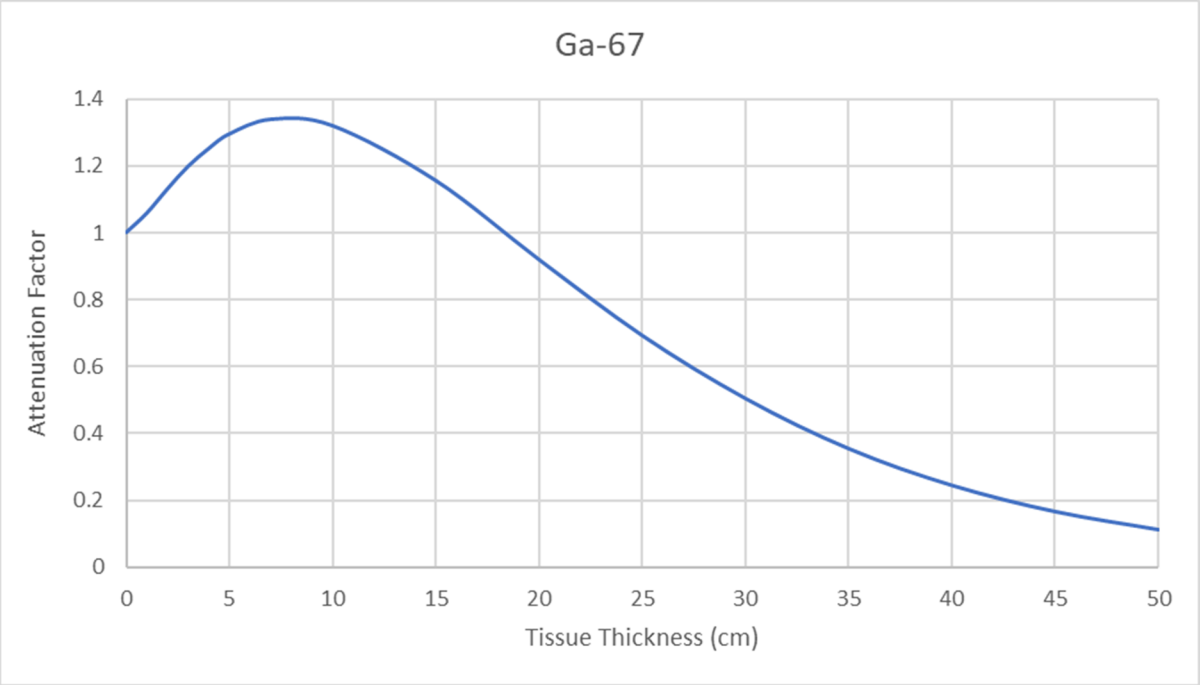
Ga-67
Attenuation Factor
1.4
1.2
1
0.8
0.6
0.4
0.2
0
0
5
10
15
20
25
30
35
40
45
50
Tissue Thickness (cm)

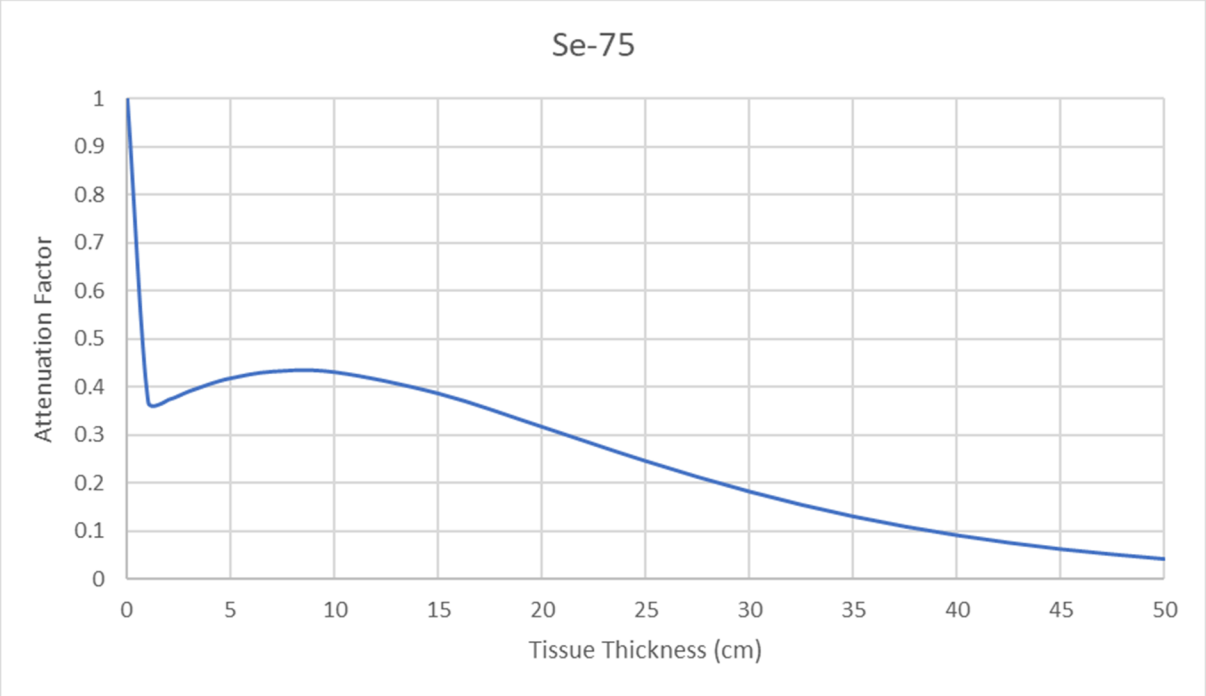
Se-75
Attenuation Factor
1
0.9
0.8
0.7
0.6
0.5
0.4
0.3
0.2
0.1
0
0
5
10
15
20
25
30
35
40
45
50
Tissue Thickness (cm)

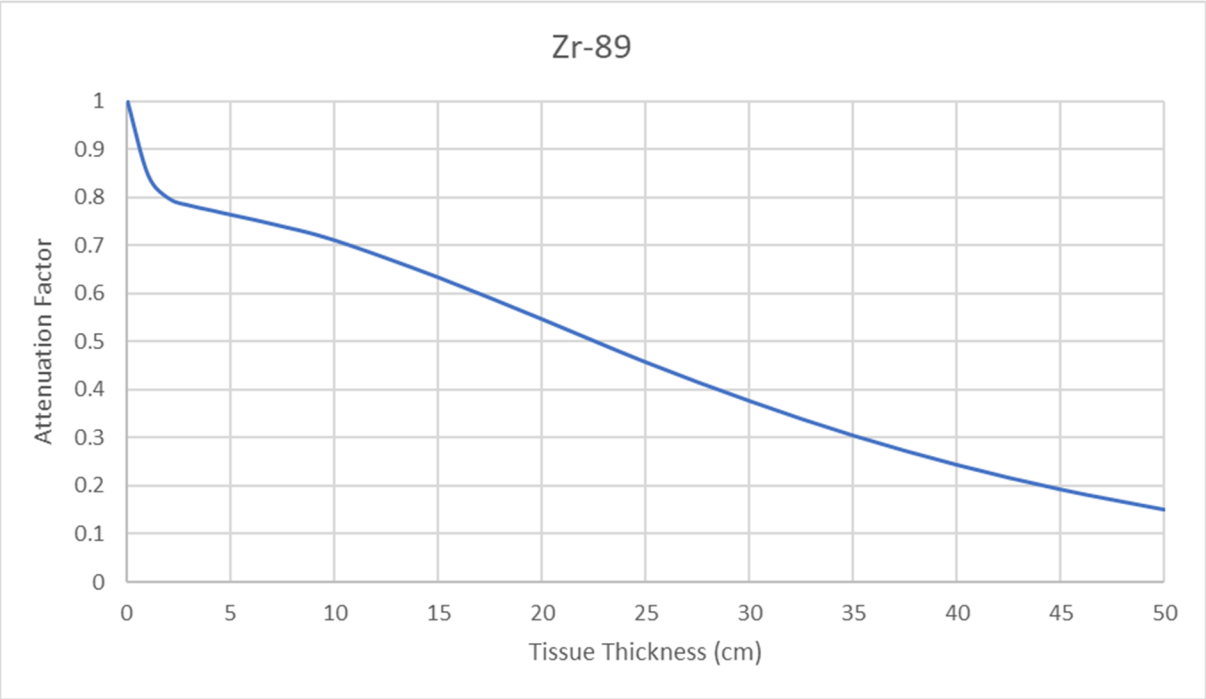
Zr-89
Attenuation Factor
1
0.9
0.8
0.7
0.6
0.5
0.4
0.3
0.2
0.1
0
0
5
10
15
20
25
30
35
40
45
50
Tissue Thickness (cm)

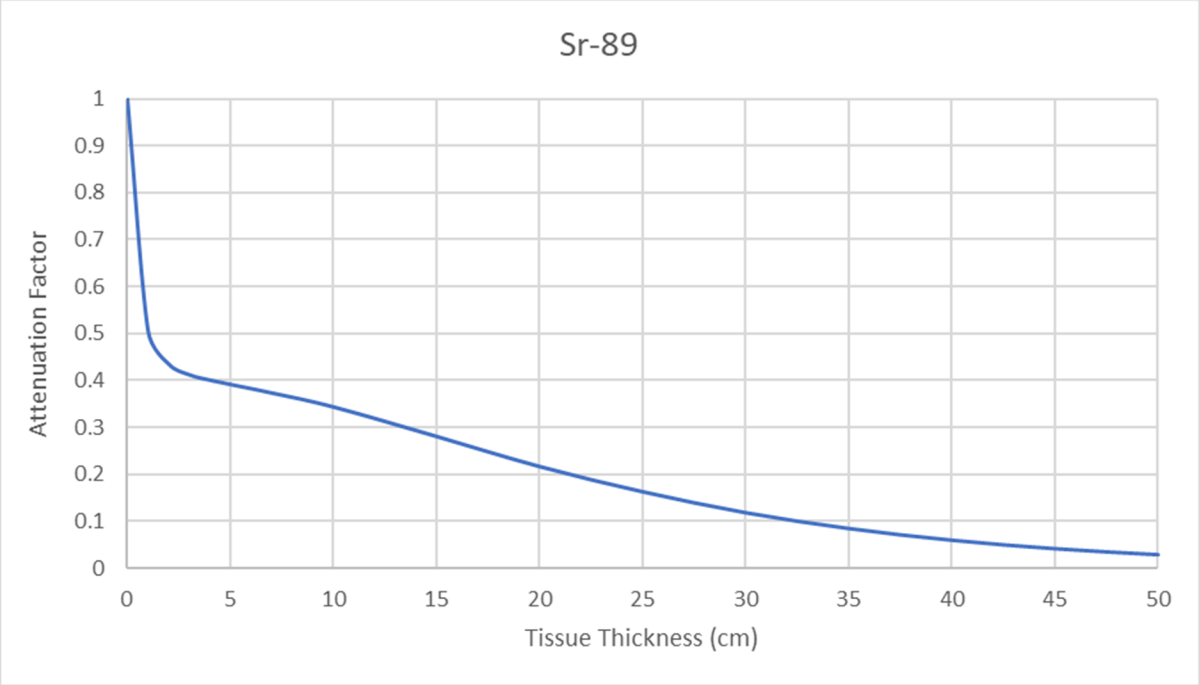
Sr-89
Attenuation Factor
1
0.9
0.8
0.7
0.6
0.5
0.4
0.3
0.2
0.1
0
0
5
10
15
20
25
30
35
40
45
50
Tissue Thickness (cm)

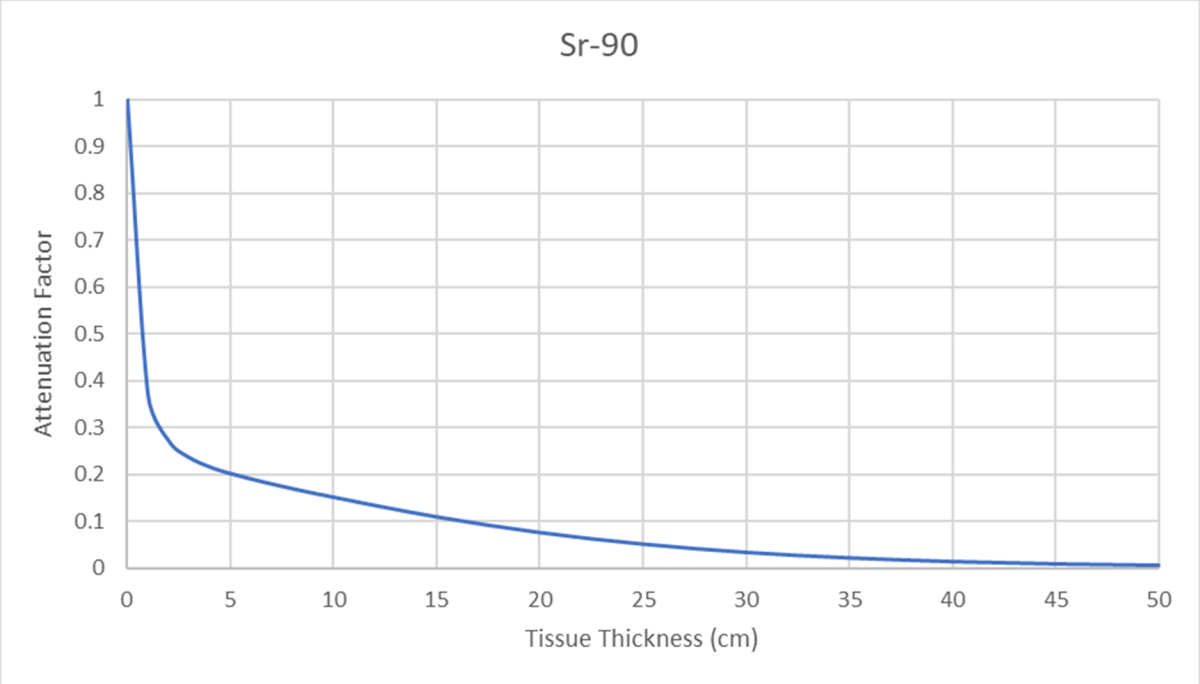
Sr-90
Attenuation Factor
1
0.9
0.8
0.7
0.6
0.5
0.4
0.3
0.2
0.1
0
0
5
10
15
20
25
30
35
40
45
50
Tissue Thickness (cm)

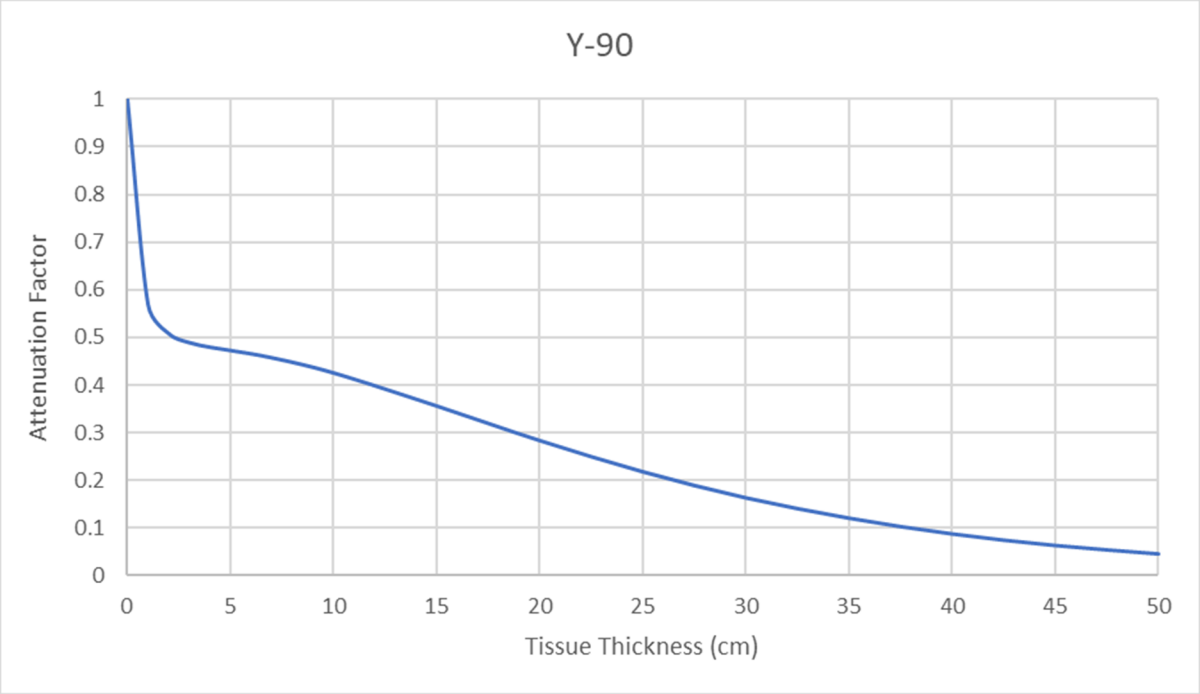
Y-90
Attenuation Factor
1
0.9
0.8
0.7
0.6
0.5
0.4
0.3
0.2
0.1
0
0
5
10
15
20
25
30
35
40
45
50
Tissue Thickness (cm)

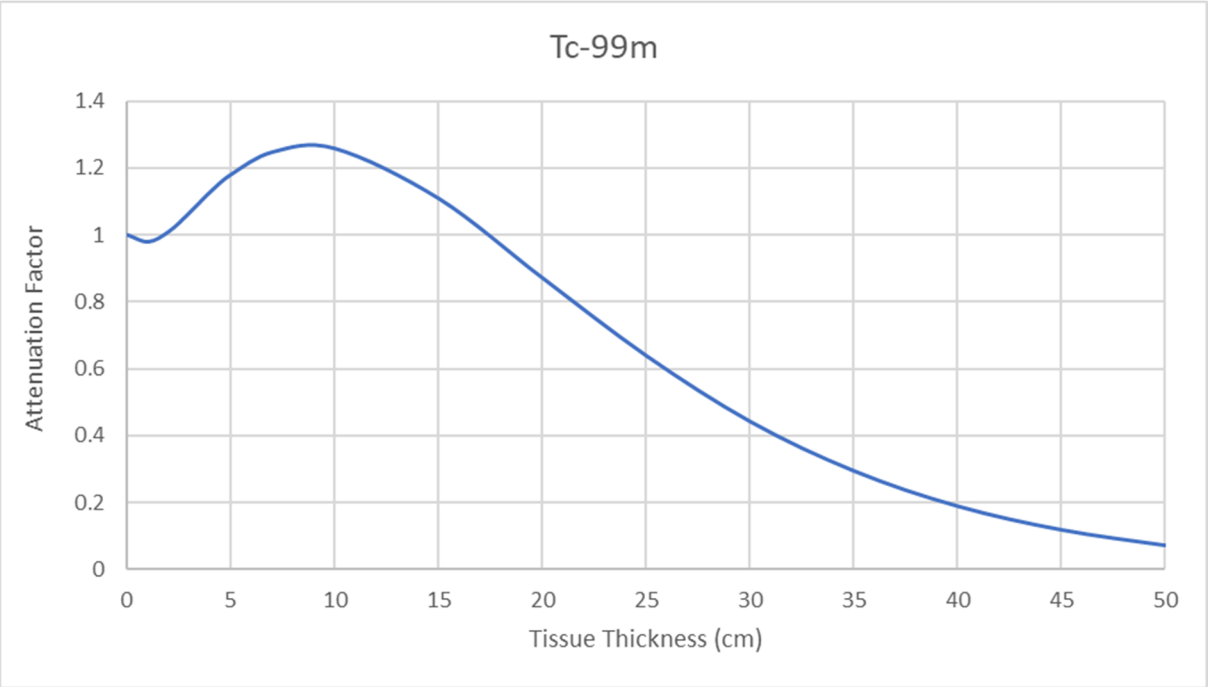
Tc-99m
Attenuation Factor
1.4
1.2
1
0.8
0.6
0.4
0.2
0
0
5
10
15
20
25
30
35
40
45
50
Tissue Thickness (cm)

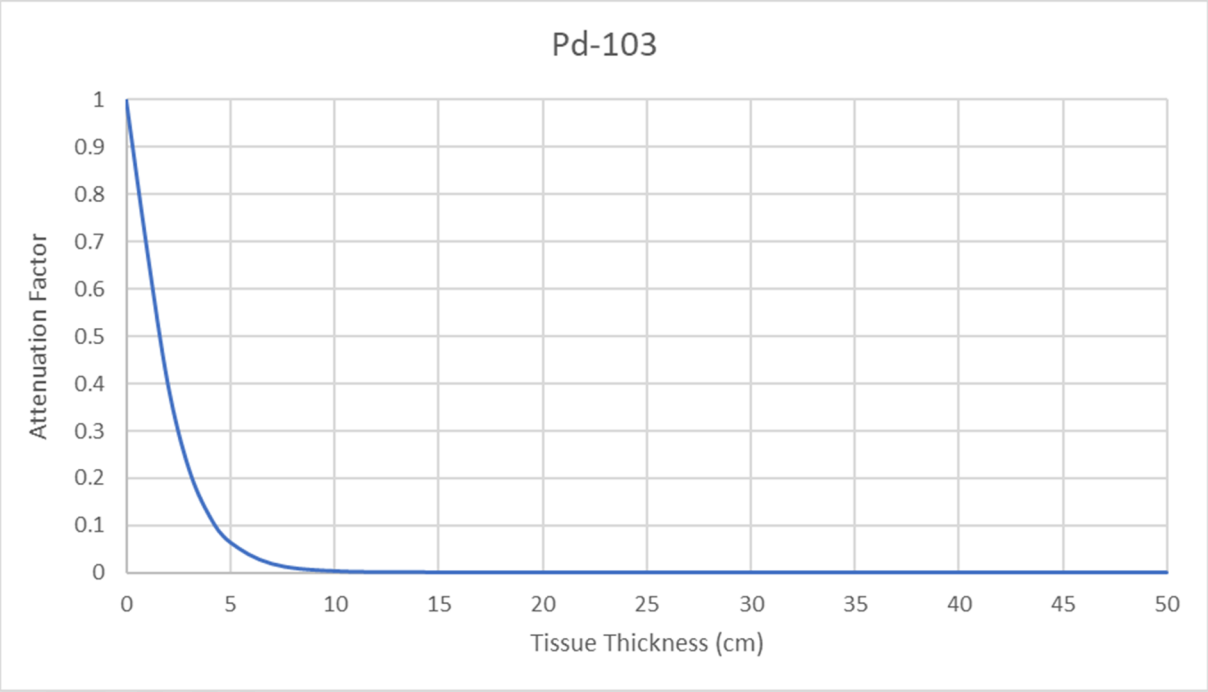
Pd-103
Attenuation Factor
1
0.9
0.8
0.7
0.6
0.5
0.4
0.3
0.2
0.1
0
0
5
10
15
20
25
30
35
40
45
50
Tissue Thickness (cm)

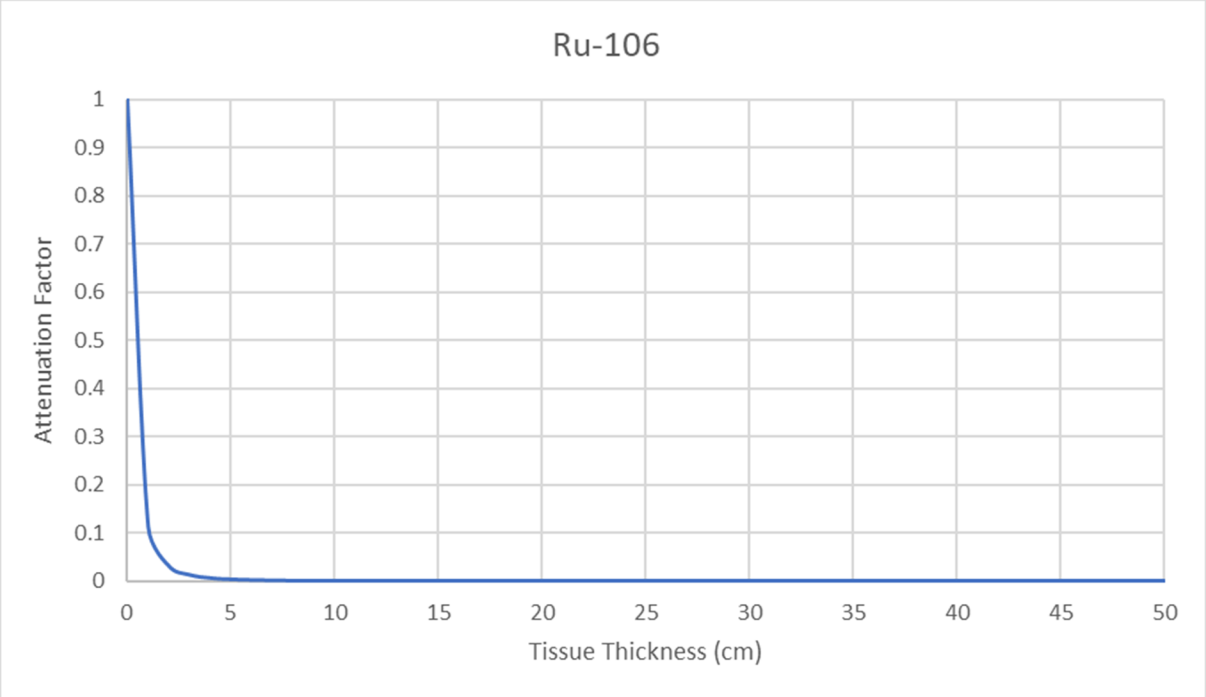
Ru-106
Attenuation Factor
1
0.9
0.8
0.7
0.6
0.5
0.4
0.3
0.2
0.1
0
0
5
10
15
20
25
30
35
40
45
50
Tissue Thickness (cm)

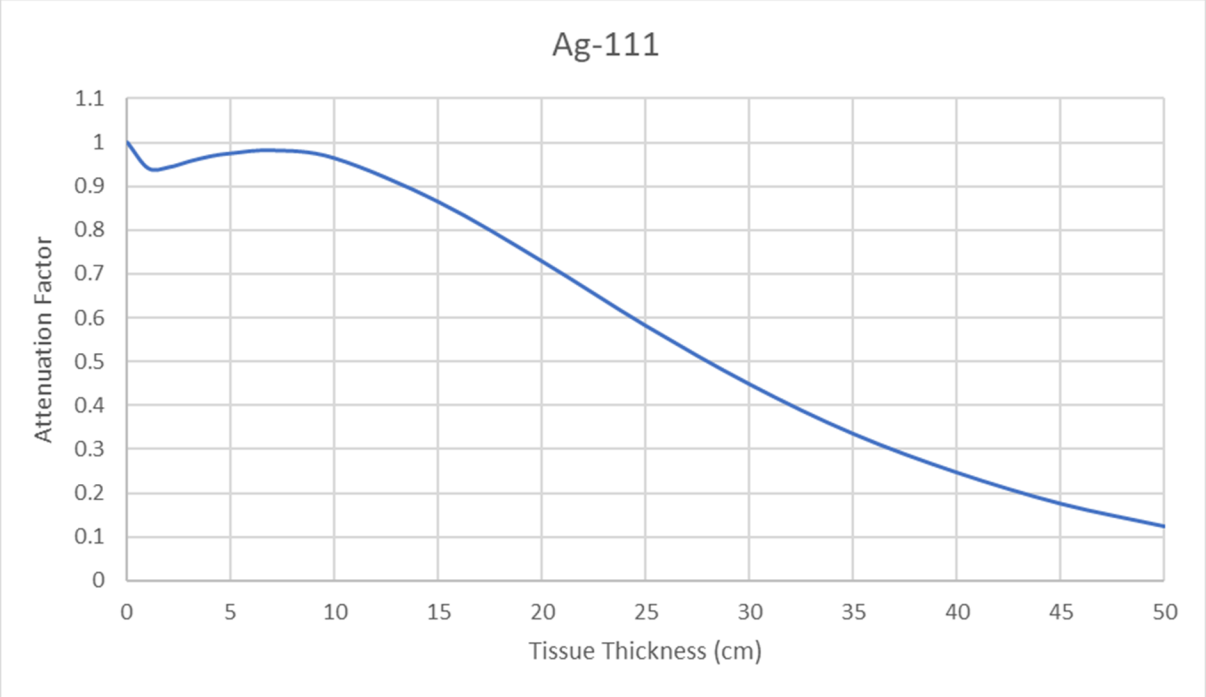
Ag-111
Attenuation Factor
1.1
1
0.9
0.8
0.7
0.6
0.5
0.4
0.3
0.2
0.1
0
0
5
10
15
20
25
30
35
40
45
50
Tissue Thickness (cm)

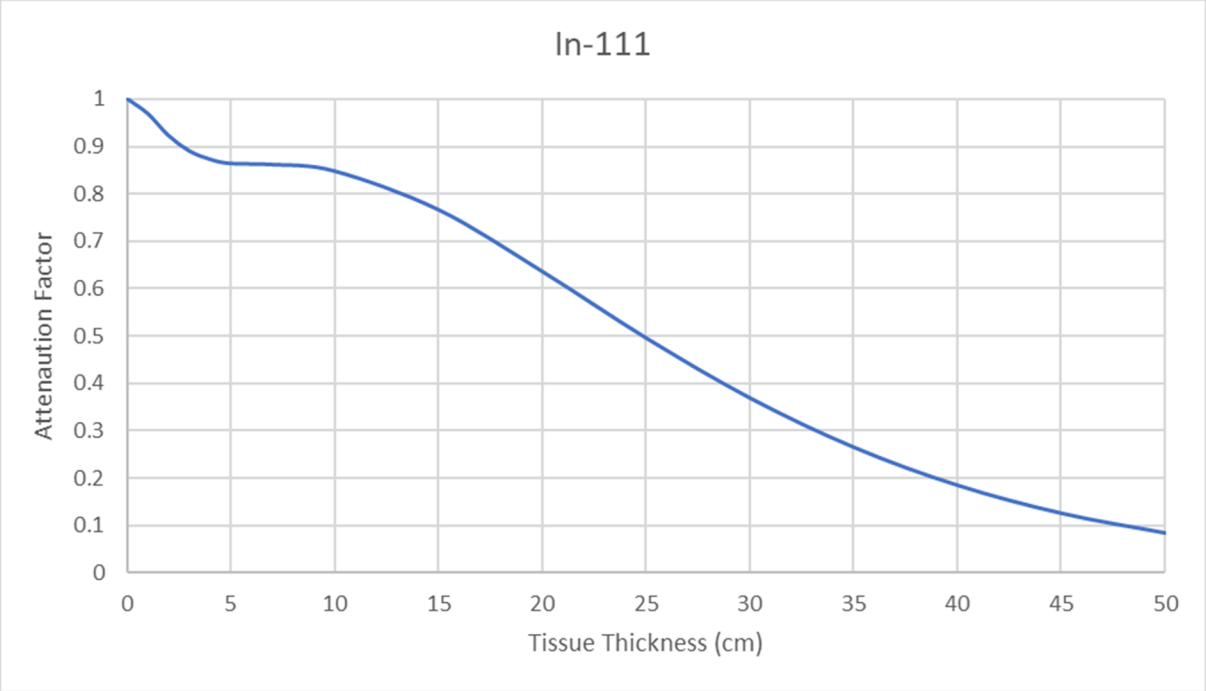
In-111
Attenaution Factor
1
0.9
0.8
0.7
0.6
0.5
0.4
0.3
0.2
0.1
0
0
5
10
15
20
25
30
35
40
45
50
Tissue Thickness (cm)

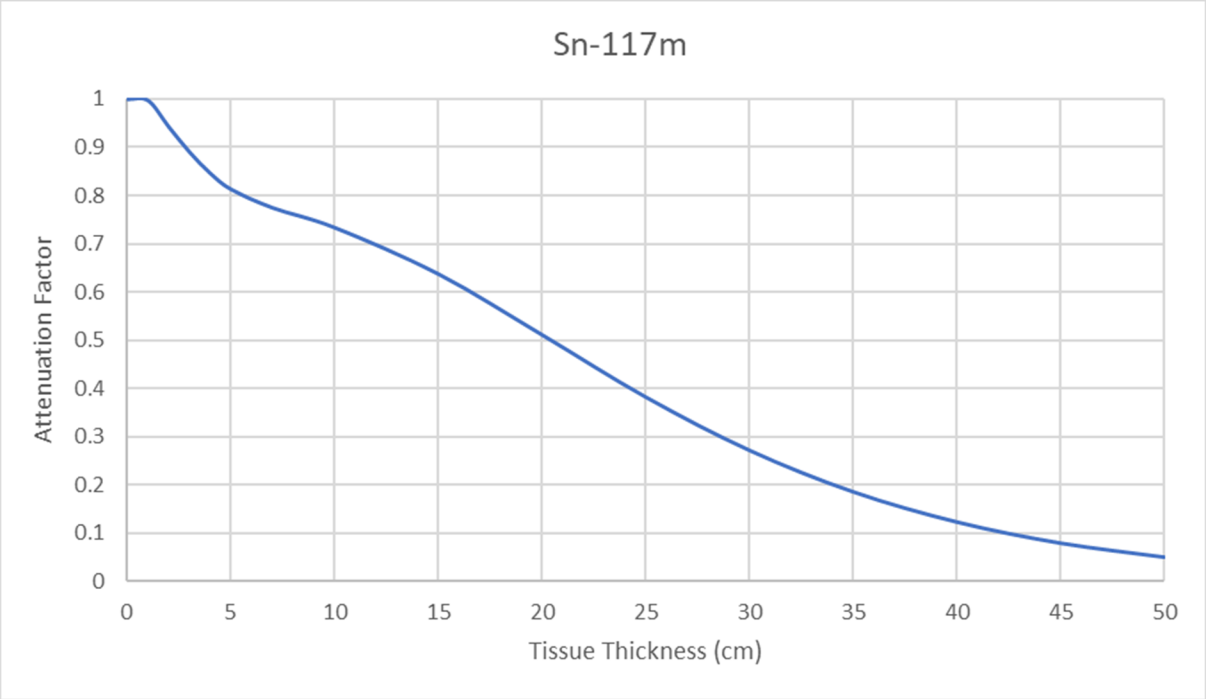
Sn-117m
Attenuation Factor
1
0.9
0.8
0.7
0.6
0.5
0.4
0.3
0.2
0.1
0
0
5
10
15
20
25
30
35
40
45
50
Tissue Thickness (cm)

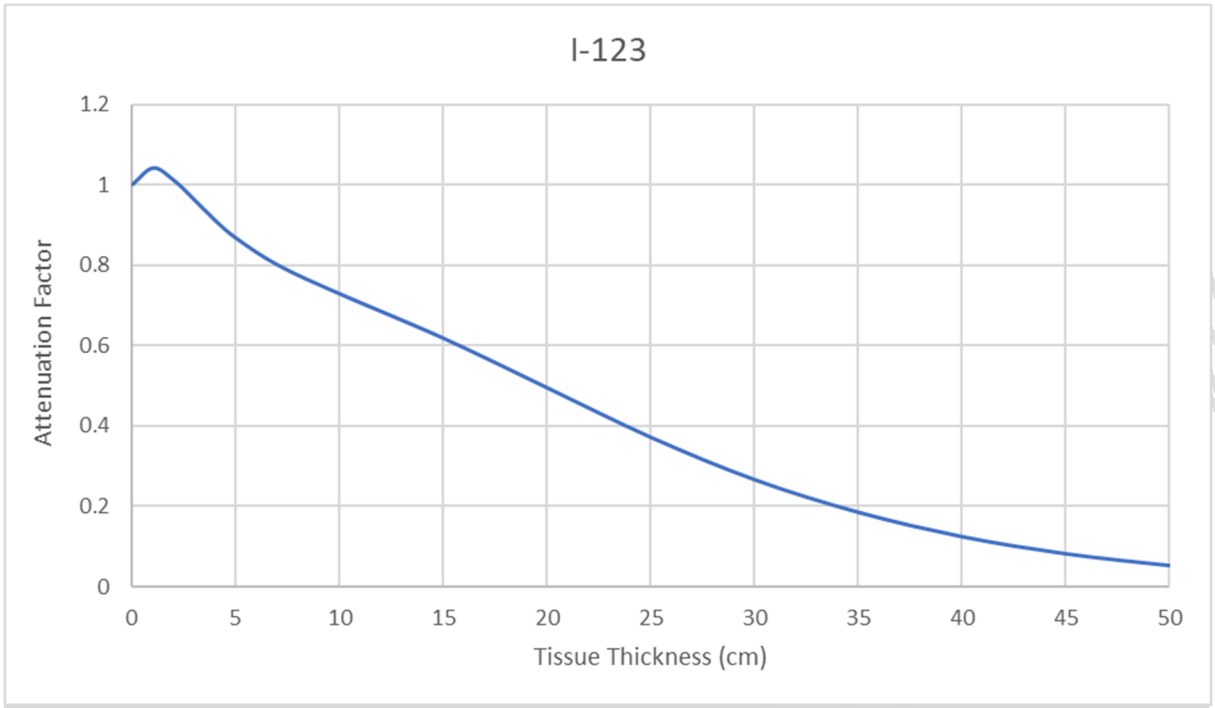
I-123
Attenuation Factor
1.2
1
0.8
0.6
0.4
0.2
0
0
5
10
15
20
25
30
35
40
45
50
Tissue Thickness (cm)

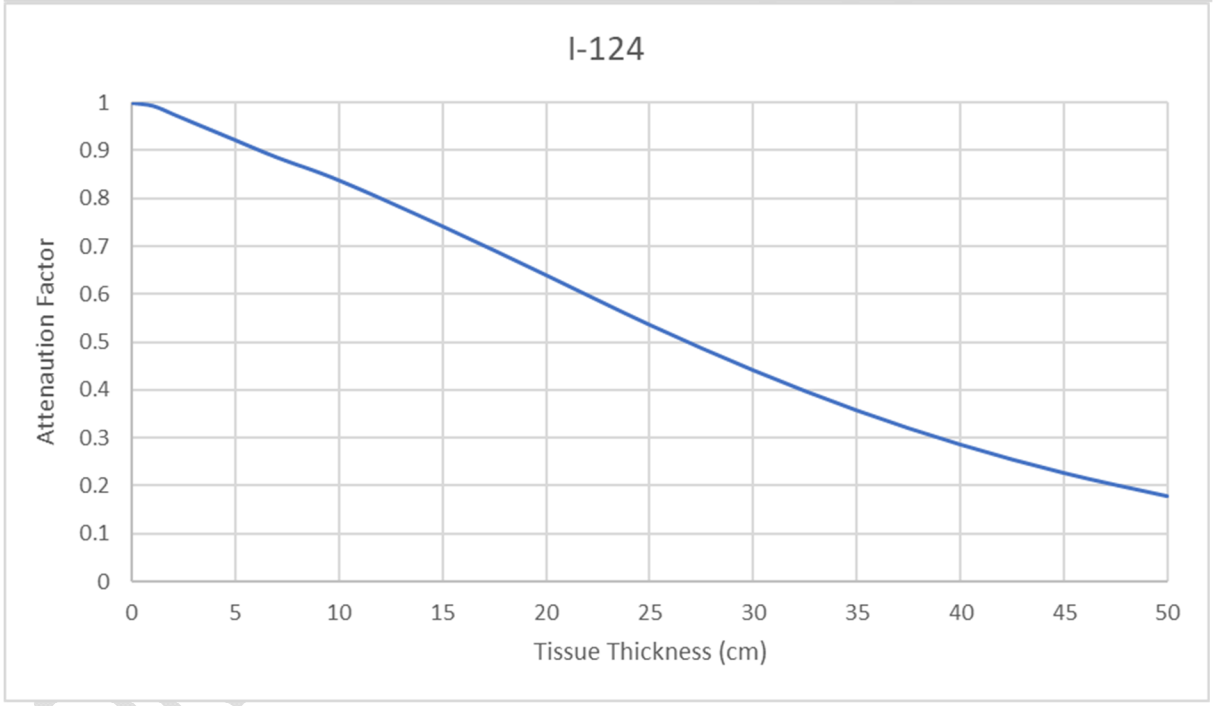
I-124
Attenaution Factor
1
0.9
0.8
0.7
0.6
0.5
0.4
0.3
0.2
0.1
0
0
5
10
15
20
25
30
35
40
45
50
Tissue Thickness (cm)

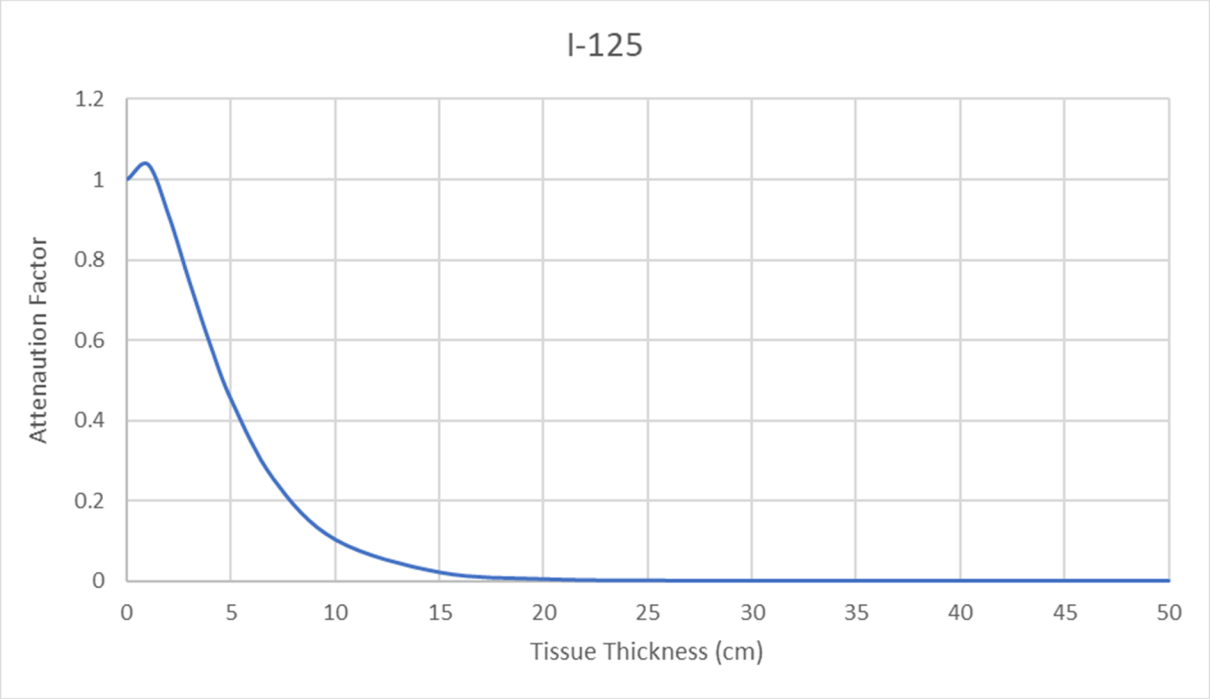
I-125
Attenaution Factor
1.2
1
0.8
0.6
0.4
0.2
0
0
5
10
15
20
25
30
35
40
45
50
Tissue Thickness (cm)

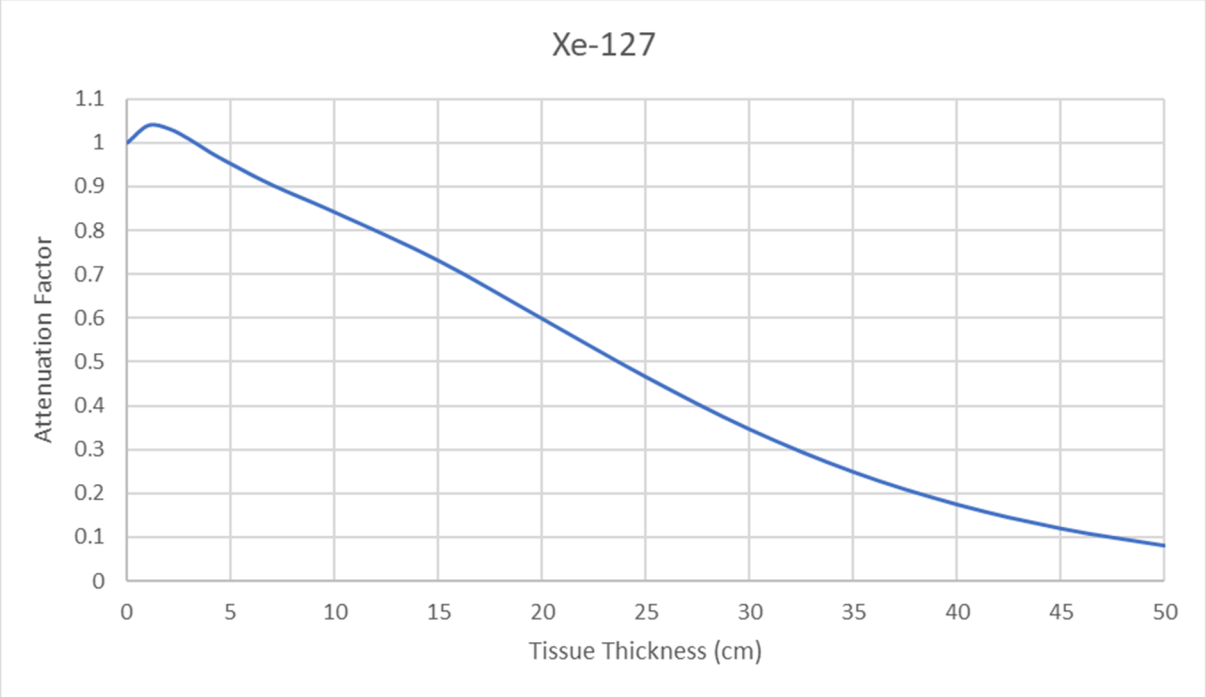
Xe-127
Attenuation Factor
1.1
1
0.9
0.8
0.7
0.6
0.5
0.4
0.3
0.2
0.1
0
0
5
10
15
20
25
30
35
40
45
50
Tissue Thickness (cm)

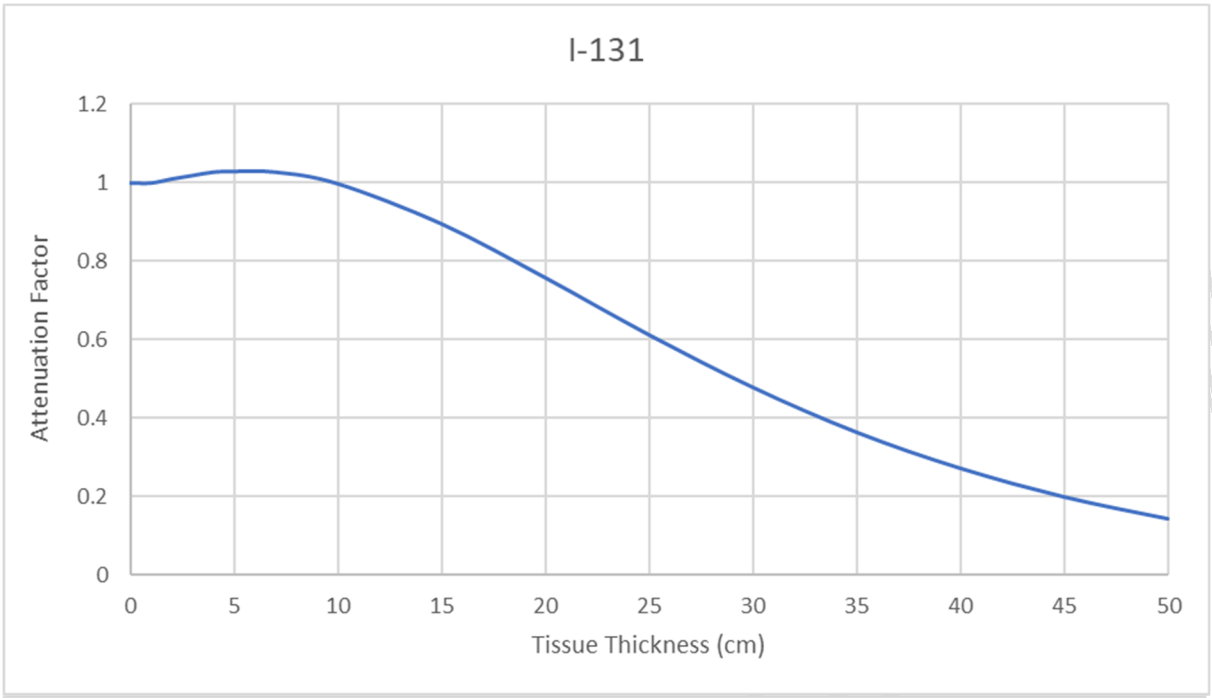
I-131
Attenuation Factor
1.2
1
0.8
0.6
0.4
0.2
0
0
5
10
15
20
25
30
35
40
45
50
Tissue Thickness (cm)

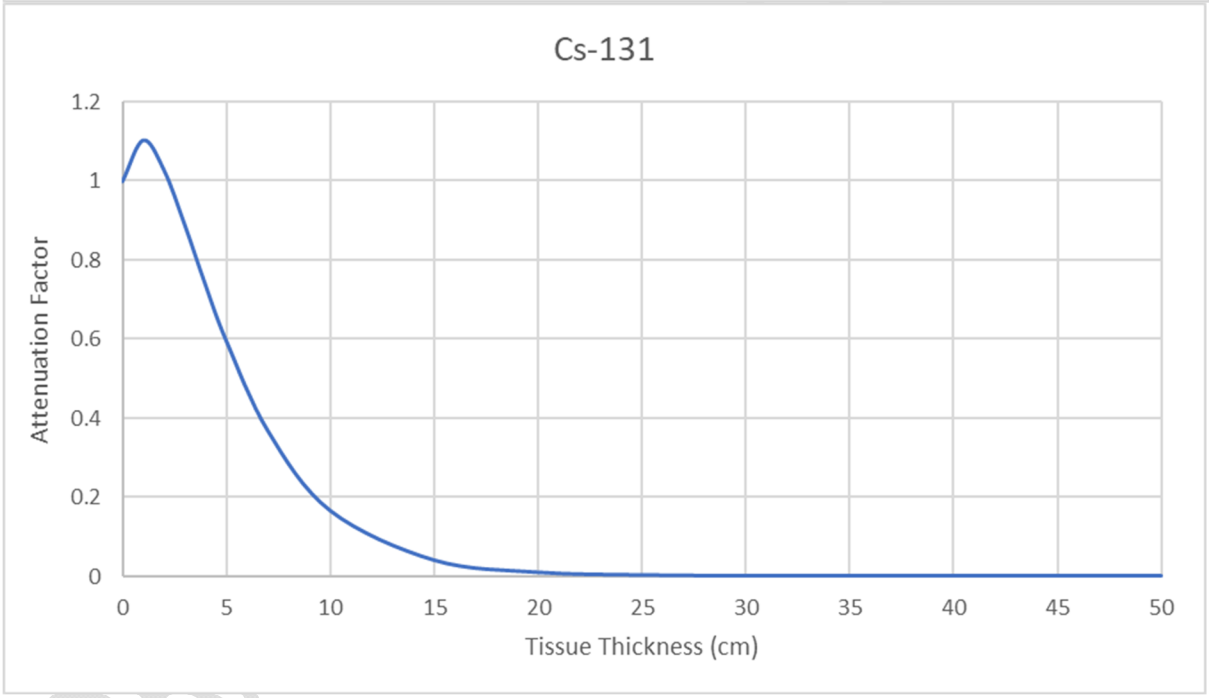
Cs-131
Attenuation Factor
1.2
1
0.8
0.6
0.4
0.2
0
0
5
10
15
20
25
30
35
40
45
50
Tissue Thickness (cm)

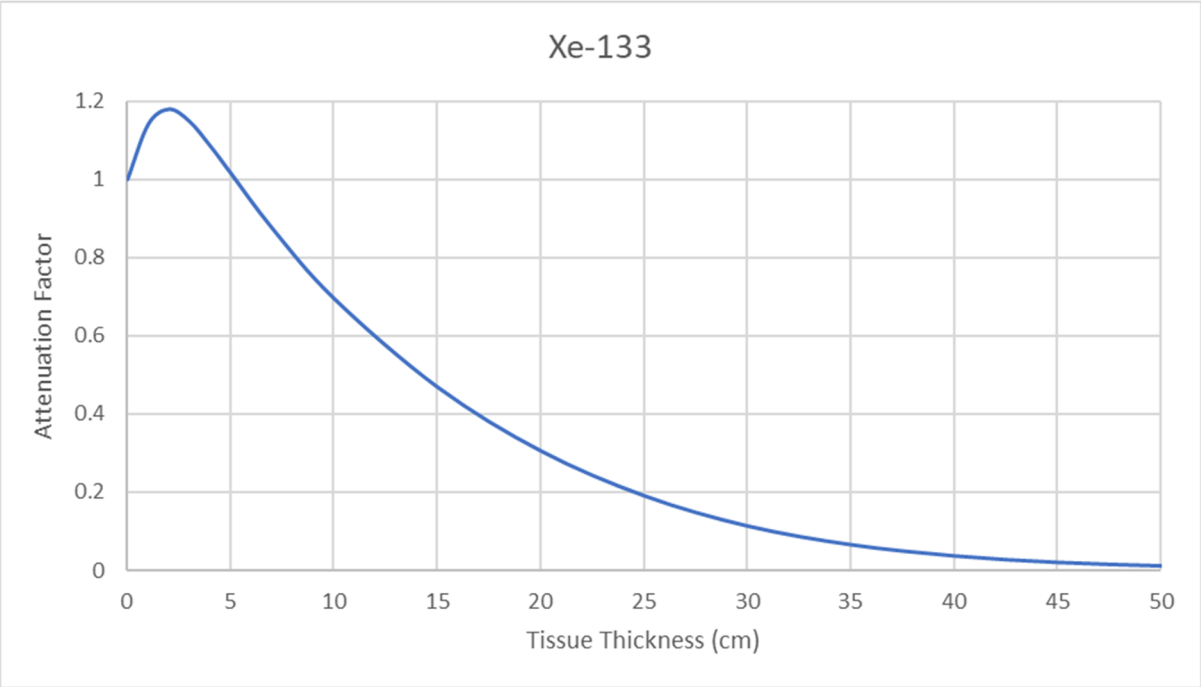
Xe-133
Attenuation Factor
1.2
1
0.8
0.6
0.4
0.2
0
0
5
10
15
20
25
30
35
40
45
50
Tissue Thickness (cm)

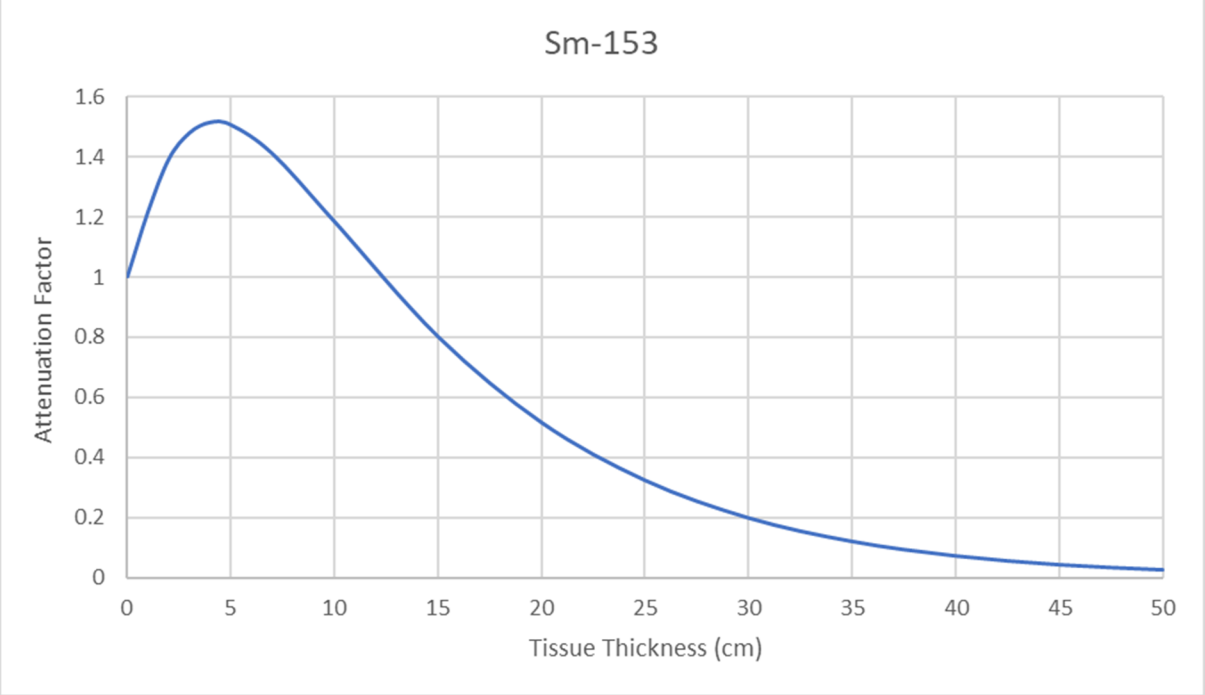
Sm-153
Attenuation Factor
1.6
1.4
1.2
1
0.8
0.6
0.4
0.2
0
0
5
10
15
20
25
30
35
40
45
50
Tissue Thickness (cm)

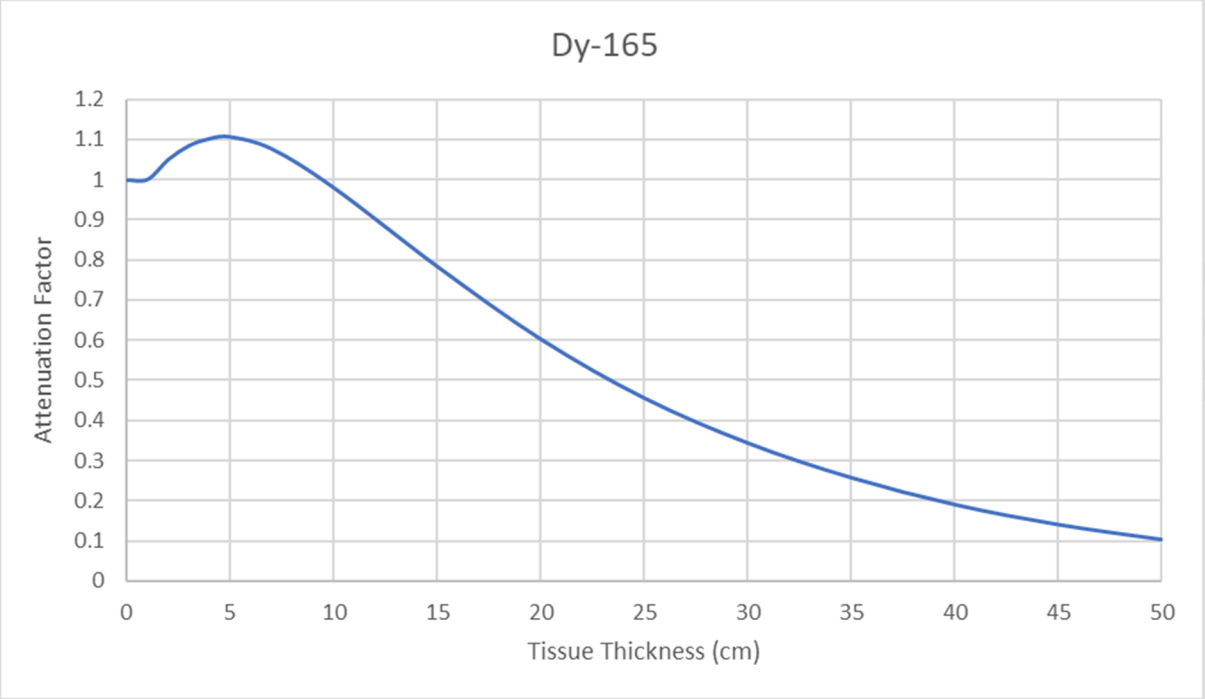
Dy-165
Attenuation Factor
1.2
1.1
1
0.9
0.8
0.7
0.6
0.5
0.4
0.3
0.2
0.1
0
0
5
10
15
20
25
30
35
40
45
50
Tissue Thickness (cm)

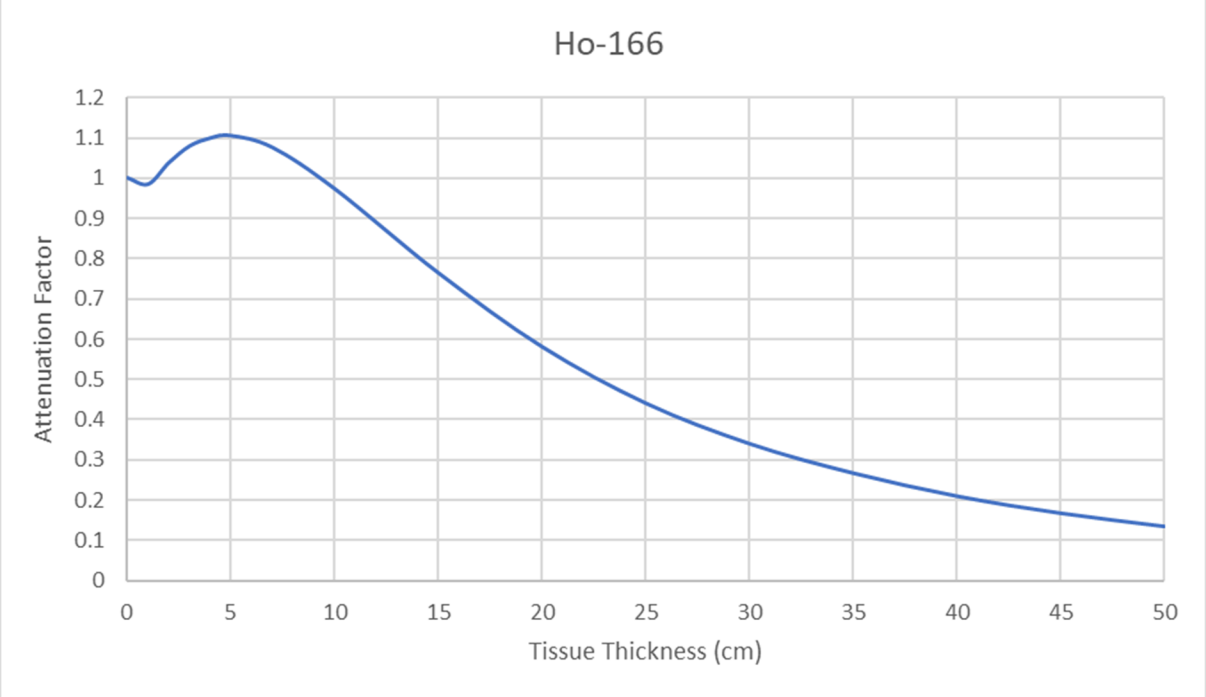
Ho-166
Attenuation Factor
1.2
1.1
1
0.9
0.8
0.7
0.6
0.5
0.4
0.3
0.2
0.1
0
0
5
10
15
20
25
30
35
40
45
50
Tissue Thickness (cm)

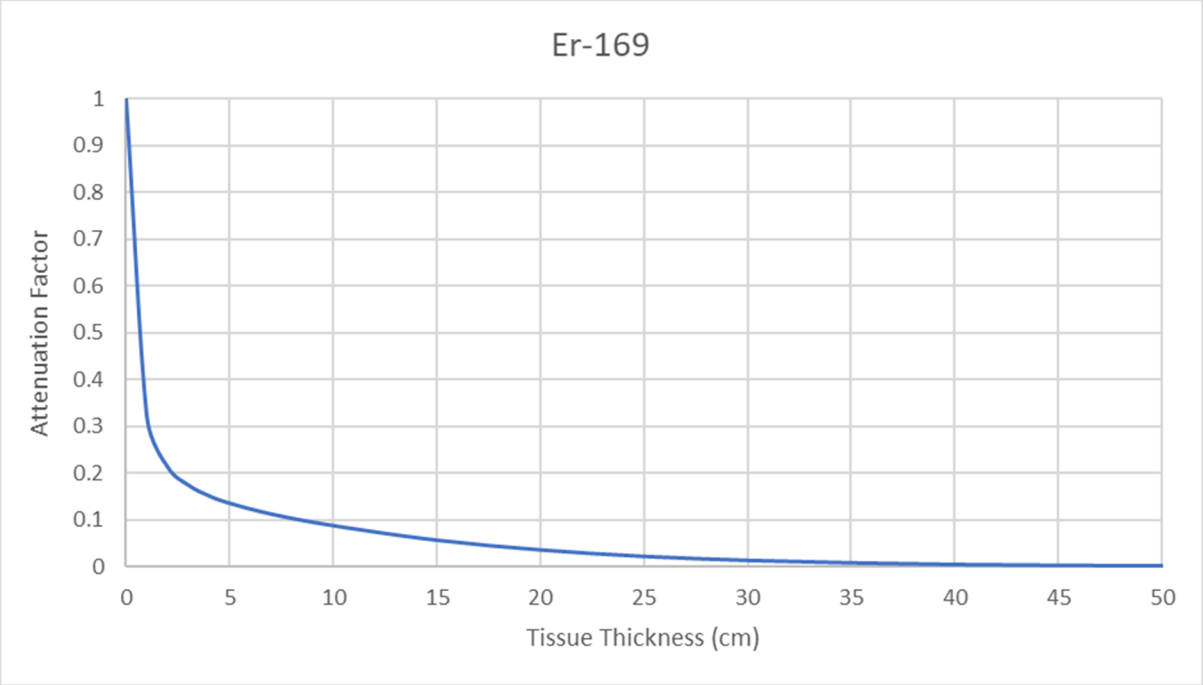
Er-169
Attenuation Factor
1
0.9
0.8
0.7
0.6
0.5
0.4
0.3
0.2
0.1
0
0
5
10
15
20
25
30
35
40
45
50
Tissue Thickness (cm)

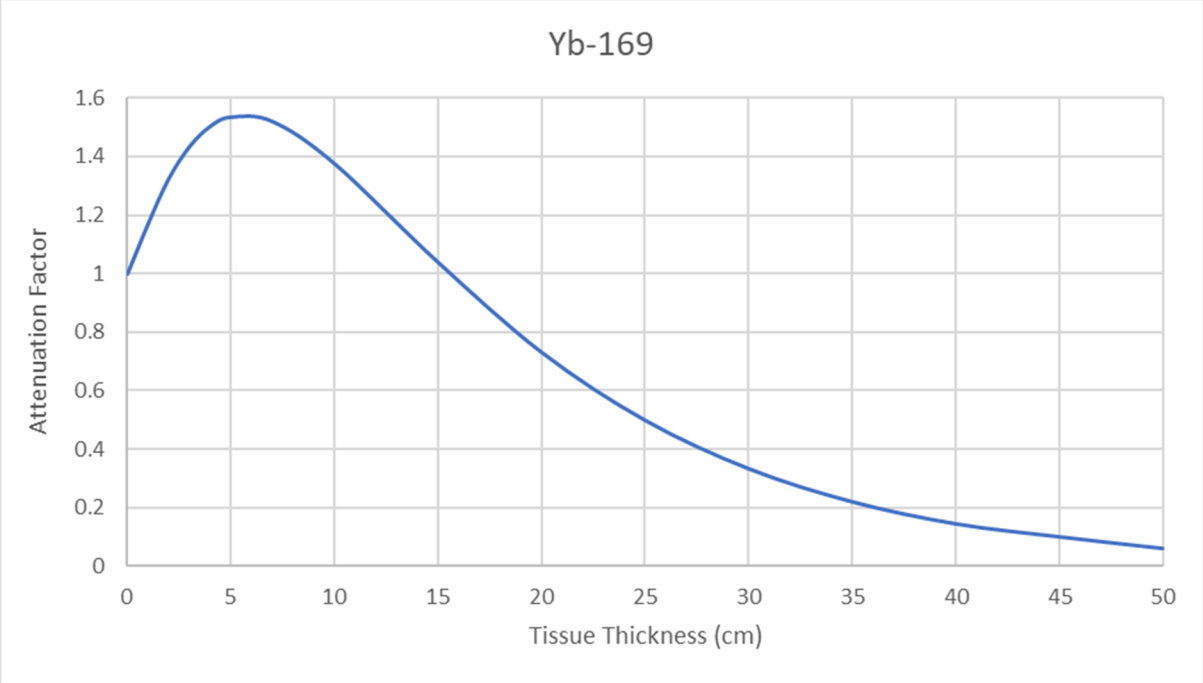
Yb-169
Attenuation Factor
1.6
1.4
1.2
1
0.8
0.6
0.4
0.2
0
0
5
10
15
20
25
30
35
40
45
50
Tissue Thickness (cm)

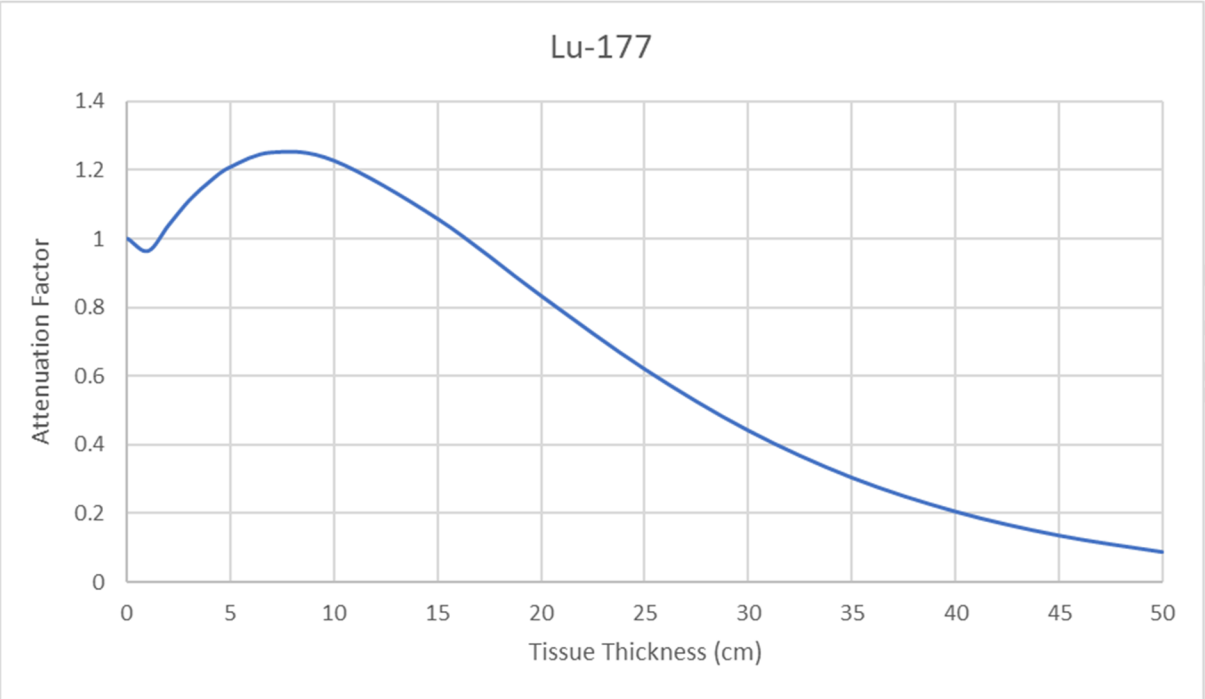
Lu-177
Attenuation Factor
1.4
1.2
1
0.8
0.6
0.4
0.2
0
0
5
10
15
20
25
30
35
40
45
50
Tissue Thickness (cm)

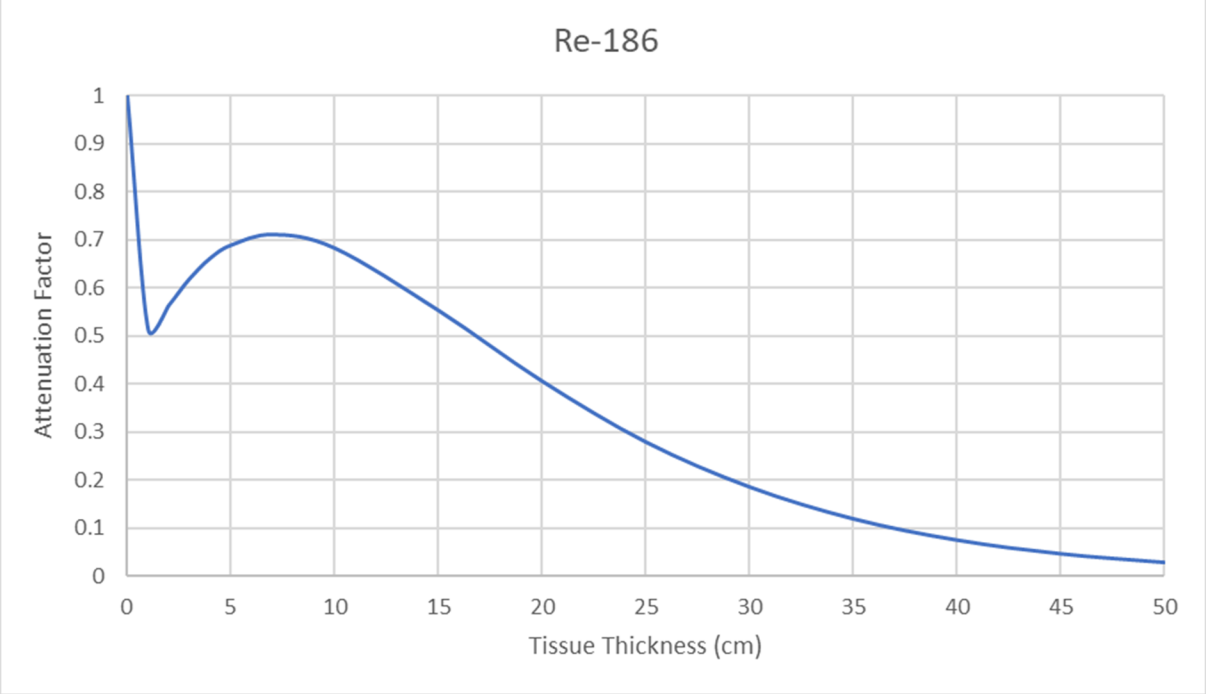
Re-186
Attenuation Factor
1
0.9
0.8
0.7
0.6
0.5
0.4
0.3
0.2
0.1
0
0
5
10
15
20
25
30
35
40
45
50
Tissue Thickness (cm)

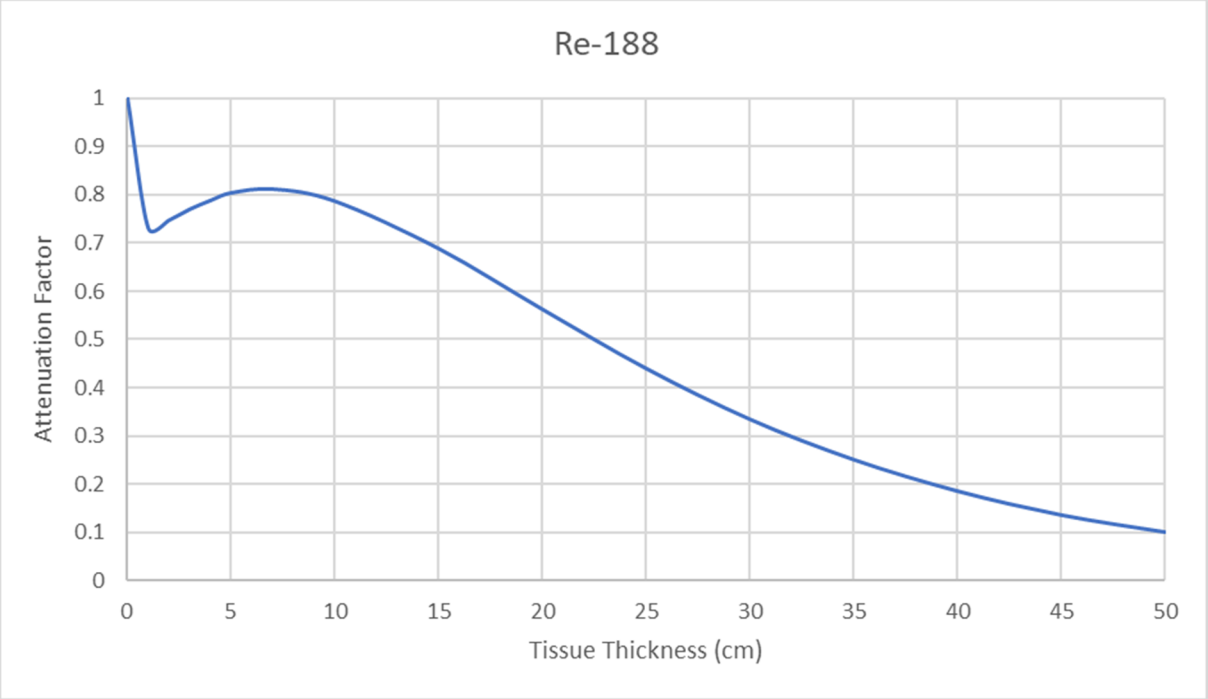
Re-188
Attenuation Factor
1
0.9
0.8
0.7
0.6
0.5
0.4
0.3
0.2
0.1
0
0
5
10
15
20
25
30
35
40
45
50
Tissue Thickness (cm)

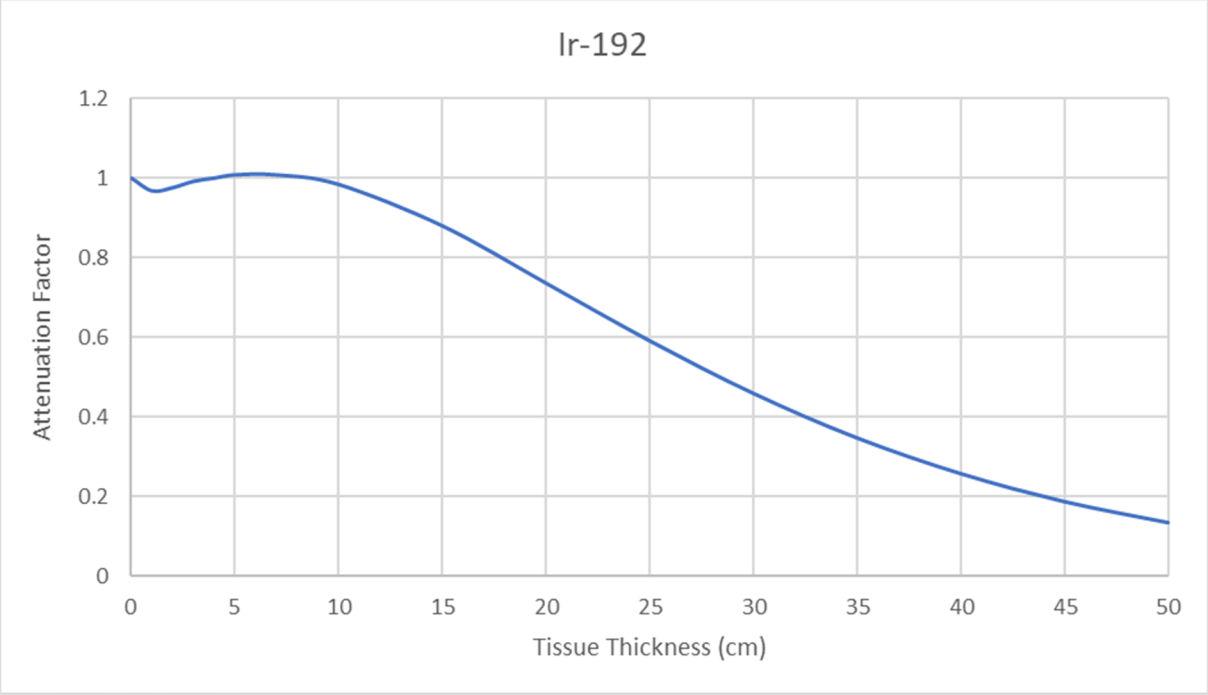
Ir-192
Attenuation Factor
1.2
1
0.8
0.6
0.4
0.2
0
0
5
10
15
20
25
30
35
40
45
50
Tissue Thickness (cm)

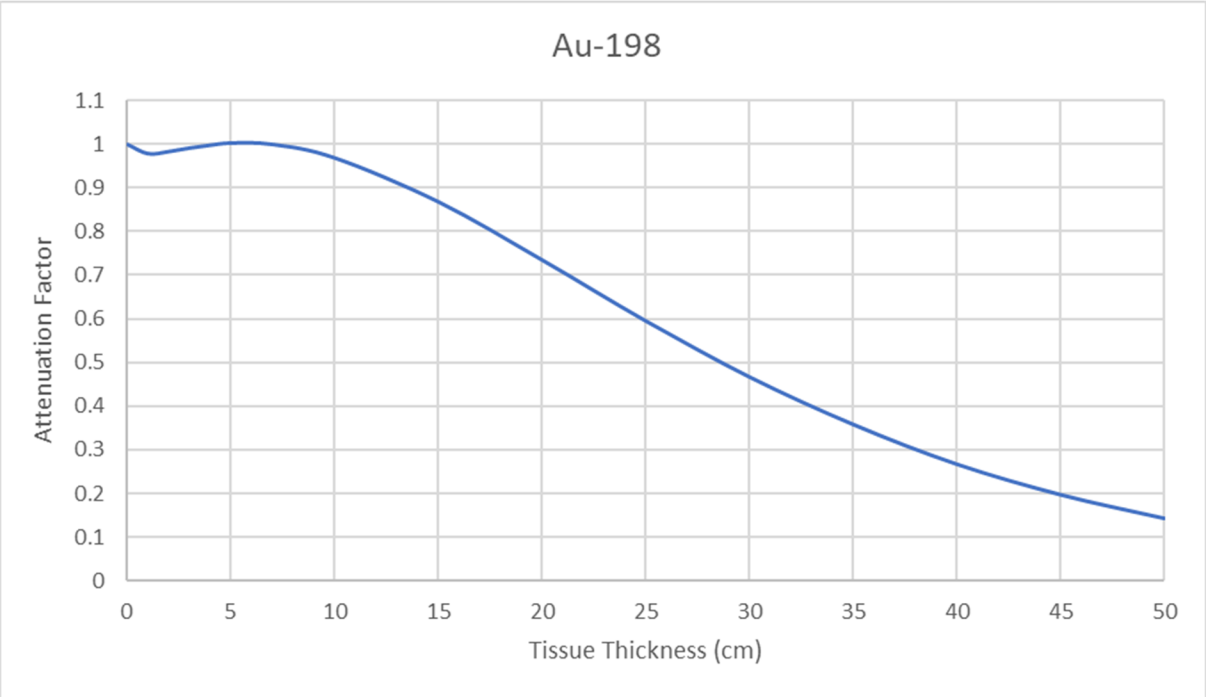
Au-198
Attenuation Factor
1.1
1
0.9
0.8
0.7
0.6
0.5
0.4
0.3
0.2
0.1
0
0
5
10
15
20
25
30
35
40
45
50
Tissue Thickness (cm)

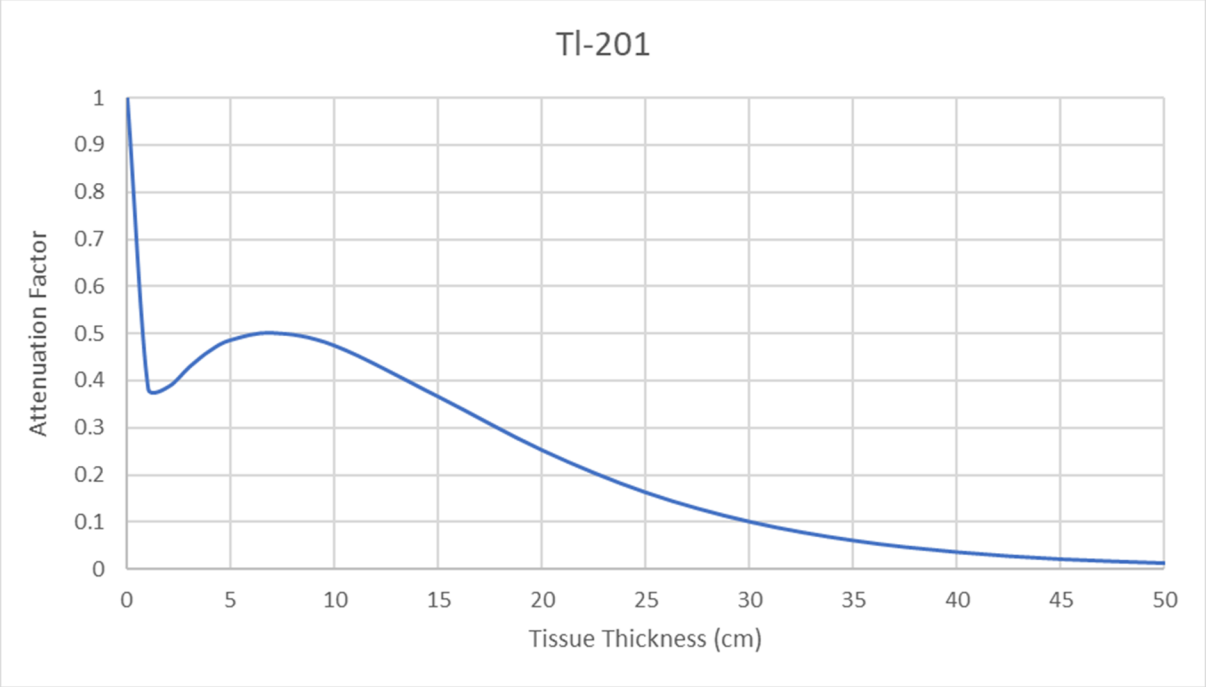
Tl-201
Attenuation Factor
1
0.9
0.8
0.7
0.6
0.5
0.4
0.3
0.2
0.1
0
0
5
10
15
20
25
30
35
40
45
50
Tissue Thickness (cm)

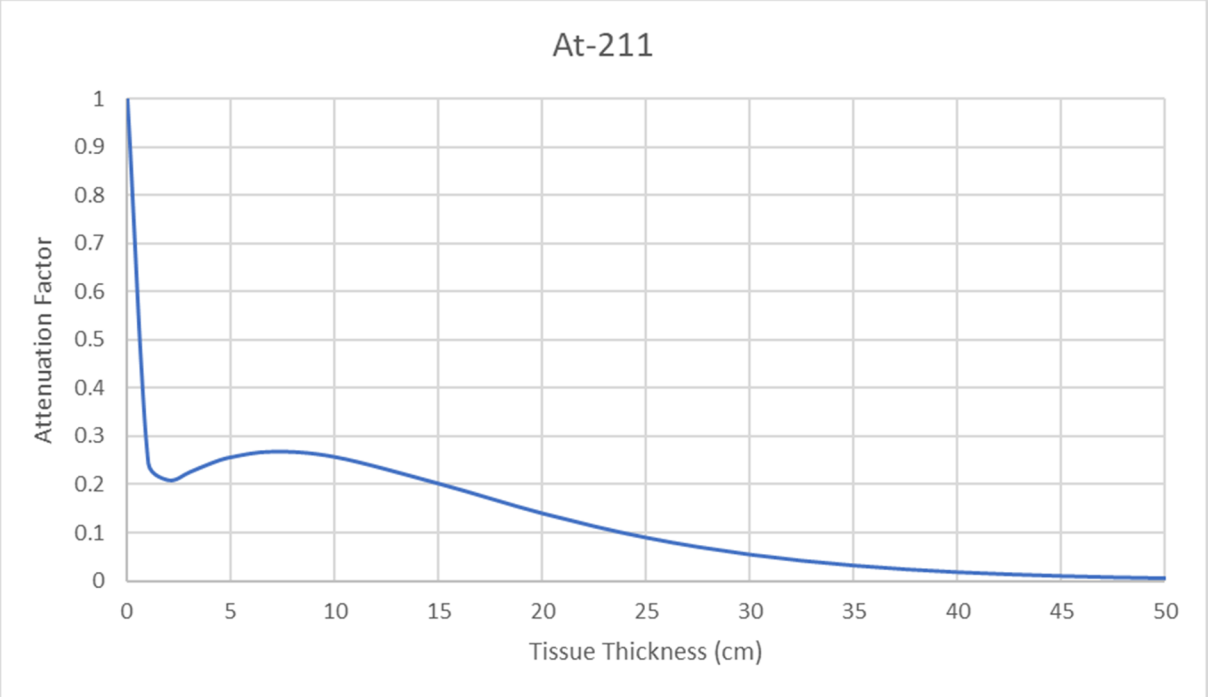
At-211
Attenuation Factor
1
0.9
0.8
0.7
0.6
0.5
0.4
0.3
0.2
0.1
0
0
5
10
15
20
25
30
35
40
45
50
Tissue Thickness (cm)

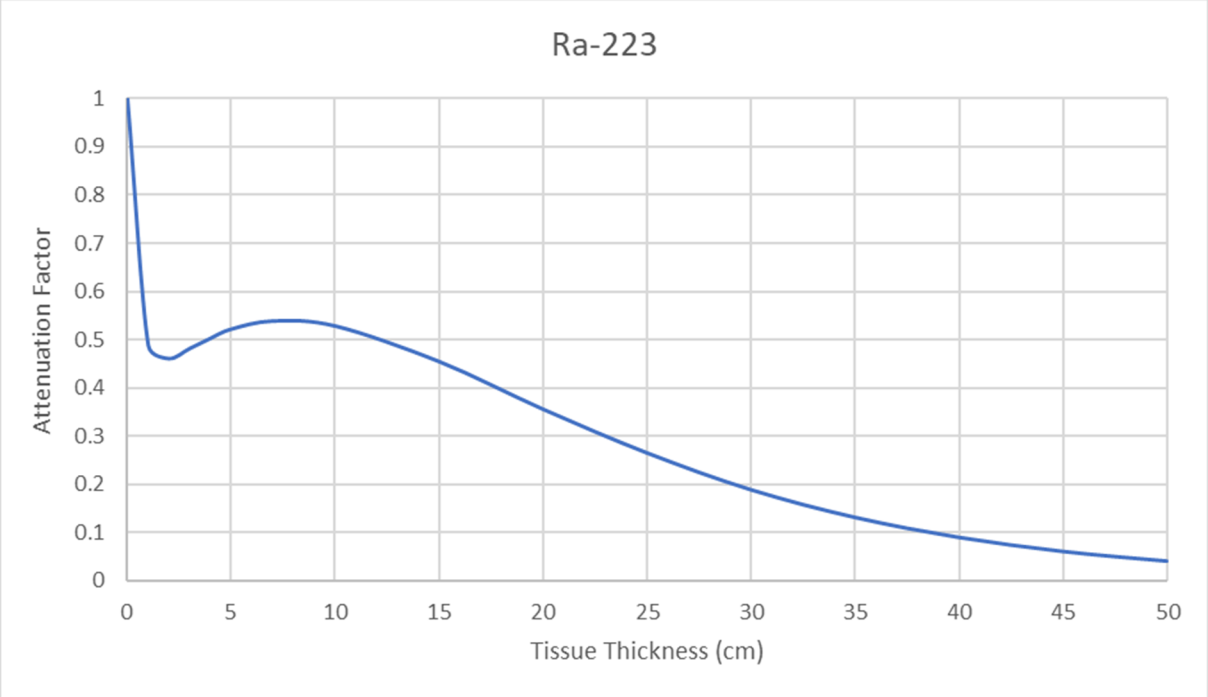
Ra-223
Attenuation Factor
1
0.9
0.8
0.7
0.6
0.5
0.4
0.3
0.2
0.1
0
0
5
10
15
20
25
30
35
40
45
50
Tissue Thickness (cm)

5. BREASTFEEDING THRESHOLDS

Regulatory Guide 8.39 Rev 1 (NRC 2020) provides direction for licensees to demonstrate compliance with 10 CFR 35.75. No determination of internal dose received by others is required of the licensee unless the patient is breastfeeding an infant or child. The regulation requires that the licensee determine breastfeeding status of female patients and assess the total effective dose equivalent (TEDE) to the feeding infant/child compared to dose limitations of 1 and 5 mSv. This chapter provides the technical basis for radiation dosimetry applicable to the breastfeeding infant, administered activity thresholds for breastfeeding patients, and breastfeeding interruption times that may be necessary to limit infant dose.

Background

Record/Instruction Activity Thresholds for Breastfeeding Patients.

In 10 CFR 35.75(a), the licensee is authorized to release a patient having received an administration of radioactive material if the external effective dose equivalent to any other person is not likely to exceed 5 mSv. If a patient is or may be nursing an infant or child, the licensee is directed to include instructions to that nursing mother on methods of reducing radiation exposure if the dose to a breastfeeding infant could exceed 1 mSv without interruption of breastfeeding (10 CFR 35.75(b)). Additionally, the licensee is required to maintain a record of the instructions provided to a nursing mother if the dose to a breastfeeding infant could exceed 5 mSv without interruption of breastfeeding (10 CFR 35.2075(b)). Therefore, it is necessary to determine activity thresholds for breastfeeding patients to keep infant doses below limits and make licensees aware of administered activities with regulatory implications.

Revisions to Regulatory Guide 8.39 Rev 1 (NRC 2020) list activity thresholds for providing instructions and maintaining records for breastfeeding patients. Tabulations also provide recommended time durations for interrupting breastfeeding if necessary, so that the infant/child is not likely to receive more than 1 mSv when breastfeeding is resumed. Threshold activities were determined for both internal (via consumption of breastmilk) and external (via direct photon exposure) of the infant or child while feeding. The external dose calculation follows a similar methodology to the external dose calculation for any other individual exposed to the patient. However, the internal dose calculation for breastfeeding requires radiopharmaceutical-specific internal dose coefficients for infants, along with secretion fractions that describe the portion of activity in the mother's body transferred to the infant during breastfeeding. The described methodology is flexible so that radiopharmaceuticals with increased biokinetic complexity can be incorporated into assessments of internal and external radiation dose received by the breastfeeding infant.

History of Recommendations for Breastfeeding Interruption.

Several relevant documents on the subject are summarized. For each document, a brief description of dosimetric assumptions for the breastfeeding infant is provided along with recommendations for interruption or cessation of breastfeeding. All of these reports assume a dose limitation of 1 mSv to the infant and provide recommendations based on specific administration levels. **Table *5-1*** provides a summary of the interruption recommendations from several different sources.

NUREG-1492 (1997b) describes the method for determining instructions for lactating patients applicable to the original 1997 Regulatory Guide 8.39 (NRC 1997a). This method established best-case and worst-case scenarios for estimating internal dose to the breastfeeding infant based on time-dependent concentrations of radioactivity

in breastmilk. The dose assessment progressed through a stepwise approach to estimate concentrations at an assumed feeding frequency (every 3 hours for up to 50 effective half-lives of the radiopharmaceutical in the mother). Complete absorption of the radiopharmaceutical in the infant's GI tract was assumed, and cumulative ingestion for various time periods was calculated. Retention of the radiopharmaceutical in the mother was estimated to follow single-exponential (monophasic) loss in all cases, including free iodine administered as NaI. The NUREG-1492 states there are specific cases for which "… effective dose equivalent should not be used for decision making, and the individual organ absorbed dose should be considered." One primary case is radiopharmaceuticals administered as sodium iodide with significant uptake by the infant's thyroid that can result in thyroid damage. NUREG-1492 also considered the possibility of radiological contaminants in ^{111}In, ^{123}I, and ^{201}Tl radiopharmaceuticals. External dose to the infant was assumed with an occupancy factor of 0.16 and a separation distance of 0.2 meters. For 25 common radiopharmaceuticals, breastfeeding interruption was found to be necessary for ten of those radiopharmaceuticals.

Stabin and Breitz (2000) provide a literature review and determine radiation dose received by breastfeeding infants for the same 25 radiopharmaceuticals as above administered to their mothers. They report that nine of the pharmaceuticals require breastfeeding interruption to meet a dose criterion of 1 mSv, with a recommendation of complete cessation for three pharmaceuticals (^{67}Ga-citrate, and ^{123}I and ^{131}I as NaI). Cessation of breastfeeding with administrations of ^{123}I, however, is based on potentially high concentrations of ^{125}I as a contaminant, otherwise pure ^{123}I as NaI has only a 24 h recommended interruption time. The authors show that half-times and secretion fractions vary considerably between subjects (and even within the same subject at different times) and those individual measurements are quite important for determining patient-specific dosimetry. Of ^{99m}Tc-labeled pharmaceuticals, the authors estimate that about 60% is secreted in the first 4 hours through breastmilk and therefore an interruption time between 12 hours and 2 days may be necessary to reduce infant dose to less than 1 mSv. Stabin and Breitz (2000) consider single-exponential loss for all compounds except ^{131}I as NaI and ^{201}Tl-chloride, in which case they consider double-exponential loss.

Additional recommendations on breastfeeding interruption are given in ICRP 106 (2008a). Several of the radiopharmaceuticals have recommendations of "greater than 3 wk" which the ICRP notes should be interpreted as "cessation" due to the mother's difficulty in maintaining the milk supply for that length of interruption. They advise a general 4-hour interruption (one feeding) for ^{99m}Tc-labeled pharmaceuticals and consideration is given to contamination of ^{123}I by ^{125}I. ICRP 128 (2015) provides similar results to that of ICRP 106 (2008a), and the methods described in NUREG-1556 (2019) are very similar to the original Regulatory Guide 8.39 (1997a).

More recently, Leide-Svegborn et al. (2016) published data on infant dosimetry and interruption recommendations for sixteen radiopharmaceuticals from 53 breastfeeding patients. In their assessment, they estimate breastmilk excretion fractions for radionuclides administered to the mother, as well as the resulting organ and effective dose to the infant with no interruption. Feeding rates were assumed to be 133 mL every 4 hours (800 mL/d) and dose was estimated until negligible activity remained in breastmilk. Their clinical data show that a single-exponential retention model is appropriate for the majority of pharmaceuticals they investigated. Two of the pharmaceuticals, ^{131}I as NaI and ^{51}Cr-EDTA, indicated a double-exponential (biphasic) model provided a better representation of retention. External dose to the infant due to close contact was considered by noting that it should be "… kept in mind when recommendations are given …", but generally thought to be insignificant when compared to internal contributions.

A subcommittee of members of the US NRC Advisory Committee on Medical Uses of Isotopes (ACMUI) prepared a report (Zanzonico et al. 2019) on guidelines for the nursing mother having received a medical administration. The ACMUI analysis considered exposure of the infant through external routes of proximity to the mother's body and to the mother's breast, and through the internal route of consumption of breastmilk. The infant was assumed

to be 7.5 cm from the breast and 15 cm from the mother's body during feeding. An occupancy factor of 0.33 was assumed, as well as a point-to-line geometry factor (breast-to-mother) of 0.32. Contributions from bremsstrahlung were not considered by Zanzonico et al. (2019) and all beta emissions in the mother were assumed to be non-contributors to external infant dose. For internal dosimetry, a breastmilk volume of 142 mL per feeding was assumed with ingestion occurring every 4 hours and dose to the infant was calculated assuming no interruption of breastfeeding. The ACMUI report provides tabulated data, but also textual recommendations that differ. It is their textual recommendations that have been included in **Table *5-1*** below.

The data compiled in **Table *5-1*** are indicative of the variability of administered activity, dosimetric methodology, parameter assumptions, biological elimination rate, etc. For a given radiopharmaceutical breastfeeding interruption recommendations can fluctuate considerably, accentuating the need for patient-specific analysis.

Table 5-1 Historical recommendations on breastfeeding interruption for infant dose less than 1 mSv

		Recommended Interruption Times (Administered Activity in MBq)						
Nuclide	Pharma ceutical	NUREG-1492 (NRC 1997b)	Stabin & Breitz (2000)	ICRP-106 (2008a)	ICRP-128 (2015)	NUREG-1556 (NRC 2019)	Leide-Svegborn et al. (2016)	Zanzonico et al. (2019)
C-11	any	-	-	none	none	-	-	none (925)
Cr-51	EDTA	none (1.85)	none (1.85)	none	none	none	none (3.7)	-
F-18	FDG	-	-	none	none	-	none (422)	4 h (370)
Ga-67	citrate	1 mo (185)	cessation (185)	> 3 wk	> 3 wk	1 mo (150)	-	28 d (185)
Ga-68	octreotate	-	-	-	-	-	-	4 h (185)
I-123	MIBG	24 h (370)	48 h (370)	> 3 wk	> 3 wk	24 h (370)	-	-
	OIH	none (74)	none (74)	12 h	12 h	none	-	4 h (37)
	NaI	none (14.8)	cessation[b](14.8)	> 3 wk	> 3 wk	none	-	3 d (15)
I-124	NaI	-	-	-	-	-	-	cessation (74)
I-125	OIH	none (0.37)	none (0.37)	12 h	12 h	none	12 h (0.40)	-
I-131	OIH	none (11.1)	none (11.1)	12 h	12 h	none	12 h (0.66)	4 h (10)
	NaI	cessation (5,550)	cessation (5,550)	> 3 wk	> 3 wk	cessation	cessation (1.85)	cessation (74)
In-111	WBC	1 wk (18.5)	none (18.5)	none	none	1 wk (20)	-	6 d (18.5)
	octreotate	-	-	none	none	-	-	6 d (185)
Lu-177	octreotate	-	-	-	-	-	-	28 d (7,800)
N-13	any	-	-	none	none	-	-	none (925)
O-15	any	-	-	none	none	-	-	none (1,850)
Ra-223	dichloride	-	-	-	-	-	-	cessation
Rb-82	chloride	-	-	-	-	-	-	none (2,220)
Tc-99m	DISIDA	none (300)	none (300)	none	none	none	-	-
	DTPA	none (740)	none (740)	none	none	none	none (190)	-
	DTPA aerosol	none (37)	none (37)	-	-	none	-	-
	glucoheptonate	none (740)	none (740)	none	none	none	-	-
	HAM	none (300)	none (300)	-	12 h	-	-	-
	MAA	12 h (148)	12 h (148)	12 h	12 h	12.6 h (150)	12 h (104)	-
	MAG3	none (370)	none (370)	none	-	none	none (68)	-
	MDP[a]	none (740)	none (740)	none	none	none	none (600)	-
	MIBI	none (1,100)	none (370)	none	none	none	none (586)	-
	pertechnetate[a]	24 h (1,100)	4 h (185)	12 h	12 h	24 h (1,100)	12 h (207)	-
	PYP	none (740)	none (740)	none	none	none	-	-
	RBC in vitro	none (740)	none (740)	none	none	none	-	-
	RBC in vivo	6 h (740)	12 h (740)	12 h	12 h	6 h (740)	none[c] (602)	-
	sulfur colloid	6 h (440)	none (444)	none	none	6 h (440)	-	-
	WBC	24 h (185)	48 h (185)	12 h	12 h	24 h (1,100)	-	-
Tl-201	chloride	2 wk (111)	96 h (111)	48 h	48 h	2 wk (110)	-	4 d (148)
Zr-89	antibodies	-	-	-	-	-	-	28 d

[a]no blocking agent
[b]due to assumed ^{125}I contamination
[c]with blocking agent

Dosimetry Methods

The infant can be exposed to radiation energy by internal and external pathways. Internal exposure is caused by the infant's consumption of contaminated breastmilk, while external exposure results from infant proximity to the mother's breast and body. Therefore, in the revised methodology for Regulatory Guide 8.39, it is assumed that the breastfeeding infant is exposed to radioactivity in the mother through three different routes: (1) internally due to the consumption of contaminated breastmilk; (2) externally from the activity in the mother's breast at the time of feeding; and (3) externally from the activity assumed to be uniformly distributed throughout the mother's body at the time of feeding. The radiopharmaceutical in the breastmilk is assumed to be in equilibrium with that in the mother's body when breastfeeding is resumed. With a daily milk production of about 850 mL during lactation (Stabin and Breitz 2000), breastmilk ingestion by the feeding infant is assumed to occur at a constant rate of 35 mL/h with complete emptying of the breast at each of six feedings per day, i.e, 140 mL/feeding. The determination of dose to the breastfeeding infant is fundamentally based on the radioactivity in the mother's body, $A(t)$, at some time, t, after initial administration, A_0, where

$$A(t) = A_0 \cdot R(t) \qquad \text{Equation [5-1]}$$

with $R(t)$ representing the fraction of A_0 retained in the body at time t. Generally, a monophasic or single-exponential retention function

$$R(t) = e^{-\lambda_e t} \qquad \text{Equation [5-2]}$$

is adequate to describe the loss of radioactivity from the mother's body. The parameter λ_e is the effective rate constant (in units of inverse time) describing the loss of radioactivity by both radiological decay and biological excretion. In the method that follows, dose to the infant is approximated by determining the time-integration of activity in the mother, $\tilde{A}$, where

$$\tilde{A} = \int_{\tau}^{T} A(t)\,dt = A_0 \int_{\tau}^{T} R(t)\,dt = A_0 \int_{\tau}^{T} e^{-\lambda_e t}\,dt = A_0 \frac{e^{-\lambda_e \tau} - e^{-\lambda_e T}}{\lambda_e}. \qquad \text{Equation [5-3]}$$

The limits of integration relate to the time after administration at which breastfeeding begins, τ, and the time at which breastfeeding ends, T. In this analysis, breastfeeding is assumed to begin after an interruption time, τ, and to continue until all radioactivity in the mother is lost, i.e., "infinite" time. While breastfeeding typically occurs from a few months to several years, an assumption of infinite time is acceptable as long as T is greater than about 10-times the number of effective half-lives of the radiopharmaceutical, i.e., less than 0.1% of A_0 would be remaining in the mother's body by the time breastfeeding ends. The longest-lived (effective half-live) pharmaceutical considered herein is 130 hours (^{223}Ra). Therefore, if breastfeeding continues for more than about 1300 hours post-administration (~2 months), the assumption of "infinite" time is entirely reasonable. With this assumption Equation [5-3] reduces to

$$\tilde{A} = A_0 \frac{e^{-\lambda_e \tau}}{\lambda_e}. \qquad \text{Equation [5-4]}$$

Likewise, for a double-exponential (biphasic) retention model, applied herein to ^{51}Cr-EDTA, all administrations of sodium iodide, and ^{201}Tl-chloride, the time-integrated activity is

$$\tilde{A} = A_0 \int_{\tau}^{T} \left(f_1\, e^{-\lambda_{e_1} t} + f_2\, e^{-\lambda_{e_2} t}\right) dt = A_0 \left[\frac{f_1 \left(e^{-\lambda_{e_1}\tau} - e^{-\lambda_{e_1} T}\right)}{\lambda_{e_1}} + \frac{f_2 \left(e^{-\lambda_{e_2}\tau} - e^{-\lambda_{e_2} T}\right)}{\lambda_{e_2}}\right] \quad \text{Equation [5-5]}$$

with a reduced form

$$\tilde{A} = A_0 \left[\frac{f_1 \left(e^{-\lambda_{e_1}\tau}\right)}{\lambda_{e_1}} + \frac{f_2 \left(e^{-\lambda_{e_2}\tau}\right)}{\lambda_{e_2}}\right]. \quad \text{Equation [5-6]}$$

Internal Dose due to the Consumption of Breastmilk. The infant is assumed to feed on breastmilk beginning at time, τ, after administration until the complete loss of radioactivity from the mother's body. The infant's internal dose as the result of breastfeeding is therefore,

$$D_{int} = A_0\, \alpha\, I\, DC \int_{\tau}^{\infty} R(t)\, dt, \quad \text{Equation [5-7]}$$

where A_0 is the activity administered to the mother [GBq]; α is the fraction of the pharmaceutical in the mother's body that is excreted to breastmilk per unit volume [mL^{-1}]; I is the mother's milk production rate, as well as the infant's consumption rate [mL h^{-1}]; DC is the radiopharmaceutical-specific dose coefficient for newborn ingestion [mSv GBq^{-1}], and $R(t)$ represents the fraction of the radiopharmaceutical retained in the mother's body at time t after administration. It is assumed that the radiopharmaceutical remains intact when transferred to the infant and that there is complete uptake in the infant's GI tract once ingested (i.e., $f_1 = 1$). The volumetric fraction excreted to breastmilk, α, is conservatively assumed to be constant throughout breastfeeding. After considering the integration of the retention function in Equation [5-7], the total internal dose to the infant is

$$D_{int} = \tilde{A}\, \alpha\, I\, DC. \quad \text{Equation [5-8]}$$

The total fraction, f, of activity initially administered to the mother that ultimately appears in breastmilk is derived from the time-integration of the rate of accumulation of activity in the breastmilk and is related to α by

$$f = \frac{A_0\, \alpha\, I \int_0^{\infty} e^{-\lambda_e t}\, dt}{A_0} = \alpha\, I \left(\frac{1}{\lambda_e}\right) \quad \text{Equation [5-9]}$$

for single-exponential retention, and by

$$f = \frac{A_0\, \alpha\, I \int_0^{\infty} \left(f_1 e^{-\lambda_{e_1} t} + f_2 e^{-\lambda_{e_2} t}\right) dt}{A_0} = \alpha\, I \left(\frac{f_1}{\lambda_{e_1}} + \frac{f_2}{\lambda_{e_2}}\right) \quad \text{Equation [5-10]}$$

for double-exponential retention. The relationship between f and α is provided because several references in the literature provide the total fraction appearing in breastmilk, f, while others provide the volumetric fraction, α. If calculations for an emerging technology are conducted without secretion information, the licensee should conservatively assume half of the total activity administered to the mother appears in the breastmilk (i.e., $f = 0.5$), and the appropriate value of α can be calculated. This assumption is consistent with previous guidance (NRC 1997b; NRC 2020).

External Dose due to Proximity to the Mother's Breast. The infant's total external dose from exposure to the mother's breast while feeding is,

$$D_{ext|br} = A_0 \, \Delta_{pr} \, F_O \, F_{G|br} \, \alpha \, \frac{V}{2} \int_{\tau}^{\infty} R(t)dt$$ Equation [5-11]

where Δ_{pr} [mSv GBq^{-1} h^{-1}] is the nuclide-specific dose-rate kernel (Chapter 2) defined at a distance of 1 meter, F_O is the occupancy factor for breastfeeding (on average, 30-minute feedings six times per day = 0.125), $F_{G|br}$ is the geometry factor for the infant exposed to the mother's breast, and V is the assumed volume of breastmilk at the beginning of feeding. Breastmilk volume is divided by two (2) to approximate the average activity in the breast during feeding. The infant-to-breast geometry factor assumes the infant is 0.6 m long and is lying on the mother's torso, over the breasts and perpendicular to her mid-line, with a separation distance of 0.10 m on center; its analytically derived value is 39. The infant's body length increases from about 0.5 m at birth to about 0.7 m by an age of 6 months (Hunt et al. 2005). The product αV is the fraction of radioactivity in the mother's body that accumulates in the breast at the beginning of feeding. The time-integration of Equation [5-11] provides total external dose to the infant due to radioactivity in the mother's breast,

$$D_{ext|br} = \tilde{A} \, \Delta_{pr} \, F_O \, F_{G|br} \, \alpha \, \frac{V}{2}.$$ Equation [5-12]

External Dose due to Proximity to the Mother's Body. The infant's external dose from exposure to the mother's body while feeding is,

$$D_{ext|bo} = A_0 \, \Delta_{pr} \, F_O \, F_{G|bo} \, (1 - \alpha \, V) \int_{\tau}^{\infty} R(t)dt,$$ Equation [5-13]

where $F_{G|bo}$ is the infant-to-body geometry factor determined by modeling the mother as a 1.7 m line source and the infant as a parallel 0.6 m line receptor, with a separation distance of 0.2 m on center; its analytically derived value is 7.6. The fraction of the radiopharmaceutical that is not in the breast, $(1 - \alpha V)$, is assumed to be uniformly distributed throughout the remainder of the mother's body. The time-integration of Equation [5-13] provides the total external dose to the infant due to radioactivity in the mother's body,

$$D_{ext|bo} = \tilde{A} \, \Delta_{pr} \, F_O \, F_{G|bo} \, (1 - \alpha \, V).$$ Equation [5-14]

The geometry factors stated have been determined using a 2D fluence-based analytical method. As a check for conservatism and precision in using 2D geometry, a 3-dimensional dose-based probabilistic method was also employed (**Figure *5-1***). The 3D estimates of geometry factor are within 10% and less than the 2D estimates, indicating that the 2D estimates are well within bounds of reasonable conservatism.

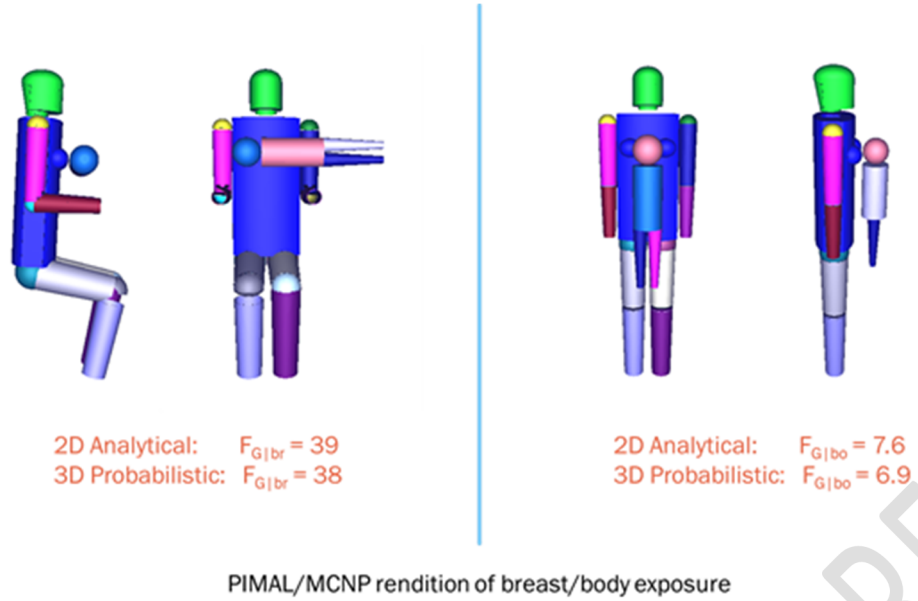

Figure 5-1 Probabilistic representation using PIMAL and MCNP to determine 3D geometry factors

Total Effective Dose Equivalent (TEDE). The infant TEDE is the sum of internal dose due to breastmilk consumption, external dose from exposure to the mother's breast, and external dose from exposure to the mother's body. The TEDE to the breastfeeding infant is therefore,

$$TEDE = \tilde{A}\left[\left(\Delta_{pr}\, F_O \left(F_{G|br}\, \alpha\, \frac{V}{2} + F_{G|bo}\,(1-\alpha\, V)\right)\right) + (\alpha\, I\, DC)\right] \quad \text{Equation [5-15]}$$

where $\tilde{A}$ is equal to Equation [5-4] for monophasic retention or Equation [5-6] for biphasic retention. Reference values of the radiopharmaceutical-specific parameters used herein are presented in

Table *5-2* and Table 5-3.

The Breastfeeding Activity Thresholds. The assumptions in calculating the infant TEDE (Equation [5-15]) are made in order to estimate the activity thresholds for breastfeeding. The intent is that this threshold is conservative, yet somewhat realistic. Setting the TEDE in Equation [5-15] equal to the appropriate total dose limitation D of either 1 or 5 mSv, assuming monophasic retention, and solving for the administered activity, A_0, that would result in that dose limit, we obtain the breastfeeding activity threshold, Q_B, where

$$Q_B = \frac{D\ \lambda_e}{\left[\left(\Delta_{pr}\ F_O\left(F_{G|br}\ \alpha\ \frac{V}{2} + F_{G|bo}\ (1-\alpha\ V)\right)\right) + (\alpha\ I\ DC)\right]}. \quad \text{Equation [5-16]}$$

Consistent with 10 CFR 35.75(b), values of Q_B are calculating assuming no interruption of breastfeeding ($\tau = 0\ h$). We have assumed that the maximum concentration in breastmilk appears instantaneously, and the first breastfeeding occurs immediately after administration. The breastfeeding activity thresholds are presented in **Table *5-4*** for both 5 and 1 mSv dose limitations.

To determine the interruption time required to meet a given dose limitation, Equation [5-15] is again rearranged to solve for τ. The calculated interruption time for monophasic retention is therefore,

$$\tau = \ln\left(\frac{A_0\left[\left(\Delta_{pr}\ F_O\left(F_{G|br}\ \alpha\ \frac{V}{2} + F_{G|bo}\ (1-\alpha\ V)\right)\right) + (\alpha\ I\ DC)\right]}{D\ \lambda_e}\right)\Bigg/\lambda_e = \frac{\ln\left({}^{A_0}/_{Q_B}\right)}{\lambda_e} \quad \text{Equation [5-17]}$$

Table *5-5* provides calculated interruption times for several pharmaceuticals given a particular administered activity, A_0. Equation [5-16] and Equation [5-17] are reformulated for biphasic retention (again, with t = 0) such that the equation for the breastfeeding activity threshold is,

$$Q_B = \frac{D}{\left(\frac{f_1}{\lambda_{e_1}} + \frac{f_2}{\lambda_{e_2}}\right)\left[\left(\Delta_{pr}\ F_O\left(F_{G|br}\ \alpha\ \frac{V}{2} + F_{G|bo}\ (1-\alpha\ V)\right)\right) + (\alpha\ I\ DC)\right]}. \quad \text{Equation [5-18]}$$

The interruption time is calculated by moving the integrated retention function to the left and allowing Q_B to equal the administered activity; thus, Equation [5-18] is rewritten as

$$f_1\ \frac{e^{-\lambda_{e_1}\tau}}{\lambda_{e_1}} + f_2\ \frac{e^{-\lambda_{e_2}\tau}}{\lambda_{e_2}} = \frac{D}{A_0\left[\left(\Delta_{pr}\ F_O\left(F_{G|br}\ \alpha\ \frac{V}{2} + F_{G|bo}\ (1-\alpha\ V)\right)\right) + (\alpha\ I\ DC)\right]}. \quad \text{Equation [5-19]}$$

Then, using Equation [5-19], the interruption time is deduced by numerically sampling different values of τ to determine the value that satisfies the equality. For a pharmaceutical that follows biphasic elimination, modeling that elimination as a monophasic or single-exponential retention function results in a significantly shorter interruption time because the function essentially ignores long-term activity. Licensees should use whatever

retention data are available for a given radiopharmaceutical when the need arises to estimate an appropriate time for breastfeeding interruption.

Contaminant Nuclides. In some cases, radiological contaminants may be present in a given administration (e.g., I-125 in I-123 administrations). If the contributions to radiological dose could be significant, the licensee should determine infant TEDE; breastfeeding activity threshold; and, if necessary, breastfeeding interruption time based on the greater dose and times calculated for each radiological constituent. **Table *5-5*** includes I-125 administered as NaI for this very reason. The licensee is cautioned that there may be times when the contaminant results in greater dose than the original radionuclide.

Table 5-2 Radiopharmaceutical-specific parameter values for calculating modified activity thresholds and potential interruption times for a monophasic retention model to protect the breastfeeding infant

Radionuclide	Pharmaceutical	λ_e [h^{-1}]	Δ_{pr}[a] [mSv GBq^{-1} h^{-1}]	α [mL^{-1}]	*f* [unitless]	*DC* [mSv GBq^{-1}]
C-11	choline	2.04	0.154	3×10^{-3}	5×10^{-2} [c]	40[d]
F-18	FDG	0.386[b]	0.148	4×10^{-4}	4×10^{-2} [g]	95[d]
Ga-67	citrate	0.0123[e]	0.0207	4×10^{-5}	1×10^{-1} [e]	640[d]
Ga-68	octreotate	0.618	0.143	4×10^{-5}	2×10^{-3} [c]	180[d]
I-123	MIBG	0.0604[c]	0.039	2×10^{-6}	1×10^{-3} [c]	2,700[e]
	OIH	0.159[b]	0.039	9×10^{-5}	2×10^{-2} [b]	150[d]
I-125	OIH	0.107[b]	0.0332	6×10^{-5}	2×10^{-2} [b]	2,400
I-131	OIH	0.110[b]	0.0576	8×10^{-5}	2×10^{-2} [b]	2,700[d]
In-111	octreotate	0.0144[c]	0.0798	1×10^{-9}	3×10^{-6} [c]	280[d]
	WBC	0.0151[c]	0.0798	4×10^{-6}	1×10^{-2} [j]	5,500[e]
Lu-177	octreotate	0.00842[c]	0.00527	5×10^{-7}	2×10^{-3} [k]	6,100[g]
N-13	any	4.17	0.154	6×10^{-3}	5×10^{-2} [c]	5.7
O-15	water	20.4	0.154	3×10^{-2}	5×10^{-2} [c]	7.7[d]
Ra-223	dichloride	0.00528[f]	0.0475	8×10^{-5}	5×10^{-1} [h]	5,300,000[g]
Rb-82	chloride	32.7	0.172	5×10^{-2}	5×10^{-2} [c]	8.5[d]
Tc-99m	DISIDA	0.185[e]	0.0194	5×10^{-4}	1×10^{-1} [c]	220[e]
	DTPA	0.202[b]	0.0194	7×10^{-7}	1×10^{-4} [b]	16[d]
	DTPA aerosol[m]	0.202[b]	0.0194	7×10^{-7}	1×10^{-4} [b]	6.5[e]
	glucoheptonate	0.185[e]	0.0194	7×10^{-6}	1×10^{-3} [e]	80[e]
	HAM	0.231[e]	0.0194	7×10^{-4}	1×10^{-1} [c]	200[e]
	MAA	0.173[b]	0.0194	2×10^{-4}	4×10^{-2} [b]	63[d]
	MAG3	0.165[b]	0.0194	3×10^{-6}	7×10^{-4} [b]	22[d]
	MDP	0.192[b]	0.0194	1×10^{-6}	3×10^{-4} [b]	63[e]
	MIBI	0.129[b]	0.0194	2×10^{-6}	5×10^{-4} [b]	53[d]
	pertechnetate	0.202[b]	0.0194	6×10^{-4}	1×10^{-1} [b]	98[d]
	PYP	0.202[e]	0.0194	6×10^{-4}	1×10^{-1} [c]	66[e]
	RBC in vitro	0.202[e]	0.0194	2×10^{-6}	3×10^{-4} [e]	39[d]
	RBC in vivo	0.202[e]	0.0194	5×10^{-6} [e]	9×10^{-4}	39[d]
	sulfur colloid	0.138[e]	0.0194	4×10^{-4}	1×10^{-1} [c]	92[e]
	WBC	0.185[e]	0.0194	5×10^{-4}	1×10^{-1} [c]	62[d]
Zr-89	panitumumab	0.0127[f]	0.207	2×10^{-4}	5×10^{-1} [h]	790[g]

[a] point kernel at 1 meter
[b] Leide-Svegborn et al. (2016)
[c] Zanzonico et al. (2019)
[d] ICRP-128 (2015)
[e] Stabin and Brietz (2000)
[f] manufacturers package insert
[g] Hicks et al. (2001)
[h] capped at 0.5
[j] estimated
[k] based on Ga-68 octreotate

[m]40.6% of administration taken up into bloodstream[e] then treated as DTP

Table 5-3 Radiopharmaceutical-specific parameter values for calculating modified activity thresholds and potential interruption times for a biphasic retention model to protect the breastfeeding infant

Radio-nuclide	Pharmaceutical	f_1 (unitless)	λ_{e_1} [h^{-1}]	f_2 (unitless)	λ_{e_2} [h^{-1}]	Δ_{pr}[a] [mSv GBq^{-1} h^{-1}]	α [mL^{-1}]	f (unitless)	DC [mSv GBq^{-1}]
Cr-51	EDTA	0.96[b]	0.113[b]	0.04[b]	0.0618[b]	0.00465	2×10^{-6}	7×10^{-4} [b]	200
I-123	NaI thyroid HYP	0.2[f]	0.142[f]	0.8[f]	0.0578[f]	0.039	1×10^{-4}	7×10^{-2} [c]	38,000
I-123	NaI thyroid CA	0.95[f]	0.142	0.05[f]	0.0562[f]	0.039	3×10^{-4}	7×10^{-2}	38,000
I-123	NaI EDE HYP	0.2	0.142	0.8	0.0578	0.039	1×10^{-4}	7×10^{-2}	2,100
I-123	NaI EDE CA	0.95	0.142	0.05	0.0562	0.039	3×10^{-4}	7×10^{-2}	2,100
I-124	NaI thyroid HYP	0.2	0.0969[f]	0.8	0.0125[f]	0.167	3×10^{-5}	7×10^{-2} [c]	2,300,000
I-124	NaI thyroid CA	0.95	0.0969	0.05	0.0109[f]	0.167	1×10^{-4}	7×10^{-2}	2,300,000
I-124	NaI EDE HYP	0.2	0.0969	0.8	0.0125	0.167	3×10^{-5}	7×10^{-2}	110,000
I-124	NaI EDE CA	0.95	0.0969	0.05	0.0109	0.167	1×10^{-4}	7×10^{-2}	110,000
I-125	NaI thyroid HYP	0.2	0.0905[f]	0.8	0.00603[f]	0.0332	2×10^{-5}	7×10^{-2} [c]	1,000,000
I-125	NaI thyroid CA	0.95	0.0905	0.05	0.00445[f]	0.0332	9×10^{-5}	7×10^{-2}	1,000,000
I-125	NaI EDE HYP	0.2	0.0905	0.8	0.00603	0.0332	2×10^{-5}	7×10^{-2}	52,000
I-125	NaI EDE CA	0.95	0.0905	0.05	0.00445	0.0332	9×10^{-5}	7×10^{-2}	52,000
I-131	NaI thyroid HYP	0.2	0.0936[f]	0.8	0.00915[f]	0.0576	1×10^{-4}	3×10^{-1} [b]	3,600,000
I-131	NaI thyroid CA	0.95	0.0936	0.05	0.00756[f]	0.0576	5×10^{-4}	3×10^{-1}	3,600,000
I-131	NaI EDE HYP	0.2	0.0936	0.8	0.00915	0.0576	1×10^{-4}	3×10^{-1}	180,000
I-131	NaI EDE CA	0.95	0.0936	0.05	0.00756	0.0576	5×10^{-4}	3×10^{-1}	180,000
Tl-201	chloride	0.64[e]	0.0256[e]	0.36[e]	0.00951[e]	0.0405	1×10^{-7}	3×10^{-4} [c]	1,300

[a]point kernel at 1 meter
[b]Leide-Svegborn et al. (2016)
[c]Zanzonico et al. (2019)
[d]ICRP-128 (2015)
[e]Johnston et al. (1996)
[f]RG 8.39, Rev 1 (NRC 2020)

Table 5-4 Modified breastfeeding activity thresholds by radiopharmaceuticals with no interruption

		Breastfeeding Thresholds			
		$Q_{B\|rec}$		$Q_{B\|ins}$	
Radionuclide	Pharmaceutical	GBq	mCi	GBq	mCi
C-11	choline	2	60	0.5	10
Cr-51	EDTA	30	800	6	200
F-18	FDG	1	30	0.2	6
Ga-67	citrate	0.08	2	0.02	0.4
Ga-68	octreotate	9	200	2	50
I-123	MIBG	1	40	0.3	8
	OIH	2	40	0.3	8
	NaI*	0.002	0.05	0.0004	0.01
I-124	NaI*	3×10^{-5}	8×10^{-4}	6×10^{-6}	2×10^{-4}
I-125	OIH	0.1	3	0.02	0.6
	NaI*	7×10^{-5}	2×10^{-3}	1×10^{-5}	4×10^{-4}
I-131	OIH	0.08	2	0.02	0.4
	NaI*	4×10^{-6}	1×10^{-4}	9×10^{-7}	2×10^{-5}
In-111	octreotate	0.9	30	0.2	5
	WBC	0.08	2	0.02	0.4
Lu-177	octreotate	0.4	10	0.08	2
N-13	any	10	400	3	70
O-15	water	10	300	2	60
Ra-223	dichloride	2×10^{-6}	5×10^{-5}	4×10^{-7}	1×10^{-5}
Rb-82	chloride	10	300	2	60
Tc-99m	DISIDA	0.2	6	0.05	1
	DTPA	50	1000	10	300
	DTPA aerosol	100	4000	30	700
	glucoheptonate	20	600	5	100
	HAM	0.2	7	0.05	1
	MAA	2	60	0.4	10
	MAG3	40	1000	8	200
	MDP	40	1000	9	200
	MIBI	30	800	6	200
	pertechnetate	0.5	10	0.1	3
	PYP	0.7	20	0.1	4
	RBC in vitro	50	1000	10	300
	RBC in vivo	40	1000	8	200
	sulfur colloid	0.5	10	0.1	3
	WBC	0.8	20	0.2	4
Tl-201	chloride	2	50	0.4	10
Zr-89	panitumumab	0.01	0.3	0.002	0.07

*Thresholds based on infant thyroid dose equivalent

Table 5-5 Recommended breastfeeding interruption times for dose limitations of 5 and 1 mSv

Radionuclide	Pharmaceutical	Typical Administered Activity (GBq)	Interruption Time (h)	
			5 mSv	1 mSv
C-11	any	0.925[b]	-	-
Cr-51	EDTA	0.00185[b]	-	-
F-18	FDG	0.74[c]	-	3
Ga-67	citrate	0.333[c]	120	250
Ga-68	octreotate	0.185[b]	-	-
I-123	MIBG	0.37[b]	-	4
	OIH	0.074[b]	-	-
	NaI*(HYP)	0.185[c]	78	110
I-124	NaI*(HYP)	0.074[b]	620	750
I-125	OIH	0.00037[b]	-	-
	NaI*(CA)	0.0185[a]	1,100	1,400
I-131	OIH	0.011[b]	-	-
	NaI*(CA)	5.55[b]	1,700	1,900
In-111	octreotate	0.185[b]	-	-
	WBC	0.037[c]	-	50
Lu-177	octreotate	7.8[b]	350	540
N-13	any	0.925[b]	-	-
O-15	water	1.85[b]	-	-
Ra-223	dichloride	0.00385[d]	1,400	1,700
Rb-82	chloride	1.85[c]	-	-
Tc-99m[+]	DISIDA	0.296[b]	1	10
	DTPA	1.11[c]	-	-
	DTPA aerosol	0.04[c]	-	-
	glucoheptonate	0.74[b]	-	-
	HAM	0.296[b]	-	8
	MAA	0.151[c]	-	-
	MAG3	0.37[c]	-	-
	MDP	1.11[c]	-	-
	MIBI	1.48[c]	-	-
	pertechnetate	0.37[c]	-	6
	PYP	0.555[c]	-	7
	RBC in vitro	1.11[c]	-	-
	RBC in vivo	1.11[c]	-	-
	sulfur colloid	0.222[c]	-	5
	WBC	0.37[c]	-	5
Tl-201	chloride	0.148[c]	-	-
Zr-89	panitumumab	0.075[d]	140	270

[+]it is generally recommended that 24-hour interruption is applied all Tc-99m pharmaceuticals
*interruption time based on most restrictive infant thyroid dose for mothers with hyperthyroidism (HYP) or thyroid cancer (CA)
[a]10% of the activity administered as I-123 (to consider nuclide contamination)
[b]Zanzonico et al. 2019
[c]SNMMI 2000
[d]manufacturer's package insert

Example Calculation

An administration of ^{131}I as NaI for hyperthyroidism is chosen to provide an example. To determine the breastfeeding activity thresholds, the internal and external radiation dose to the infant, and recommended breastfeeding interruption time (if required), the following parameterization is necessary:

A_0 = 5.55 [GBq]	T_r = 192.497 [h]	Δ_{pr} = 0.0576 [mSv GBq^{-1} h^{-1}]	
f_1 = 0.20	T_{b_1} = 7.7 [h]	T_{e_1} = 7.4 [h]	λ_{e_1} = 0.0936 [h^{-1}]
f_2 = 0.80	T_{b_2} = 125 [h]	T_{e_1} = 75.8 [h]	λ_{e_2} = 0.00915 [h^{-1}]
F_0 = 0.125	$F_{G\|br}$ (0.1 m) = 39	$F_{G\|bo}$ (0.2 m) = 7.6	
V = 140 [mL]	I = 35 [mL h^{-1}]	α = 9.9x10^{-5} [mL^{-1}]	DC = 3.6x10^6 [mSv GBq^{-1}]

The total fraction of administered ^{131}I excreted in breastmilk is related to the volumetric fraction, α, by:

$$f = \alpha\, I \left(\frac{f_1}{\lambda_{e_1}} + \frac{f_2}{\lambda_{e_2}}\right) = 9.9x10^{-5}\ [mL^{-1}] \cdot 35\ [mL\ h^{-1}] \left(\frac{0.20}{0.0936} + \frac{0.80}{0.00915}\right) = 0.31$$

The breastfeeding activity threshold for an assumption of no interruption (t = 0) is calculated for biphasic retention and a 1 mSv dose limitation (instruction):

$$Q_{B|ins} = \frac{1\ [mSv]}{\left(f_1\ \frac{e^{-\lambda_{e_1}\tau}}{\lambda_{e_1}} + f_2\ \frac{e^{-\lambda_{e_2}\tau}}{\lambda_{e_2}}\right)\left[\left(\Delta_{pr}\, F_O \left(F_{G|br}\ \alpha\ \frac{V}{2} + F_{G|bo}\ (1 - \alpha\, V)\right)\right) + (\alpha\ I\ DC)\right]}.$$

$$= \frac{1\ [mSv]}{\left(\frac{0.20}{0.0936} + \frac{0.80}{0.00915}\right)\left[\left(0.0576 \cdot 0.125 \left(39 \cdot 9.9x10^{-5} \cdot \frac{140}{2} + 7.6 \cdot (1 - 9.9x10^{-5} \cdot 140)\right)\right) + (9.9x10^{-5} \cdot 35 \cdot 3.6x10^6)\right]}.$$

$$Q_{B|ins} = 9.0x10^{-7}\ [GBq]$$

and for a 5 mSv dose limitation (record keeping):

$$Q_{B|rec} = \frac{5\ [mSv]}{\left(f_1\ \frac{e^{-\lambda_{e_1}\tau}}{\lambda_{e_1}} + f_2\ \frac{e^{-\lambda_{e_2}\tau}}{\lambda_{e_2}}\right)\left[\left(\Delta_{pr}\, F_O \left(F_{G|br}\ \alpha\ \frac{V}{2} + F_{G|bo}\ (1 - \alpha\, V)\right)\right) + (\alpha\ I\ DC)\right]}.$$

$$= \frac{5\ [mSv]}{\left(\frac{0.20}{0.0936} + \frac{0.80}{0.00915}\right)\left[\left(0.0576 \cdot 0.125 \left(39 \cdot 9.9x10^{-5} \cdot \frac{140}{2} + 7.6 \cdot (1 - 9.9x10^{-5} \cdot 140)\right)\right) + (9.9x10^{-5} \cdot 35 \cdot 3.6x10^6)\right]}.$$

$$Q_{B|rec} = 4.5x10^{-6}\ [GBq]$$

The administered activity of 5.55 GBq is much greater than both thresholds, therefore, interruption of breastfeeding is necessary. Using Equation [5-19] and iteratively solving for τ, an interruption time of 1,710 hours is derived (compare to Table 5-5).

$$f_1 \frac{e^{-\lambda_{e_1}\tau}}{\lambda_{e_1}} + f_2 \frac{e^{-\lambda_{e_2}\tau}}{\lambda_{e_2}} = \frac{D}{A_0\left[\left(\Delta_{pr} F_O \left(F_{G|br}\, \alpha \frac{V}{2} + F_{G|bo}\,(1-\alpha V)\right)\right) + (\alpha\, I\, DC)\right]}.$$

6. PATIENT DEATH

This analysis examines the potential event of patient death shortly after administration of radioactive material and release from a medical facility under 10 CFR 35.75, "Medical Use of Byproduct Material." The dosimetry analysis evaluated the potential impact on first responders and funeral workers who may be exposed to doses near 10 CFR Part 20 limits due to the handling of the deceased patient.

An external dosimetry assessment was conducted for first responders and those involved in burial preparation when handling the remains of individuals who received medical administrations of radiopharmaceuticals. The outcome of the assessment is heavily dependent on the administered activity assumed; where possible, the assessment considers the suggested administrations of package inserts or typically administered activities. The radionuclides analyzed were obtained from RG 8.39, Rev 1 (NRC 2020). The analysis shows that a small fraction of the radionuclides listed could result in first responders or funeral workers exceeding the 0.02 mSv/h dose rate limit or the 1 mSv dose limit of 10 CFR 20 if, under conservative conditions, a patient was administered a radiopharmaceutical and died within hours of release.

Four specific radionuclides (^{131}I, ^{166}Ho, ^{177}Lu, and ^{188}Re) and eight related radiopharmaceutical procedures were identified for future study to determine if cremation or cadaver care is an issue for consideration in regulatory guidance. Future, more rigorous and realistic analyses could provide supporting information if additional instruction for funeral practitioners would be appropriate.

Background

Patient release following 10 CFR 35 is based on the licensee determining that any other individual coming into contact with the patient will not exceed a dose limit of 5 mSv (for release) or 1 mSv (with instruction) over the effective life of the radiopharmaceutical. If a patient dies, regulatory requirements adhere to 10 CFR 20 dose limits to any member of the public of 0.02 mSv/h or 1 mSv per year. Based on administered activity, pharmaceutical biokinetics, and radiation emission characteristics, it is possible for living patients undergoing certain therapeutic procedures to be released with enough activity to cause external dose rates to others in excess of 0.02 mSv/h (or total dose in excess of 1 mSv). First responders (e.g., police officers, emergency medical technicians) and funeral workers (e.g., embalmers, crematorium operators) are the most likely candidates to receive these potentially high exposures.

Under 10 CFR 35.75, once a licensee administers the radioactive material and releases the patient, the radioactivity (whether sealed or unsealed) is no longer licensed. While the probability of a burial or cremation with radioactive contamination is of low incidence, it has occurred in recent years (Yu et al. 2019). During that event, an older male suffering from pancreatic cancer received a radiation therapy administration (^{177}Lu) from an Arizona hospital. Two days later, he died unexpectedly at a different hospital and was subsequently cremated. Crematorium workers remained unaware of the patient's treatment history until staff from the administering hospital learned of the untimely death and commissioned the Arizona Bureau of Radiation Control to inspect the facility.

Their survey revealed radiation contamination on the crematorium's oven, vacuum filter, and bone crusher. Additionally, traces of ^{99m}Tc were detectable in the urine of one operator at the same crematorium indicating that a separate cremation must have occurred previously without knowledge that the cadaver was radioactive. To further complicate requirements for crematoriums, the authors noted

that while one state in the Union has no regulation regarding informing a crematorium of deceased patients who have received a radiopharmaceutical, another state requires that no radionuclides be incinerated with human remains. Yu et al. (2019) concluded that, "… *future safety protocols for radiopharmaceuticals should include postmortem management, such as evaluating radioactivity in deceased patients prior to cremation and standardizing notification of crematoriums."* As well, the American College of Radiology recommends that, " *… the NRC play a more proactive role in education of the crematorium and funeral home industries that could reduce or eliminate RSOs' administrative burden in Section 2.4 [of RG 8.39, Rev 1].*"

And, in March 2019, the National Funeral Directors Association (NFDA 2019) stated:

Importantly, one of the tenets of the National Funeral Directors Association's Certified Crematory Operator Program™ is to ensure that crematory operators have the necessary information about the decedent to conduct cremation safely. NFDA guidance on authorizations includes the need to obtain representation that there are no radioactive or other implants … in the remains as they may create a hazardous condition when placed in the cremation chamber and subjected to heat.

During the revision of Regulatory Guide 8.39, the NRC added a new section in Rev 1 (NRC 2020) on the death of a patient which discusses in general terms what should be considered by the licensee to instruct the patient for potential precautions if untimely death occurs. The guidance states that the licensee (if notified by the family of the patient's death) should inform the morgue or funeral home that the decedent contains radioactive material and then provide precautions to minimize exposures to professionals involved in embalming, burial, cremation, etc.

The potential for first responders or funeral workers to receive external radiation exposures in excess of regulatory dose limits is evaluated in this chapter. Radiopharmaceuticals of potential concern in terms of exceeding regulatory limits are also identified.

Methodology

A screening assessment was performed to identify radionuclides of potential concern and then the specific pharmaceutical administrations containing those nuclides that may result in elevated dose rates or total integrated dose near the cadaver. Because of the two dose limitations set forth in 10 CFR 20, the screening assessment examines external dose potentially received in two unrelated exposure scenarios at different points in time. The assessment considers both the dose rate limit of 0.02 mSv/h and the annual dose limit of 1 mSv. For conservatism, and due to the relatively short timeframes examined (described below), the radioactive material in the cadaver is assumed to be lost only by physical decay between the time of administration and death. Further, the exposed individuals and cadaver are modeled as point-to-point geometry with 1-meter separation and full occupancy.

The first scenario is designed to model an example exposure of a first responder where a conservative assumption is made that the patient is released and dies at 6 hours post-administration. The exposed individual comes into close contact with the cadaver at that time; in this case, the dose equivalent rate at 1 meter from the cadaver cannot exceed 0.02 mSv/h. The calculation of dose rate is carried out using

$$\dot{D}(t)\left[\frac{mSv}{h}\right] = A_0[GBq] \cdot \Delta_{pr}\left[\frac{mSv}{GBq \cdot h}\right] \cdot e^{-\lambda t} \qquad \text{Equation [6-1]}$$

where A_0 is the assumed administered activity (SNMMI 2018), Δ_{pr} is the nuclide-specific gamma-ray dose rate constant at 1 meter from Chapter 2, λ is the radiological decay constant (ICRP 2008), and t is the time since radiopharmaceutical administration (i.e., 6 hours).

The second scenario is designed to model an example exposure of a funeral worker where it is assumed that the patient is released and dies within the first twenty-four hours after administration. The exposed individual comes into close contact with the cadaver at hour 24 and is exposed continuously for the next 8 hours; in this case, the funeral worker's dose equivalent cannot exceed 1 mSv. The total dose is determined by integrating dose equivalent rate over the time of exposure, such that

$$D[mSv] = A_0 \cdot \Delta_{pr} \cdot \int_{\tau_1}^{\tau_2} e^{-\lambda t}\, dt = A_0 \cdot \Delta_{pr} \cdot \frac{e^{-\lambda\tau_1} - e^{-\lambda\tau_2}}{\lambda} \qquad \text{Equation [6-2]}$$

where τ_1 is the beginning of exposure (i.e., 24 hours) and τ_2 is the end of exposure (i.e., 32 hours). Again, for conservatism physical decay is the only removal mechanism post-administration, and an average distance of 1 meter and full occupancy are assumed during the eight-hour exposure.

Results

The results of the screening study are based on conservative assumptions for modeling exposures to first responders and funeral workers. All dose and dose rates are proportionately dependent on the assumed administered activity; as such, assumptions thereof originate from package inserts, the research literature, or activity thresholds associated with a 10 CFR 35.75 bystander dose of 1 mSv.

Table *6-1*, below, provides a listing of 44 radionuclides used commonly or historically for diagnostic and therapeutic medical administrations, per RG 8.39, Rev 1 (NRC 2020). The table shows an assumed administration for each radionuclide, the external dose equivalent rate at 6-hours post-administration, and the total external dose equivalent to an individual exposed between Hour 24 and Hour 32 after administration. Based on these conservative assumptions, dose rates exceeding the 0.02 mSv/h limit are indicated for about 15% of the listed radionuclides and two (^{131}I, ^{166}Ho) exceed the total dose limit of 1 mSv.

Diagnostic procedures typically require lower activity administrations than those for therapeutic purposes. Patient death shortly after release of a therapy patient represents the greatest potential for high radiological dose rates to others from the radioactive cadaver. **Table *6-2*** presents the list of 44 radionuclides with a patient death activity threshold. This threshold represents the administered activity required to create a dose rate of 0.02 mSv/h at 1 meter, 6 hours after administration. The use of these thresholds will be more appropriate if the administered activity of a given nuclide is known. In that case, the licensee could use of **Table *6-2*** to determine the likelihood of exceeding 10 CFR 20 dose rate limits if a released patient should die shortly after administration when biological removal prior to death is neglected.

Table *6-3* presents external dose rates at 1 m immediately after radiopharmaceutical administration for eight identified therapeutic procedures involving high levels of radioactivity. Four radionuclides, including ^{131}I (in five different pharmaceuticals), ^{166}Ho, ^{177}Lu, and ^{188}Re, were found to exhibit the realistic potential to result in dose rates exceeding 0.02 mSv/h by as much as a factor of 50. The rightmost column in Table 6-3 provides a conservative indication of the time that would be required for dose rates to fall below 0.02 mSv/h due to radiological decay alone (without biological removal). As shown, the highest external dose rate (1.1 mSv/h) arises from the administration of 18.5 GBq ^{131}I-iobenguane (Azedra).

Conclusions

For the vast majority of administered radiopharmaceuticals, activity levels in released patients will not result in situations where exposure to a radioactive cadaver could exceed the dose limits of 10 CFR 20. Depending on therapeutic need however, administration of ^{131}I (in five different pharmaceuticals), ^{166}Ho, ^{177}Lu, and ^{188}Re could result in dose rates exceeding 0.02 mSv/h or total dose in excess of 1 mSv within days of release. Driven entirely by the administered activity of a given pharmaceutical, dose and dose rate limits could be exceeded by several procedures. With more than 20 million procedures annually in the United States (SNMMI 2018), a small fraction of this total rises to a level of concern.

The screening assessment reveals that the dose-rate limitation (as opposed to that for total dose) is the driving force for decision making (

Table *6-1*). The two nuclides with a hypothetical total dose above 1 mSv exceeded the limit by no more than a factor of two. For radionuclides with dose rates exceeding 0.02 mSv/h, the limit could be exceeded by more than an order of magnitude. Therefore, limiting dose rate to an acceptable level for all nuclides will also limit total dose. Additionally, during this screening process, no radioactive implant was identified as potentially important from the perspective of external exposure following patient death. For patient death occurring outside the medical facility, this screening assessment indicates there is a low likelihood that regulatory limits on external dose would be exceeded if the radioactive implant were to remain in place. **Table *6-2*** lists the threshold level of activity for 44 nuclides that would result in a dose rate of 0.02 mSv/h at one meter, 6 hours after administration.

Yittrium-90 therapy was determined not to be a hazard for external exposure to first responders or funeral workers unless cremation is to be carried out. The ^{90}Y that is obtained from the neutron bombardment reaction is quite pure. But, because of the less-than-pure purification process of ^{90}Y from ^{90}Sr and other fission products, sources of ^{90}Y originating from fission could be potentially contaminated with other long-lived radionuclides, e.g., ^{57}Co, ^{60}Co, ^{88}Y, ^{89}Y, ^{154}Eu, and ^{156}Eu (Nelson et al. 2008). During cremation of a patient having received contaminated ^{90}Y microspheres, the long-lived contaminants could expose crematorium workers, contaminate cremation ovens, and escape into the atmosphere becoming available for inhalation by members of the public near the cremation facility (Gadodia et al. 2020). This assessment indicates that ^{90}Y itself is not an issue to external dose, but the screening analysis did not examine the potential for internal exposures due to ^{90}Y or its long-lived contaminants. Further inhalation analysis from cremation may be warranted.

Additional examination of the ^{131}I (in five different pharmaceuticals), ^{166}Ho, ^{177}Lu, and ^{188}Re is justified to reduce the conservatism provided in this study. These additional considerations include more realistic biological clearance, probabilistic geometric considerations, and the back-calculation of time required to

reach the 10 CFR 20 dose limit following a specific administration. Contamination buildup in the crematorium oven/chimney could be investigated as well, along with an additional internal pathway analysis for alpha-emitting radionuclides.

Table 6-1 Potential dose rate and total dose at 1 m from deceased to a first responder or funeral worker

Radionuclide	Administered Activity[a] A_0 (GBq)	Dose-Rate Constant[b] Δ_{pr} (mSv GBq^{-1} h^{-1})	Dose Rate at 6 h (mSv/h)	Total Dose Hour 24-32 (mSv)
Ag-111	0.92	0.00417	0.004	0.028
At-211	16	0.00604	0.054	0.054
Au-198	0.18	0.0605	0.010	0.065
Bi-213	48	0.0193	0.004	---
C-11	0.925	0.152	---	---
Cr-51	0.0074	0.00476	---	---
Cs-131	0.20	0.0148	0.003	0.022
Cu-64	2.0	0.0274	0.039	0.096
Cu-67	0.66	0.0171	0.011	0.066
Dy-165	62	0.00488	0.051	0.001
Er-169	120	0.0000258	0.003	0.023
F-18	0.74	0.147	0.011	---
Ga-67	0.333	0.0234	0.007	0.049
Ga-68	0.185	0.141	0.001	---
Ho-166	77.2	0.00526	0.348	1.58
I-123	0.185	0.0394	0.005	0.014
I-124	0.074	0.163	0.012	0.080
I-125	0.0185	0.0301	0.001	0.004
I-131	5.0	0.0582	0.285	2.11
In-111	0.185	0.0736	0.013	0.082
Ir-192	0.0033	0.122	---	0.003
Lu-177	7.4	0.00548	0.040	0.287
N-13	0.925	0.152	---	---
O-15	1.85	0.153	---	---
P-32	0.37	0.000473	---	0.001
P-33	71	0.0000161	0.001	0.009
Pd-103	0.14	0.0122	0.002	0.013
Ra-223	0.00385	0.0219	---	0.001
Rb-82	1.85	0.166	---	---
Re-186	2.2	0.00356	0.007	0.050
Re-188	4.0	0.00948	0.030	0.097
Ru-106	1,200	0.0000000654	---	0.001
Sc-47	0.54	0.0160	0.008	0.054
Se-75	0.0042	0.0574	---	0.002
Sm-153	0.93	0.0160	0.014	0.078
Sn-117m	0.062	0.0343	0.002	0.016
Sr-89	1.5	0.000381	0.001	0.004
Sr-90	0.04	0.0000691	---	---
Tc-99m	1.5	0.0196	0.015	0.010

Radionuclide	Administered Activity[a] A_0 (GBq)	Dose-Rate Constant[b] Δ_{pr} (mSv GBq^{-1} h^{-1})	Dose Rate at 6 h (mSv/h)	Total Dose Hour 24-32 (mSv)
Tl-201	0.148	0.0157	0.002	0.014
Xe-133	0.74	0.0151	0.011	0.077
Y-90	14	0.000798	0.010	0.066
Yb-169	0.014	0.0633	0.001	0.007
Zr-89	0.075	0.165	0.012	0.077

[a]assumed administrated activity from package inserts, Society of Nuclear Medicine (SNMMI 2018)
[b]point kernel at 1 meter
--- indicates a dose rate less than 0.001 mSv/h

Table 6-2 Patient death activity threshold for 44 radionuclides

Radionuclide	Patient Death Activity Threshold (GBq)
Ag-111	4.9
At-211	5.9
Au-198	0.35
Bi-213	240
C-11	26,000
Cr-51	4.2
Cs-131	1.4
Cu-64	1.0
Cu-67	1.3
Dy-165	24
Er-169	790
F-18	1.3
Ga-67	0.90
Ga-68	5.7
Ho-166	4.4
I-123	0.69
I-124	0.13
I-125	0.67
I-131	0.35
In-111	0.29
Ir-192	0.16
Lu-177	3.8
N-13	>>
O-15	>>
P-32	43
P-33	1,200
Pd-103	1.7
Ra-223	0.93
Rb-82	>>
Re-186	5.9
Re-188	2.7
Ru-106	>>
Sc-47	1.3
Se-75	0.35
Sm-153	1.4
Sn-117m	0.59
Sr-89	53
Sr-90	290
Tc-99m	2.0

Radionuclide	Patient Death Activity Threshold (GBq)
Tl-201	1.4
Xe-133	1.4
Y-90	27
Yb-169	0.32
Zr-89	0.13

>> indicates very large activity required

Table 6-3 Therapeutic procedures resulting in high dose rates at the time of administration

Administration	Half-Life (d)	Maximum Dose Rate at Administration (mSv/h)	Time Required for Activity to Decay to 0.02 mSv/h (d)
18.5 GBq ^{131}I iobenguane	8.0	1.1	46
8 GBq Na-^{131}I for differentiated thyroid cancer	8.0	0.47	36
5 GBq ^{131}I meta-iodobenzylguanidine (MIBG)	8.0	0.29	31
3 GBq ^{131}I labeled monoclonal antibody therapy	8.0	0.17	25
2 GBq ^{131}I ethiodized oil lipiodol therapy	8.0	0.12	20
7.4 GBq ^{177}Lu dotatate	6.6	0.041	7
77.2 GBq ^{166}Ho injection[a]	1.1	0.41	5
4 GBq ^{188}Re hydroxyethylidine diphosphonate (HEDP)[b]	0.71	0.038	1

[a] Largest activity in administered range of 19.2 – 77.2 GBq for injections of various chemical forms (IAEA 2009, Annex V)
[b] Largest activity in listed range of 1.2 – 4 GBq (IAEA 2009, Annex V)

7. EMERGING TECHNOLOGIES

To find information on emerging technologies in radiopharmaceuticals, an in-depth search from the past 5 years was performed in the publications of: *Journal of Nuclear Medicine*; *The Lancet Oncology*; and *Theranostics*. Internet searches limited to the same time frame were conducted on several key terms: theranostics, radioimmunotherapy, novel, radiopharmaceutical, and radiochemistry.

Radionuclides

The emerging technologies search revealed that a vast number of radionuclides have been mentioned to be in development or up for consideration (**Table *7-1***). Radionuclides appearing in the literature that are already included in the Regulatory Guide 8.39 revisions are not restated. The nature of novel radiopharmaceuticals and radionuclides is such that many articles are written on the same nuclide. As a result, an effort was made to provide only the most recent reference. Thirty-eight nuclides appearing in **Table *7-1*** are under different stages of development and not currently included in the regulatory guide.

Table 7-1 Potential new radionuclides

Radionuclides	Source
^{203}Pb, ^{212}Pb	Banerjee et al (2020)
^{55}Co	Andersen et al (2020)
^{225}Ac, ^{43}Se, ^{44}Sc, ^{149}Tb, ^{152}Tb, ^{155}Tb, ^{161}Tb	Nicolas et al (2018)
^{134}Ce and ^{134}La, ^{227}Th	Bailey et al (2019)
^{191}Pt, ^{193m}Pt	De Kruijff et al (2019)
^{52}Mn	Martinez et al (2019)
^{227}Ac, ^{228}Th, ^{32}Si, ^{44}Ti, ^{22}Na, ^{26}Al, ^{177m}Lu	SNMMI (2018)
^{109}Cd, ^{57}Co, ^{69}Ge, ^{45}Ti, ^{52}Mn	Lamb and Holland (2018)
^{223}Ra, ^{212}Bi, ^{221}Fr (^{225}Ac progeny)	Poty et al (2018a; 2018b)
^{195m}Pt	Muns et al (2018)
^{63}Zn, ^{52}Mn	Bartnicka and Blower (2018)
^{161}Tb	Hindié et al (2016)
^{149}Pm, ^{170}Tm	Mishiro et al(2019)

Radiolabeling

Recent and significant advancements in molecular imaging and molecular science relate to radiolabeling. Jeon (2019) shows the various ways that radionuclides are molecularly attached to substances to be used in the diagnosis and treatment of various diseases (**Figure *7-1***). While it can be difficult to unfold the complex nature of radiopharmaceuticals, a basic premise is consistent. Radionuclides are attached to molecules that are synthesized to selectively target a type of cell or a process in the body. When evaluating absorption, this molecule is often a sugar which will concentrate in areas of higher biological metabolism. Infectious processes can be evaluated by radiolabeling agents of the immune system like white blood cells, antigens, or antibodies. Similarly, antigens can be radiolabeled if they are specific to tumor receptors; perhaps the most recognizable of these relationships is prostate-specific membrane antigen

(PSMA). In these instances, the glycoprotein (e.g., PSMA) is a marker that is present in greater concentrations on the targeted mass and the antigen is the molecule to which it will selectively bind. This can aid in the diagnosis of disease or be used for delivering a therapeutic radiation dose.

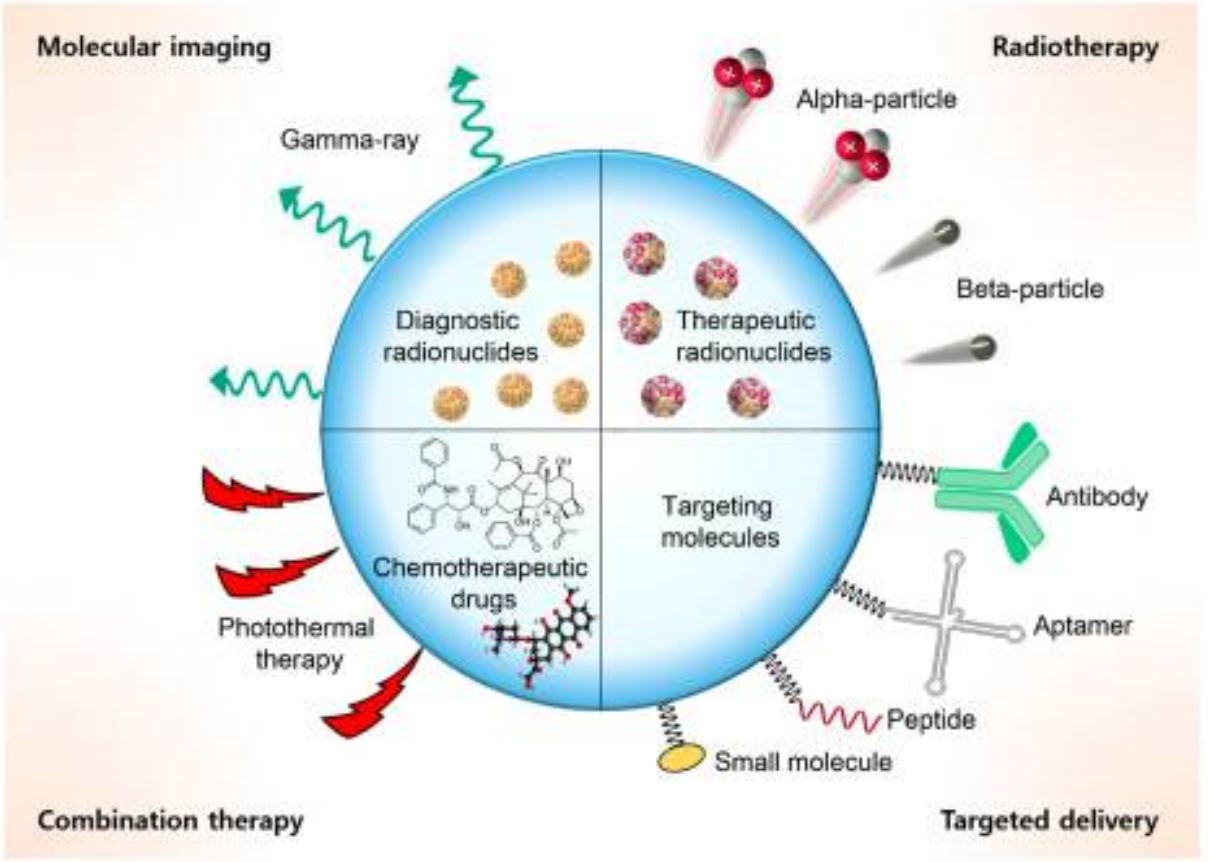

Figure 7-1 Applications of radiolabeled materials (from Jeon 2019)

It helps to consider that the biodistribution of a given radiopharmaceutical should not change given the radionuclide with which it is conjugated; the biological half-life of a radiopharmaceutical is independent of the radiological half-life. Because of this relationship (or lack thereof), we can use the same pharmaceutical to diagnose or treat, simply by attaching the appropriate radionuclide. For example, Ga-68 is a common positron emitter used for PET imaging delivered as DOTATATE, and this same pharmaceutical can be conjugated with Lu-177 to deliver a beta dose to the same area of the body (https://uihc.org/health-topics/what-theranostics). Being able to see in real time where the dose is being absorbed can contribute to the understanding of biodistribution of therapies, and this technique is being used when the biodistribution of various chemotherapy agents are being investigated. While none of these technologies is particularly new, many different applications have emerged. **Table *7-2*** contains a comprehensive list of radiopharmaceuticals that have been in various stages of investigation in the last 5 years. The radionuclides associated with these imaging pharmaceuticals are already included in the Regulatory Guide 8.39 revisions.

Table 7-2 Imaging radiopharmaceuticals

Name	Source
^{11}C-LSN3172176	Nabulsi et al (2019)
^{11}C-GSK1482160	Territo et al (2017)
4-^{11}C-MBZA	Garg et al (2017)
^{11}C-PS13, ^{11}C-MC1	Kim et al (2018)
^{11}C-Me-NB1	Krämer et al (2018)
^{11}C-RO6931643 ^{11}C-RO6924963 ^{18}F-RO6958948	Honer et al (2018)
^{11}C-RO-643 ^{11}C-RO-963 ^{18}F-RO-948	Wong et al (2018)
^{18}F-FAP Inhibitor	Toms et al (2020)
^{18}F-SKI-249380 (^{18}F-SKI)	Krebs et al (2020)
^{18}F-FGln	Grkovski et al (2020)
^{18}F-DMFB	Pyo et al (2019)
^{18}F-JNJ-64413739	Koole et al (2019)
^{18}F-P3BZA	Ma et al (2019)
^{18}F-Flortaucipir (Tauvid)	Nasrallah et al (2018)
^{18}F-Fluciclovine	Miller et al (2017)
^{18}F-THK-5351	Hsiao et al (2017)
^{18}F-5-fluoroaminosuberic acid (FASu)	Yang et al (2017)
^{18}F-JNJ64349311	Declercq et al (2017)
^{68}Ga-pentixafor	Kircher et al (2020)
^{68}Ga-NODAGA-exendin-4	Boss et al (2020)
^{68}Ga-BBN-RGD	Zhang et al (2017)

Radiolabeled Chemotherapy Agents

Chemotherapy agents can be radiolabeled to further our understanding of biodistribution and to gain information about the dose delivered to the area of interest, as well as dose delivered to areas not wanting to be targeted. **Table *7-3*** provides a list of recent pharmaceutical agents that have been studied with radioactive tracing. The radionuclides associated with these chemotherapy agents are already included in the Reg Guide 8.39 revisions.

Table 7-3 Radiolabeled chemotherapy agents

Name	Source
^{11}C-preladenant	Sakata et al (2017)
^{11}C-preladenant	Zhou et al (2017)
^{11}C-phenytoin	Mansor et al (2017)
^{11}C-vorozole	Biegon et al (2019)
^{18}F-clofarabine	Barrio et al (2017)
^{64}Cu-rituximab	James et al (2017)
^{89}Zr-radiolabeled onartuzumab	Klingler et al (2020)
^{89}Zr-daratumumab	Ghai et al (2018)
^{89}Zr-trastuzumab	O'Donoghue et al (2018)
^{89}Zr-bevacizumab	van Es et al (2017)
^{89}Zr-pertuzumab	Ulaner et al (2018)
^{89}Zr-Df-pembrolizumab	England et al (2017)
^{177}Lu-3BP-227	Baum et al (2018)

Radioimmunotherapy

Radioimmunotherapy is a technique where alpha or beta emitting radionuclides are conjugated with antibodies or antibody fragments in the aim of depositing concentrated radiological dose directly to targeted tissues, while sparing healthy tissues. This technique has been used to treat immunological cancers like lymphomas and leukemias. Several emerging agents have been identified (**Table *7-4***). The radionuclides associated with these radioimmunotherapy agents are already included in the Reg Guide 8.39 revisions.

Table 7-4 Emerging radioimmunotherapy agents

Name	Source
^{89}Zr-IAB22M2C	Pandit-Taskar et al (2020)
^{124}I-omburtamab	Pandit-Taskar et al (2019)
^{177}Lu-lilotomab-satetraxetan (Betalutin)	Malenge et al (2020)
^{177}Lu-lilotomab satetraxetan	Blakkisrud et al (2017)

Personalized Dosimetry and Implications

In addition to new radiopharmaceuticals and radionuclides used in diagnosis and therapy, the advancement of dosimetry techniques and ability to collect and process large amounts of data as well as advancing radiomics has shed light on our understanding of other interactive elements in the biodistribution and retention of radiopharmaceuticals.

Biegon et al. (2018) posited that “hormonal changes associated with the menstrual cycle are an underappreciated but avoidable source of vulnerability and risk to female reproductive organs, specifically ovaries, endometrium, and breasts.” So much so that uptake could be confused with ovarian tumors and in some cases, dose could exceed regulatory limits for ovaries defined for research studies. Concluding remarks in that paper stated a “need for new guidelines for radiotracer development and use” that is inclusive of premenopausal fluctuations in female hormones. Additional research has shown that sex is a biologic variable that needs consideration in imaging and metabolism (Chan et al. 2018).

Also in the Journal of Nuclear Medicine was a study citing the changes in uptake of MIBG in cardiac patients who are also being treated with some novel antidepressant therapy (Werner et al. 2018). This highlights the importance of acquiring complete pharmaceutical histories, even if they seem irrelevant to the procedure at hand. This study specifically looked at the interference of antidepressant drugs in norepinephrine transporters (NETs) with MIBG uptake, but it is noted that there are other tracers using NETs such as in radiotheranostics.

8. INTERNATIONAL HARMONIZATION

Guidance on the release of patients after the administration of radiopharmaceuticals is also addressed by international regulatory programs and in the related literature. This chapter provides insight on how well the revised regulatory guide harmonizes with international aims.

Background

The Bonn Call for Action (WHO 2012) is a joint effort between the World Health Organization (WHO) and the International Atomic Energy Agency (IAEA) addressing radiation protection in diagnostic, therapeutic and interventional procedures in medicine that use ionizing radiation. Of the goals of the Bonn Call for Action, "implement[ing] harmonized criteria for release of patients after radionuclide therapy and develop[ing] further detailed guidance as necessary" was part of the initiative to "enhance the implementation of the principle of optimization of protection and safety" from potential harmful effects of radiation in medicine, with aims for the eventual full integration of radiation protection into international health care systems. Importance is placed on guidance by IAEA, scientific basis by the ICRP (Lau 2008), implementation by internationally recognized professional organizations, and enacted policies and laws enforced by health authorities and regulators.

IAEA (2009) published detailed criteria for the release of patients after radiopharmaceutical administration. Based on science from the ICRP with flexibility for individual regulating authorities, this IAEA guidance is based on retained activity in the patient such that doses to a caregiver or bystander would not exceed a few mSv. Special considerations are mentioned for patients using public transportation, hotels and public lodging, and close contact with children. These patient considerations include the need for hospitalization, judgement on collection and disposal of urine based on the patient's mental or emotional capacity to understand and follow directions, as well as home exposure situations with children or people living in a smaller space.

IAEA recommends special considerations for patients who are or may become pregnant, patients who are breastfeeding children, as well as patients who unexpectedly die soon after treatment. These considerations include recommending that the patient avoid becoming pregnant for a period of time to ensure dose to an embryo or fetus does not exceed 1 mGy differentiated by radionuclide. For patients who are breastfeeding, IAEA recommends that nursing be suspended indefinitely beginning 2-3 weeks before radiopharmaceutical administration.

Patients should be given understandable, procedure-specific pre-treatment information as well as post-treatment instructions for patients and caregivers. Doses to the public from photon emitting nuclides are estimated based on administered activity and measured dose rates. By collecting dose rate measurements at 3 m from the patient immediately after administration and again at other times, the retained activity can then be estimated with the following equation:

$$A_R = A_0 \frac{D}{D_0} \qquad \text{Equation [8-1]}$$

where D is the dose rate at the time of measurement, A_0 is the administered activity, and D_0 is the dose rate measured immediately after administration. If a dose estimate is needed at distances closer than 3 meters, then the following adjustment is made:

$$D = \frac{D_1}{x^{1.5}}$$ Equation [8-2]

where D_1 is the dose at 1 meter.

Findings

Members of the European Union must adhere to standards set by EURATOM guidelines (EURATOM 1997), which are guided by the recommendations of the IAEA. Heads of the European Radiological Protection Competent Authorities (HERCA 2010) drive European policy on radiation protection. Specific guidelines for medical examinations and procedures (e.g., I-131 therapy) address IAEA recommendations and provide cultural autonomy of each country with respect to rulemaking and guidance implementation. Some countries (e.g., Finland) have a comprehensive set of regulations and explicit recommendations or rules. Other countries (e.g., Cyprus) simply state conformance with EURATOM, European Basic Safety Standard (BSS) and IAEA on all issues related to ionizing radiation without country specific policies or guidelines (DLI 2020).

Finland published a detailed set of recommendations (STUK 2013) with references to both scientific literature as well as the specific acts and laws from which the particular recommendation is derived. There is guidance on record keeping and how to inform patients before and after procedures. There is a set of reference levels, instructions on how to assess those levels, and what to do if the measured values do not conform to the reference levels. The dose constraint is set per family member and per treatment episode and is specified by age: 1 mSv for children and fetuses; 3 mSv for adults under 60; and 15 mSv for adults over 60. The dose constraint of 0.3 mSv is specified for any nonfamily member. There are recommendations for patients who are pregnant and potentially pregnant as well as breastfeeding patients. These recommendations are based on ICRP 106 (2008a).

Australia (ARPANSA 2002) incorporates a similar approach as the United States, with a comprehensive regulatory document that is easily available and published online. This regulatory document outlines procedures for the general public, but does not have specific recommendations for pregnancy, breastfeeding or exposure to children beyond the requirement that treatment specialist should consider these circumstances. It is based on science from ICRP 53 (1987) and ICRP 73 (2014); the recommended dose constraint is set at 5 mSv per treatment episode to the caregiver or family member who is not a child.

Canada has a radiation protection program centered on the principle of “as low as reasonably achievable” (ALARA). General regulations comply with the standards set by the Bonn Call to Action (2012), but do not reside in one comprehensive regulatory framework. Standards are loosely set in various regulatory documents that require the individual providers be licensed federally with responsibility to instruct patients on which personal activities to limit (CNSC 2011). Specific guidelines for handling deceased patients after the administration of radiopharmaceuticals are outlined in their regulatory context (CNSC 2018). The lack of a federal regulatory framework is largely due to the health professions act (Aldridge, 2008), which grants professional organizations the authority to establish acceptable health activities that

must adhere to dose constraint and ALARA standards. Basically, there is flexibility with the administration of rules as long as compliance is achieved with the overall regulatory limits of 5 mSv per episode to public, including family and caregivers. The responsible professional associations include the Canadian Association of Medical Radiation Technologists (CAMRT) and the Canadian Medical Association (CMA).

As medical radiation exposures from therapeutic and nuclear medicine procedures become more prevalent, developing nations in Africa are aiming to adhere to the recommendations set by the Bonn Call to Action (2012). The AFROSAFE (2018) organization is developing a legal and policy framework that better aligns with WHO recommendations. South Africa (Herbst 2012) is realizing the gaps in their regulatory capacity, as well. Although regulatory guidance set by ARPANSA (2002) and the ICRP is generally followed, a less mature regulatory framework and mercurial nature of regulatory bodies have hampered the implementation of radiation protection practices in clinical settings.

Devoted to ensuring the safe use of radiation, LATINSAFE (2020) establishes best practices and guidelines based on affiliations with American professional associations, such as the American Society of Radiologic Technologists (ASRT), the American Association of Physicists in Medicine (AAPM), American College of Radiology (ACR), and the Radiological Society of North America (RSNA). Although the intentions of LATINSAFE were stated, implementation strategies were less available compared to those of AFROSAFE with its detailed "Implementation Tool Matrix" to track action items and objectives (2018).

Discussion

Revisions to Regulatory Guide 8.39 Rev 1 (NRC 2020) are intended to provide a thorough accounting of criteria for the release of patients following radionuclide administration. Additionally, applicable regulations are to be clearly referenced and easy to access. The baseline criteria for release is an expected dose to another individual that does not exceed 5 mSv.

IAEA and European recommendations base dose estimates on measured dose rates and extrapolate exposure to others according to Equation [8-2], with the rationale that the body is not a point source for distances closer than 3 meters (HURSOG 1997). The U.S estimate originates from dosimetric methods described in NCRP 155 (2006). This method of dose estimation considers not just nuclide-specific activity, but half-life as well. However, it does not account for the body being a volume source (rather, it has an inverse square relationship with distance, as a point source would) as the international literature recommends. In revisions to Regulatory Guide 8.39 Rev 1 (2020), modifying factors describing biokinetics, occupancy, geometry, and attenuation are applied for patient-specific release/instruction decisions.

The US regulatory guide aligns well with the IAEA publication in its details for releasing patients. There are recommended patient instructions for the general public, nursing mothers, and patients who live with or are in contact with children. There are general instructions for pathology staff if a patient dies after the administration of radiopharmaceuticals in how to handle autopsies and preparation for burial or cremation. The guide also contains nuclide-specific activity thresholds and dose rates at which actions can be taken with regard to release and when specific instructions are required.

Most countries have policies of radiation protection that are in line with framework suggestions by WHO and recommendations by IAEA and ICRP. The United States guidance aligns well with the international guidelines and meets or exceeds detailed requirements.

9. REFERENCES

Advanced Accelerator Applications USA, Inc. (AAA). Lutathera (lutetium Lu 177 dotatate) injection, for intravenous use. Package Insert. New Jersey. 2019.

AFROSAFE. "*Implementation Tool Matrix*". Kenya: AFROSAFE. 2018.

Aldridge, S. "The Regulation of Health Professionals: An Overview of the British Columbia Experience." Elsevier. 2008.

American National Standards Institute (ANSI). "Gamma ray attenuation coefficient and buildup factors for engineering materials". ANSI/ANS-6.4.3. American Nuclear Society. LaGrange Park, Illinois. 1991.

Andersen TL, Baun C, Olsen BB, Dam JH, Thisgaard H. Improving Contrast and Detectability: Imaging with [55Co]Co-DOTATATE in Comparison with [64Cu]Cu-DOTATATE and [68Ga]Ga-DOTATATE. *J Nucl Med.* 61(2): 228-233. 2020.

Attix, F.H. Introduction to Radiological Physics and Radiation Dosimetry. John Wiley & Sons. New York. 1986.

Australian Radiation Protection and Nuclear Safety Agency (ARPANSA). Discharge of Patients Undergoing Treatment with Radioactive Substances. Radiation Protection Series Publication No. 4. Commonwealth of Australia. Canberra. 2002.

Bailey T., Lake, A., A, D., Gauny S., Abergel R., Biodistribution Studies of Chelated Ce-134/La-134 as Positron Emitting Analogues of Alpha Emitting Therapy Radionulides. *J Nucl Med.* Supplement 1 130. 2019.

Banerjee SR, Minn I, Kumar V, Josefsson A, Lisok A, Brummet M, Chen J, Kiess AP, Baidoo K, Brayton C, Mease RC, Brechbiel M, Sgouros G, Hobbs RF, Pomper MG. Preclinical Evaluation of $^{203/212}$Pb-Labeled Low-Molecular-Weight Compounds for Targeted Radiopharmaceutical Therapy of Prostate Cancer. *J Nucl Med.* 61(1): 80-88. 2020.

Barrio MJ, Spick C, Radu CG, Lassmann M, Eberlein U, Allen-Auerbach M, Schiepers C, Slavik R, Czernin J, Herrmann K. Human Biodistribution and Radiation Dosimetry of 18F-Clofarabine, a PET Probe Targeting the Deoxyribonucleoside Salvage Pathway. *J Nucl Med.* 58(3): 374-378. 2017.

Bartnicka JJ, Blower PJ. Insights into Trace Metal Metabolism in Health and Disease from PET: "PET Metallomics". *J Nucl Med.* 59(9): 1355-1359. 2018.

Baum RP, Singh A, Schuchardt C, Kulkarni HR, Klette I, Wiessalla S, Osterkamp F, Reineke U, Smerling C. 177Lu-3BP-227 for Neurotensin Receptor 1-Targeted Therapy of Metastatic Pancreatic Adenocarcinoma: First Clinical Results. *J Nucl Med*. 59(5): 809-814. 2018.

Bethe, H.A.; Heitler, W. On the stopping of fast particles and on the creation of positive electrons. *Proceedings of the Royal Society of London*. Series A, Containing Papers of a Mathematical and Physical Character. 146(856): 83-112. 1934.

Biegon A, Franceschi D, Schweitzer ME. Nuclear Medicine Procedures in Women: Unappreciated Risks to Reproductive Organs? *Radiology*. 289(1): 25-27. 2018.

Biegon, Anat et. al.. (2019). Initial studies with [11 C]vorozole positron emission tomography detect over-expression of intra-tumoral aromatase in breast cancer. *J Nucl Med*. 61: 2019.

Blakkisrud J, Løndalen A, Martinsen AC, Dahle J, Holtedahl JE, Bach-Gansmo T, Holte H, Kolstad A, Stokke C. Tumor-Absorbed Dose for Non-Hodgkin Lymphoma Patients Treated with the Anti-CD37 Antibody Radionuclide Conjugate 177Lu-Lilotomab Satetraxetan. *J Nucl Med.* 58(1): 48-54. 2017.

Boss M, Buitinga M, Jansen TJP, Brom M, Visser EP, Gotthardt M. PET-Based Human Dosimetry of 68Ga-NODAGA-Exendin-4, a Tracer for β-Cell Imaging. *J Nucl Med.* 61(1): 112-116. 2020.

Brodsky, A. Resuspension factors and probabilities of intake of material in process. *Health Physics*. 39(6): 992-1000. 1981.

Buchanan, R.C.T.; Brindle, J.M. Radioiodine therapy to out-patients – The contamination hazard. British *Journal of Radiology*. 44(523): 557. 1971.

Calais, P.J.; Turner, J.H. Radiation safety of outpatient ^{177}Lu-octreotate radiopeptide therapy of neuroendocrine tumors. *Ann Nucl Med*. 28:51-539; 2014.

Canadian Nuclear Safety Commission (CNSC). REGDOC 1-6-1. “License Application Guide: Class II Nuclear Facilities and Prescribed Equipment”. § E.2.4. Ottawa: 2011.

Canadian Nuclear Safety Commission (CNSC). REGDOC 2-7-3. “Radiation Protection Guidelines for Safe Handling of Decedents”. Ottawa: 2018.

Chan SR, Salem K, Jeffery J, Powers GL, Yan Y, Shoghi KI, Mahajan AM, Fowler AM. Sex as a Biologic Variable in Preclinical Imaging Research: Initial Observations with ^{18}F-FLT. *J Nucl Med.* 59(5): 833-838. 2018.

Declercq L, Rombouts F, Koole M, Fierens K, Mariën J, Langlois X, Andrés JI, Schmidt M, Macdonald G, Moechars D, Vanduffel W, Tousseyn T, Vandenberghe R, Van Laere K, Verbruggen A, Bormans G. Preclinical Evaluation of 18F-JNJ64349311, a Novel PET Tracer for Tau Imaging. *J Nucl Med.* 58(6): 975-981. 2017.

De Kruijff R., et al. Developing radio-assised Chemotherapy. *J Nucl Med.* Supplement 1 633. 2019.

Department of Labour Inspection (DLI). “*Radiation Protection, Medical Exposure*”. Nicosia: Cyprus. 2020.

England CG, Ehlerding EB, Hernandez R, Rekoske BT, Graves SA, Sun H, Liu G, McNeel DG, Barnhart TE, Cai W. Preclinical Pharmacokinetics and Biodistribution Studies of 89Zr-Labeled Pembrolizumab. *J Nucl Med.* 58(1): 162-168. 2017.

EURATOM. "*Council Directive 97/43/EURATOM*". Luxembourg: Official Journal of the European Communities. 1997.

Gadodia, G.; Tritle, B.; Miller, M.A.; Martin, C. Recommendation for addressing post-mortem considerations in patients treated with Y-90 radioembolization. *International Oncology Learning*. IO Learning. 8: E39-E40. 2020.

Garg PK, Nazih R, Wu Y, Singh R, Garg S. 4-11C-Methoxy N-(2-Diethylaminoethyl) Benzamide: A Novel Probe to Selectively Target Melanoma. *J Nucl Med.* 58(5): 827-832. 2017.

Ghai A, Maji D, Cho N, Chanswangphuwana C, Rettig M, Shen D, DiPersio J, Akers W, Dehdashti F, Achilefu S, Vij R, Shokeen M. Preclinical Development of CD38-Targeted [89Zr]Zr-DFO-Daratumumab for Imaging Multiple Myeloma. *J Nucl Med.* 59(2): 216-222. 2018.

Grkovski M, Goel R, Krebs S, Staton KD, Harding JJ, Mellinghoff IK, Humm JL, Dunphy MPS. Pharmacokinetic Assessment of 18F-(2S,4R)-4-Fluoroglutamine in Patients with Cancer. *J Nucl Med.* 61(3): 357-366. 2020.

Gulec, S.A.; Siegel, J.A. Posttherapy radiation safety considerations in radiomicrosphere treatment with ^{90}Y microspheres. *Journal of Nuclear Medicine*. 48: 2080-2086. 2007.

Harima, Y. An approximation of gamma-ray buildup factors by modified geometric progression. *Nuclear Science and Engineering.* 83: 299-309. 1986.

Harima, Y., Sakamoto, Y., Tanaka, S., Kawai, M. Validity of the geometric progression. *Nuclear Science and Engineering.* 94: 24-35. 1986.

Harima, Y., Tanaka, S., Sakamoto, Y., Hirayama, H. Development of new gamma-ray buildup factors and applications to shielding calculations. *Journal of Nuclear Science and Technology*. 28: 74-78. 1991.

Herbst, C P. "Radiation Protection and the Safe Use of X-Ray Equipment: Laws, Regulations and Responsibilities". *South African Journal of Radiology*. 16(2): 50-54. 2012.

HERCA. I-131 Therapy: Patient Release Criteria. Paris: Heads of the European Radiological protection Competent Authorities. 2010.

Hicks, R.J.; Binns, D.; Stabin, M.G. Pattern of Uptake and Excretion of ^{18}F-FDG in the Lactating Breast. *J Nucl Med.* 42: 1238-1242. 2001.

Hindié E, Zanotti-Fregonara P, Quinto MA, Morgat C, Champion C. Dose Deposits from 90Y, 177Lu, 111In, and 161Tb in Micrometastases of Various Sizes: Implications for Radiopharmaceutical Therapy. *J Nucl Med.* 57(5): 759-64. 2016.

Honer M, Gobbi L, Knust H, Kuwabara H, Muri D, Koerner M, Valentine H, Dannals RF, Wong DF, Borroni E. Preclinical Evaluation of 18F-RO6958948, 11C-RO6931643, and 11C-RO6924963 as Novel PET Radiotracers for Imaging Tau Aggregates in Alzheimer Disease. *J Nucl Med.* 59(4): 675-681. 2018.

Hospital and University Radiation Safety Officers Group (HURSOG), "*Guide to Radioidone Therapy Facility Design*". New South Wales: Australia. 1997.

Hsiao IT, Lin KJ, Huang KL, Huang CC, Chen HS, Wey SP, Yen TC, Okamura N, Hsu JL. Biodistribution and Radiation Dosimetry for the Tau Tracer 18F-THK-5351 in Healthy Human Subjects. *J Nucl Med.* 58(9): 1498-1503. 2017.

Hunt, J.G.; Nosske, D.; dos Santos, D.S. Estimation of the dose to the nursing infant due to direct irradiation from activity present in maternal organs and tissues. *Radiation Protection Dosimetry*. 113(3): 290-299. 2005.

International Atomic Energy Agency (IAEA). Release of Patients After Radionuclide Therapy. Safety Reports Series. Report No. 63. Vienna. 2009.

International Commission on Radiation Units and Measurements (ICRU). Radiation Quantities and Units. ICRU Report No. 33. Bethesda, MD: 1980.

International Commission on Radiological Protection. Radionuclide Transformations – Energy and Intensity of Emissions. Publication 38. Annals of the ICRP. 11-13. 1983.

International Commission on Radiological Protection (ICRP). Radiation Dose to Patients from Radiopharmaceuticals. Publication 53. Annals of the ICRP. 18(1-4). 1987.

International Commission on Radiological Protection (ICRP). Dose Coefficients for Intakes of Radionuclides by Workers. Publication 68. Annals of the ICRP. 24(4). 1994.

International Commission on Radiological Protection (ICRP). Radiological Protection and Safety in Medicine. Publication 73. 2014.

International Commission on Radiological Protection (ICRP). Radiation Dose to Patients from Radiopharmaceuticals. Publication 106. Annals of the ICRP. 38(1-2). 2008a.

International Commission on Radiological Protection (ICRP). Nuclear Decay Data for Dosimetric Calculations. Annals of the ICRP. Publication 107. 38(3). 2008.

International Commission on Radiological Protection (ICRP). Radiation Dose to Patients from Radiopharmaceuticals: A Compendium of Current Information Related to Frequently Used Substances. Publication 128. Annals of the ICRP. 44(2s). 2015.

Jacobson, A.P.; Plato, P.A.; Toeroek, D. Contamination of the home environment by patients treated with iodine-131. *American Journal of Public Health*. 68(3): 225-230. 1978.

James ML, Hoehne A, Mayer AT, Lechtenberg K, Moreno M, Gowrishankar G, Ilovich O, Natarajan A, Johnson EM, Nguyen J, Quach L, Han M, Buckwalter M, Chandra S, Gambhir SS. Imaging B Cells in a Mouse Model of Multiple Sclerosis Using 64Cu-Rituximab PET. *J Nucl Med.* 58(11): 1845-1851. 2017.

Jeon J. Review of Therapeutic Applications of Radiolabeled Functional Nanomaterials. *Int J Mol Sci*. 20(9): 2323. 2019.

Johns, H.E.; Cunningham, J.R. The Physics of Radiology. 4th ed. Charles C Thomas. Springfield, IL. 1983.

Johnston, R.E.; Mukherji, S.K.; Perry, J.R., Stabin, M.G. Radiation dose from breast feeding following administration of thallium-201. *J Nuc Med*. 37:2079-2082. 1996.

Kim MJ, Shrestha SS, Cortes M, Singh P, Morse C, Liow JS, Gladding RL, Brouwer C, Henry K, Gallagher E, Tye GL, Zoghbi SS, Fujita M, Pike VW, Innis RB. Evaluation of Two Potent and Selective PET Radioligands to Image COX-1 and COX-2 in Rhesus Monkeys. *J Nucl Med.* 59(12): 1907-1912. 2018.

Kim, Y-C.; Kim, Y-H.; Uhm, S-H.; Seo, Y.S.; Park, E-K.; Oh, S-Y.; Jeong, E.; Lee, S.; Choe J-G. Radiation safety issues in Y-90 microsphere selective hepatic radioembolization therapy: possible radiation exposure from the patients. *Nuclear Medicine and Molecular Imaging*. 44: 252-260. 2010.

Kircher M, Tran-Gia J, Kemmer L, Zhang X, Schirbel A, Werner RA, Buck AK, Wester HJ, Hacker M, Lapa C, Li X. Imaging Inflammation in Atherosclerosis with CXCR4-Directed 68Ga-Pentixafor PET/CT: Correlation with 18F-FDG PET/CT. *J Nucl Med.* 61(5): 751-756. 2020.

Klingler S, Fay R, Holland JP. Light-Induced Radiosynthesis of 89Zr-DFO-Azepin-Onartuzumab for Imaging the Hepatocyte Growth Factor Receptor. *J Nucl Med.* 61(7): 1072-1078. 2020.

Koole M, Schmidt ME, Hijzen A, Ravenstijn P, Vandermeulen C, Van Weehaeghe D, Serdons K, Celen S, Bormans G, Ceusters M, Zhang W, Van Nueten L, Kolb H, de Hoon J, Van Laere K. 18F-JNJ-64413739, a Novel PET Ligand for the P2X7 Ion Channel: Radiation Dosimetry, Kinetic Modeling, Test-Retest Variability, and Occupancy of the P2X7 Antagonist JNJ-54175446. *J Nucl Med.* 60(5): 683-690. 2019.

Krämer SD, Betzel T, Mu L, Haider A, Herde AM, Boninsegni AK, Keller C, Szermerski M, Schibli R, Wünsch B, Ametamey SM. Evaluation of 11C-Me-NB1 as a Potential PET Radioligand for Measuring GluN2B-Containing NMDA Receptors, Drug Occupancy, and Receptor Cross Talk. *J Nucl Med.* 59(4): 698-703. 2018.

Krane, K. Modern Physics. 2nd ed. John Wiley & Sons. New York. 1996.

Krebs S, Veach DR, Carter LM, Grkovski M, Fornier M, Mauro MJ, Voss MH, Danila DC, Burnazi E, Null M, Staton K, Pressl C, Beattie BJ, Zanzonico P, Weber WA, Lyashchenko SK, Lewis JS, Larson SM, Dunphy MPS. First-in-Humans Trial of Dasatinib-Derivative Tracer for Tumor Kinase-Targeted PET. *J Nucl Med.* 61(11): 1580-1587. 2020.

Lamb J, Holland JP. Advanced Methods for Radiolabeling Multimodality Nanomedicines for SPECT/MRI and PET/MRI. *J Nucl Med.* 59(3): 382-389. 2018.

LATINSAFE. Retrieved from http://latinsafe.org/global/. August 2020.

Leide-Svegborn, S.; Ahlgren, L.; Johansson, L.; Mattsson, S. Excretion of radionuclides in human breast milk after nuclear medicine examinations: biokinetics and dosimetric data and recommendations on breastfeeding interruption. *Eur J Nuc Med Mol Imaging*. 43:808-821. 2016.

Levart, D.; Kalogianni, E.; Corcoran, B.; Mulholland, N.; Vivian, G. Radiation precautions for inpatient and outpatient ^{177}Lu-dotatate peptide receptor radionuclide therapy of neuroendocrine tumours. *ENJMMI Physics*. 6:7. 2019.

Ma X, Wang S, Wang S, Liu D, Zhao X, Chen H, Kang F, Yang W, Wang J, Cheng Z. Biodistribution, Radiation Dosimetry, and Clinical Application of a Melanin-Targeted PET Probe, 18F-P3BZA, in Patients. *J Nucl Med.* 60(1): 16-22. 2019.

Malenge MM, Patzke S, Ree AH, Stokke T, Ceuppens P, Middleton B, Dahle J, Repetto-Llamazares AHV. 177Lu-Lilotomab Satetraxetan Has the Potential to Counteract Resistance to Rituximab in Non-Hodgkin Lymphoma. *J Nucl Med.* 61(10): 1468-1475. 2020.

Manjunatha, H.C.; Rudraswamy, B. Exposure of bremsstrahlung from beta-emitting therapeutic radionuclides. *Radiation Measurements*. 44:206-210. 2009.

Mansor S, Yaqub M, Boellaard R, Froklage FE, de Vries A, Bakker ED, Voskuyl RA, Eriksson J, Schwarte LA, Verbeek J, Windhorst AD, Lammertsma AA. Parametric Methods for Dynamic 11C-Phenytoin PET Studies. *J Nucl Med.* 58(3): 479-483. 2017.

Martinez O, Sosabowski J, Maher J, Papa S. New Developments in Imaging Cell-Based Therapy. *J Nucl Med.* 60(6): 730-735. 2019.

Mehmedovic, M. New age of theranostics with new radiation safety concerns; challenges and solutions. https://jnm.snmjournals.org/content/61/supplement_1/3066 (accessed April 19, 2021).

Miller MP, Kostakoglu L, Pryma D, Yu JQ, Chau A, Perlman E, Clarke B, Rosen D, Ward P. Reader Training for the Restaging of Biochemically Recurrent Prostate Cancer Using 18F-Fluciclovine PET/CT. *J Nucl Med.* 58(10): 1596-1602. 2017.

Mishiro, Kenji & Hanaoka, Hirofumi & Yamaguchi, Aiko & Ogawa, Kazuma. Radiotheranostics with radiolanthanides: Design, development strategies, and medical applications. *Coordination Chemistry Reviews.* 383. 104-131. 2019.

Muns JA, Montserrat V, Houthoff HJ, Codée-van der Schilden K, Zwaagstra O, Sijbrandi NJ, Merkul E, van Dongen GAMS. In Vivo Characterization of Platinum(II)-Based Linker Technology for the Development of Antibody-Drug Conjugates: Taking Advantage of Dual Labeling with 195mPt and 89Zr. *J Nucl Med.* 59(7): 1146-1151. 2018.

Nabulsi NB, Holden D, Zheng MQ, Bois F, Lin SF, Najafzadeh S, Gao H, Ropchan J, Lara-Jaime T, Labaree D, Shirali A, Slieker L, Jesudason C, Barth V, Navarro A, Kant N, Carson RE, Huang Y. Evaluation of 11C-LSN3172176 as a Novel PET Tracer for Imaging M1 Muscarinic Acetylcholine Receptors in Nonhuman Primates. *J Nucl Med.* 60(8): 1147-1153. 2019.

Nasrallah IM, Chen YJ, Hsieh MK, Phillips JS, Ternes K, Stockbower GE, Sheline Y, McMillan CT, Grossman M, Wolk DA. 18F-Flortaucipir PET/MRI Correlations in Nonamnestic and Amnestic Variants of Alzheimer Disease. *J Nucl Med.* 59(2): 299-306. 2018.

National Council on Radiation Protection and Measurements (NCRP). Management of Radionuclide Therapy Patients. NCRP Report No. 155. Bethesda, MD: December 2006.

National Funeral Directors Association (NFDA). Radiation Protection Guidelines for Safe Handling of Decedents. (accessed online 10/08/2020). March 2019.

Nelson, K.L.; Sheetz, M.A. Radiation safety observations associated with ^{177}Lu dotatate patients. *Health Physics*. 117(6): 680-687. 2019.

Nelson, K; Vause, P.E.; Koropova, P. Post-mortem consideration of yttrium-90 (^{90}Y) microsphere therapy procedures. *Health Physics*. 95(s5): S156-S161. 2008.

Nicolas GP, Morgenstern A, Schottelius M, Fani M. New Developments in Peptide Receptor Radionuclide Therapy. *J Nucl Med.* 118.213496. 2018.

Nuclear Regulatory Commission (NRC). "Release of Patients Administered Radioactive Material." Draft Regulatory Guide 8.39, Revision 1. Washington, DC: April 2020.

Nuclear Regulatory Commission (NRC). "Consolidated Guidance About Materials Licenses, Program-Specific Guidance About Medical Use Licenses," NUREG-1556, Volume 9, Revision 3. Washington, DC: September 2019.

Nuclear Regulatory Commission (NRC). "Release of Patients Administered Radioactive Materials," Regulatory Guide 8.39, Revision 0. Washington, DC: April 1997a.

Nuclear Regulatory Commission (NRC). "Regulatory Analysis on Criteria for the Release of Patients Administered Radioactive Materials," NUREG-1492, Final Report. Washington, DC: February 1997b.

O'Donoghue JA, Lewis JS, Pandit-Taskar N, Fleming SE, Schöder H, Larson SM, Beylergil V, Ruan S, Lyashchenko SK, Zanzonico PB, Weber WA, Carrasquillo JA, Janjigian YY. Pharmacokinetics, Biodistribution, and Radiation Dosimetry for 89Zr-Trastuzumab in Patients with Esophagogastric Cancer. *J Nucl Med.* 59(1): 161-166. 2018.

Olarinoye, I.O.; Odiaga, R.I.; Paul, S. EXABCal: a program for calculating photon exposure and energy absorption buildup factors. *Heliyon*. 5: e02017. 2019.

Pandit-Taskar, N., M.A. Postow, M.D. Hellmann, J.J. Harding, C.A. Barker, J.A. O'Donoghue, M. Ziolkowska, S. Ruan, S.K. Lyashchenko, F. Tsai, M. Farwell, T.C. Mitchell, R. Korn, W. Le, J.S. Lewis, W.A. Weber, D. Behera, I. Wilson, M. Gordon, A.M. Wu, J.D. Wolchok. First-in-Humans Imaging with 89Zr-Df-IAB22M2C Anti-CD8 Minibody in Patients with Solid Malignancies: Preliminary Pharmacokinetics, Biodistribution, and Lesion Targeting. *J Nucl Med.* 61(4): 512-519; 2020.

Pandit-Taskar N, Zanzonico PB, Kramer K, Grkovski M, Fung EK, Shi W, Zhang Z, Lyashchenko SK, Fung AM, Pentlow KS, Carrasquillo JA, Lewis JS, Larson SM, Cheung NV, Humm JL. Biodistribution and Dosimetry of Intraventricularly Administered 124I-Omburtamab in Patients with Metastatic Leptomeningeal Tumors. *J Nucl Med.* 60(12): 1794-1801. 2019.

Peplow, D.E. Specific gamma-ray dose constants with current emission data. *Health Physics*. 118(4): 402-416. 2020.

Poty S, Francesconi LC, McDevitt MR, Morris MJ, Lewis JS. α-Emitters for Radiotherapy: From Basic Radiochemistry to Clinical Studies -Part 1. *J Nucl Med.* 59(6): 878-884. 2018a.

Poty S, Francesconi LC, McDevitt MR, Morris MJ, Lewis JS. α-Emitters for Radiotherapy: From Basic Radiochemistry to Clinical Studies -Part 2. *J Nucl Med.* 59(7): 1020-1027. 2018b.

Pyo A, Kim HS, Kim HS, Yun M, Kim DY, Min JJ. N-(2-(Dimethylamino)Ethyl)-4-18F-Fluorobenzamide: A Novel Molecular Probe for High-Contrast PET Imaging of Malignant Melanoma. *J Nucl Med.* 60(7): 924-929. 2019.

Radiation and Nuclear Safety Authority (STUK). Radiation Safety in Nuclear Medicine. Guide ST 6.3. Helsinki: Finland. 2013.

Sakata M, Ishibashi K, Imai M, Wagatsuma K, Ishii K, Zhou X, de Vries EFJ, Elsinga PH, Ishiwata K, Toyohara J. Initial Evaluation of an Adenosine A2A Receptor Ligand, 11C-Preladenant, in Healthy Human Subjects. *J Nucl Med*. 58(9): 1464-1470. 2017.

Shivaramu. Modified Kramers' law for bremsstrahlung produced by complete beta particle absorption in thick targets and compounds. *Journal of Applied Physics*. 68(3): 1225-1228. 1990.

Shultis, J.K.; Faw, R.E. Radiation Shielding. American Nuclear Society. La Grange Park, IL. 2000.

Sirtex Medical (Sirtex). SIR-Spheres Y-90 Resin Microspheres. Available online at: https://www.sirtex.com/media/169247/ssl-us-14-sir-spheres-microspheres-ifu-us.pdf. Accessed June 25, 2020.

Smith, D.S.; Stabin M.G. Exposure rate constants and lead shielding values for over 1,100 radionuclides. *Health Physics*. 102(3): 271-291. 2012.

Society of Nuclear Medicine and Molecular Imaging (SNMMI). SNMMI Submits Comments to NRC on Radioactive Materials. *J Nucl Med.* 59(1): 16N. 2018.

Society of Nuclear Medicine and Molecular Imaging (SNMMI). Online resource. Nuclear Medicine Radiation Dose Tool. V 4.10. April 23, 2018. (accessed Nov 30, 2020).

Sorenson, J.A.; Phelps, M.E. Physics in Nuclear Medicine. 2nd ed. Orlando, FL. Grune & Stratton. pg 164. 1987.

Stabin, M.G.; Breitz, H.B. Breast milk excretion of radiopharmaceuticals: mechanisms, findings, and radiation dosimetry. *J Nucl Med*. 41:863-873. 2000.

Territo PR, Meyer JA, Peters JS, Riley AA, McCarthy BP, Gao M, Wang M, Green MA, Zheng QH, Hutchins GD. Characterization of 11C-GSK1482160 for Targeting the P2X7 Receptor as a Biomarker for Neuroinflammation. *J Nucl Med*. 58(3): 458-465. 2017.

Toms J, Kogler J, Maschauer S, Daniel C, Schmidkonz C, Kuwert T, Prante O. Targeting Fibroblast Activation Protein: Radiosynthesis and Preclinical Evaluation of an 18F-Labeled FAP Inhibitor. *J Nucl Med.* 61(12): 1806-1813. 2020.

Ulaner GA, Lyashchenko SK, Riedl C, Ruan S, Zanzonico PB, Lake D, Jhaveri K, Zeglis B, Lewis JS, O'Donoghue JA. First-in-Human Human Epidermal Growth Factor Receptor 2-Targeted Imaging Using 89Zr-Pertuzumab PET/CT: Dosimetry and Clinical Application in Patients with Breast Cancer. *J Nucl Med.* 59(6): 900-906. 2018.

van Es, S.C., Adrienne H. Brouwers, Shekar V.K. Mahesh, Annemarie M. Leliveld-Kors, Igle J. de Jong, Marjolijn N. Lub-de Hooge, Elizabeth G.E. de Vries, Jourik A. Gietema, Sjoukje F. Oosting. 89Zr-Bevacizumab PET: Potential Early Indicator of Everolimus Efficacy in Patients with Metastatic Renal Cell Carcinoma. *J Nucl Med.* 58(6): 905-910. 2017.

Webb, C.; Frye, S.; Muzaffar, R.; Osman, M. Radiation safety challenges in Lu-177 PSMA: A technologist's perspective. https://jnm.snmjournals.org/content/61/supplement_1/3035 (accessed April 19, 2021).

Werner RA, Kobayashi R, Javadi MS, Köck Z, Wakabayashi H, Unterecker S, Nakajima K, Lapa C, Menke A, Higuchi T. Impact of Novel Antidepressants on Cardiac ^{123}I-Metaiodobenzylguanidine Uptake: Experimental Studies on SK-N-SH Cells and Healthy Rabbits. *J Nucl Med.* 59(7): 1099-1103. 2018.

World Health Organization (WHO) and International Atomic Energy Agency (IAEA). "*Bonn Call for Action, 10 Actions to Improve Radiation Protection in Medicine in the Next Decade*". Vienna: 2012.

Wong DF, Comley RA, Kuwabara H, Rosenberg PB, Resnick SM, Ostrowitzki S, Vozzi C, Boess F, Oh E, Lyketsos CG, Honer M, Gobbi L, Klein G, George N, Gapasin L, Kitzmiller K, Roberts J, Sevigny J, Nandi A, Brasic J, Mishra C, Thambisetty M, Mogekar A, Mathur A, Albert M, Dannals RF, Borroni E. Characterization of 3 Novel Tau Radiopharmaceuticals, 11C-RO-963, 11C-RO-643, and 18F-RO-948, in Healthy Controls and in Alzheimer Subjects. *J Nucl Med.* 59(12): 1869-1876. 2018.

Wyard, S.J. Intensity distributions of bremsstrahlung from beta rays. *Proceedings of the Physical Society of London*. A65: 377. 1952.

Yang H, Jenni S, Colovic M, Merkens H, Poleschuk C, Rodrigo I, Miao Q, Johnson BF, Rishel MJ, Sossi V, Webster JM, Bénard F, Schaffer P. 18F-5-Fluoroaminosuberic Acid as a Potential Tracer to Gauge Oxidative Stress in Breast Cancer Models. *J Nucl Med*. 58(3): 367-373. 2017.

Yu, N.Y.; Rule, W.G.; Sio, T.T.; et al. Radiation contamination following cremation of a deceased patient treated with a radiopharmaceutical. *Journal of the American Medical Association* (JAMA). 321(8): 803-804. 2019.

Zanzonico, P.; Dilsizian, V.; Metter, D.; Palestro, C. Sub-Committee on Nursing Mother Guidelines for the Medical Administration of Radioactive Materials. Final Report. Advisory Committee on Medical Uses of Isotopes (ACMUI). US NRC. Washington, DC. January 31, 2019.

Zanzonico, P.B.; Binkert, B.L.; Goldsmith, S.J. Bremsstrahlung radiation exposure from pure b-ray emitters. *J Nucl Med*. 40: 1024-1028. 1999.

Zhang J, Niu G, Lang L, Li F, Fan X, Yan X, Yao S, Yan W, Huo L, Chen L, Li Z, Zhu Z, Chen X. Clinical Translation of a Dual Integrin αvβ3- and Gastrin-Releasing Peptide Receptor-Targeting PET Radiotracer, 68Ga-BBN-RGD. *J Nucl Med.* 58(2): 228-234. 2017

Zhou X, Boellaard R, Ishiwata K, Sakata M, Dierckx RAJO, de Jong JR, Nishiyama S, Ohba H, Tsukada H, de Vries EFJ, Elsinga PH. In Vivo Evaluation of 11C-Preladenant for PET Imaging of Adenosine A2A Receptors in the Conscious Monkey. *J Nucl Med.* 58(5): 762-767. 2017.